Università degli Studi di Milano

PhD program in Experimental Medicine and Medical Biotechnologies

XXXII ciclo

Curriculum Immunological and Hemato-oncological

Department of Medical Biotechnology and Translational Medicine

PhD thesis

Immunotherapeutic potential and prognostic relevance of γδ T cell subsets in patients affected by liver metastatic colorectal cancer

Med/04

PhD student:

Elena Bruni

Tutor:

Prof. Domenico Mavilio

Dr. Joanna Mikulak

Coordinator:

Prof. Massimo Locati

Academic year 2019/2020

Table of contents

Declaration

The work described in this dissertation was performed at the IRCCS Clinical and Research Institute Humanitas, between October 2016 and October 2019. I declare that this dissertation has not been submitted in part or in whole to any other academic institution. The work reported here was entirely carried out by the author, unless otherwise indicated. Part of the results included in this dissertation have been already published in The Journal for ImmunoTherapy of Cancer.

List of Publications

1. **Bruni E**, Cazzetta V, Donadon M, Cimino M, Torzilli G, Spata G, Leonardi G, Dieli F, Mikulak J, Mavilio D. Chemotherapy accelerates immune-senescence and functional impairments of circulating Vδ2^{pos} T cells in elderly patients affected by liver metastatic colorectal cancer. *Journal* for *ImmunoTherapy of Cancer (JITC).* 2019 Dec 11; doi: 10.1186/s40425-019-0825-4.*

2. Salomé B, Gomez-Cadena A, Loyon R, Suffiotti M, Salvestrini V, Wyss Lozano Hoyos T, Vanoni G, Rossi M, Tozzo A, Tentorio P, **Bruni E**, Riether C, Jacobsen EM, Jandus P, Malmberg KJ, Conrad C, Hoenig M, Schulz A, Michaud K, Della Porta MG, Salvatore S, Ho PC, Gfeller D, Ochsenbein A, Mavilio D, Curti A, Marcenaro E, Steinle A, Romero P, Trabanelli S, Jandus C. CD56 marks and ILC1 like population with NK cell properties that is functionally impaired in AML patients at diagnosis but restored upon remission. *Blood Advances.* Nov 25; doi: 10.1182/bloodadvances.2018030478.**

3. Mikulak J, Oriolo F, **Bruni E**, Roberto A, Colombo FS, Villa A, Bosticardo M, Bortolomai I, Lo Presti E, Meraviglia S, Dieli F, Vetrano S, Danese S, Della Bella S, Carvello MM, Sacchi M, Cugini GC, Klinger M, Spaggiari P, Roncalli M, Santos BS, Spinelli A, Mavilio D. NKp46 identifies a subset of gut-resident intraepithelial Vδ1 T cells endowed with high anti-tumor activity against colorectal cancer. *Journal of Clinical Investigation (JCI) Insight.* 2019 Nov 6; doi: 10.1172/jci.insight.125884.*

4. Mikulak J, **Bruni E**, Oriolo F, Di Vito C, Mavilio D. Hepatic natural killer cells: organ-specific sentinels of liver immune homeostasis and physiopathology. *Frontiers Immunology*. 2019 Apr 10; doi: 10.3389/fimmu.2019.00946.*

5. Trabanelli S, Chevalier MF, Martinez-Usatorre A, Gomez-Cadena A, Salomé B, Lecciso M, Salvestrini V, Verdeil G, Racle J, Papayannidis C, Morita H, Pizzitola I, Grandclément C, Bohner P, **Bruni E**,Girotra M, Pallavi R, Falvo P, Leibundgut EO, Baerlocher GM, Carlo-Stella C, Taurino D, Santoro A, Spinelli O, Rambaldi A, Giarin E, Basso G, Tresoldi C, Ciceri F, Gfeller D, Akdis CA, Mazzarella L, Minucci S, Pelicci PG, Marcenaro E, McKenzie ANJ, Vanhecke D, Coukos G, Mavilio D, Curti A, Derré L, Jandus C. Tumour-derived PGD2 and NKp30-B7H6 engagement drives an immunosuppressive ILC2-MDSC axis. *Nature Communication*. 2017 Sep 19; doi: 10.1038/s41467-017-00678-2.**

* Publications related to the present thesis

** Publications not pertaining to the current thesis, in which I contributed, that were published during my Ph.D. program.

List of Figures

List of Tables

List of Abbreviations

ADCC	Antibody Dependent Cellular Cytotoxicity
Ag	Antigen
AML	Acute Myeloid Leukaemia
APC	Antigen Presenting Cell
BTN	B7-related Butyrophilin
CDR	Complementarity Determining Region
CHT	Chemotherapy
CLM	Colon-derived Liver Metastases
CMV	Cytomegalovirus
CRC	Colorectal cancer
CSC	Cancer Stem Cell
CTLA4	Cytotoxic T Lymphocyte Associated Antigen 4
DAMP	Damage Associated Molecular Pattern
DETC	Dendritic Epidermal T Cell
EGFR	Epidermal Growth Factor Receptor
FAP	Familial Adenomatous Polyposis
FDPS	Farnesyl Diphosphate Synthase
HER2	Epidermal Growth Factor Receptor 2
HMBPP	Hydroxy Methylbutenyl Pyrophosphate
HNPCC	Hereditary Non Polypotic Colorectal Cancer
IBD	Inflammatory Bowel Disease
IEL	Intraepithelial Lymphocytes
IFN	Interferon
IPP	Isopentenyl Pyrophosphate
mAb	monoclonal Antibody
MDSC	Myeloid Derived Suppressor Cell
MICA/B	MHC class I-related molecule A/B
MM	Multiple Myeloma
NCR	Natural Cytotoxicity Receptor
NK	Natural Killer
NKG2D	Natural Killer Group 2D
OS	Overall Survival
PAg	Phosphoantigen
PAMP	Pathogen Associated Molecular Pattern
PB	Peripheral Blood
PBMC	Peripheral Blood Mononuclear Cell
TF	Transcription Factor
TNF	Tumor Necrosis Factor
TRAIL	TNF-Related Apoptosis Inducing Ligand
t-SNE	t-Stochastic Neighbor Embedding

1

Introduction

1.1 Clinical features of colorectal cancer

Colorectal cancer (CRC) is the third most diagnosed cancer worldwide and the second leading cause of cancer-related death.[1] Globally, the estimated cases of CRC in 2018 were 1.8 million with a mortality rate of almost 50%.[1] According to the World Health Organization, CRC is the third most diagnosed cancer in men and the second in women, representing worldwide almost the 10% of all malignancies, excluding non-melanoma skin cancer.[1] In Italy, CRC is the second most frequent diagnosed tumor in both male and female, counting for the 13% of all cancer cases in man and the 15% in woman, preceded only by prostate and breast cancer respectively[2] (**Figure 1.1**). Although the mortality rate associated with CRC has been progressively decreasing in the past years[3], it remains a major health issue, particularly in industrialized states, where Caucasian males of older age are the main affected[4].

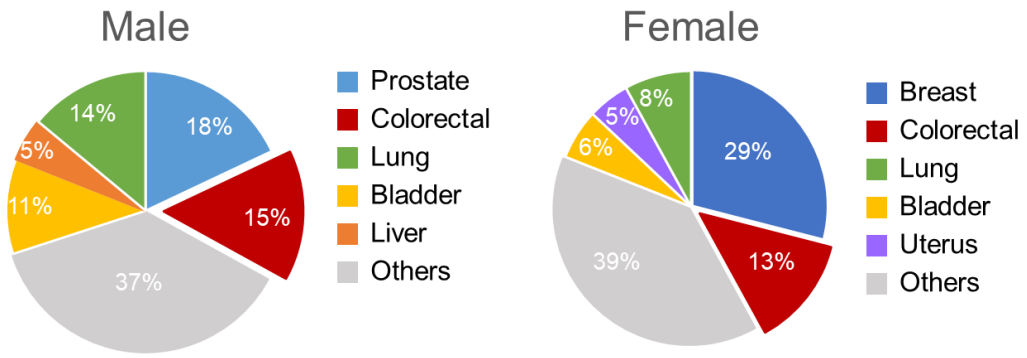

Figure 1.1. Estimated cancer statistic for Italy 2018 according to gender.[2] *Pie charts representing the distribution of the top five diagnosed cancers in male (left graph) and female (right graph). For each sex, the area of the pie chart corresponds to the proportion of the total number of cases, skin cancer excluded. Statistic data refer to the GLOBOCAN 2018 database.*

1.1.1 Pathogenesis and evolution of CRC

The incidence of CRC can be influenced by both genetic[5] and environmental factors[5,6]; however, sporadic cases are the most frequent event, counting for the 75% of all CRC patients[7]. The remaining 25% of cases are associated with a positive family history of CRC or hereditary syndromes that include Lynch syndrome, or Hereditary Non Polypotic Colorectal Cancer (HNPCC) and the Familial Adenomatous Polyposis or FAP.[7]

When CRC manifests spontaneously, i.e. with no apparent genetic cause, the onset of the disease can be related to several risk factors. Most common ones include, as mentioned above, age, gender and ethnicity, which are also known as intrinsic/non-modifiable risk

factors diversely from extrinsic/modifiable risk factors, which include mainly high-fat diet, obesity, alcohol, sedentary life and smoking[6] (**Figure 1.2**). In addition, intestinal chronic inflammation, generally associated with Inflammatory Bowel Diseases (IBD), such as Crohn or ulcerative colitis, also plays a major role in the development of CRC.[8]

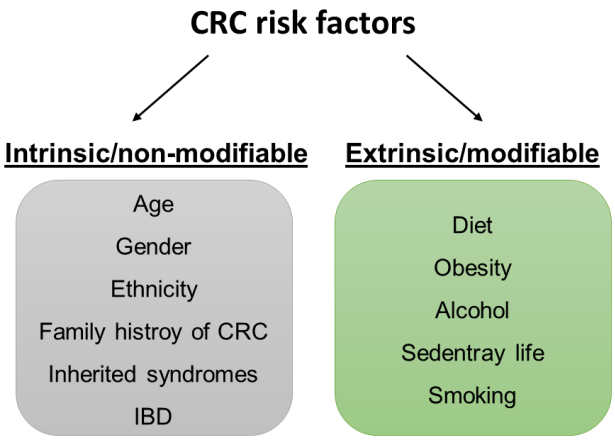

***Figure 1.2. CRC risk factors**. List of intrinsic/non-modifiable and extrinsic/modifiable risk factors in CRC. Data refer to Associazione Italiana di Oncologia Medica (AIOM), "I numeri del cancro in Italia 2017". IBD: Intestinal Bowel Disease*

A common feature of above-mentioned risk factors is their predisposition to polyp's formation.[9] These lesions are epithelial protrusions found in the colon lumen, whose incidence increases with age.[6] When polyps are malignant, they indicate the presence of an adenoma, which is considered the precursor lesion of CRC.[9] Adenomas can rapidly evolve into adenocarcinomas and finally progress into invasive carcinomas.[9] This transition from a normal mucosa into an adenocarcinoma is a multi-step process that results in the accumulation of several genomic mutations, which make CRC, at the molecular level, a heterogeneous group of diseases.[10] The most common genetic pathways dysregulated in CRC are associated with genomic instability and generally include mutations in the proto-oncogenes *Kras*, *p53* and adenomatous polyposis coli (*APC*).[10]

Upon CRC diagnosis, patients are classified in relation to the American Joint Committee on Cancer (AJCC) TNM system.[11] This type of classification takes into consideration three variables: the size of the tumor (T), the lymph node infiltration (N) and the presence of metastases (M). According to the TNM staging system, which reflects the progression of the tumor, CRC is divided into five stages from 0 to IV (**Figure 1.3**). The presence of an *in situ* carcinoma is considered the earliest stage (stage 0); whereas the most advanced condition of an invasive and metastatic tumor, which has spread to distant organs of the body, correspond to stage IV[11] (**Figure 1.3**).

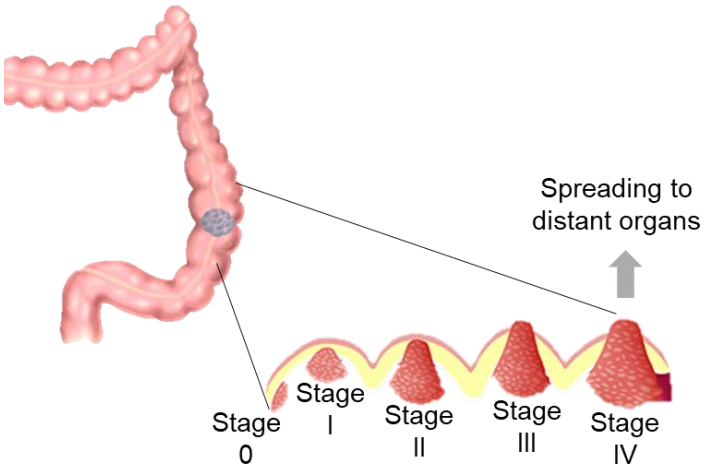

Figure 1.3. Staging classification of CRC patients.[11] *Classification of CRC patients according to the progression status of the tumor from earliest stage (stage 0) to most advanced conditions (stage IV).*

1.1.2 Colon-derived liver metastases (CLM)

Metastases result from the spreading of cancer cells from the primary tumor to distant organs. This complex process involves different steps, during which malignant cells detach from the original tumor, enter the circulatory system, survive during the transit, and, through extravasation, finally seed and form new tumor colonies in distant tissues.[12]

In primary CRC, the liver is the first site of metastatic dissemination.[13] The main reason of this high occurrence is the vascular connection, via the portal venous system, between the lower gastrointestinal tract and the liver.[13] In fact, more than 50% of patients diagnosed for CRC will eventually develop metastatic disease to the liver, which, in about 30 to 40% of advanced cases, will be the only site of metastasis.[13] In a minority of patients (around 25% of all CRC patients), liver metastases will already appear at the time of CRC diagnosis or within a year (early liver metastases), while about 30% of the remaining ones will develop hepatic metastases after one year and within 3 years after the onset of the primary tumor (late liver metastases)[14] (**Figure 1.4**). Typically, early metastases are usually more aggressive and associated with a higher T stage.[14]

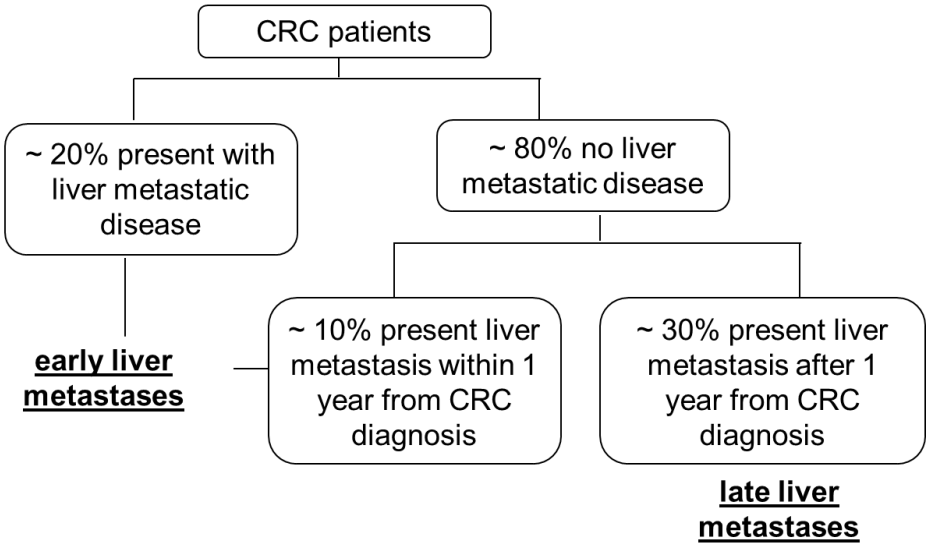

Figure 1.4. Incidence of colon-derived liver metastases in CRC patients.[14] *Schematic representation of the occurrence of liver metastases in primary CRC.*

In general, the presence of liver metastases is one of the major causes of death in CRC patients that without treatment have an average survival of less than 8 months after the presentation of the disease.[14] Moreover, the prognosis of patients is worst when large metastases or higher number of them (more than 4) are present.[15] In case of early CLM disease, 5-year survival post-resection is lower compared to late CLM.[15]

Finally, except from the liver, other common sites of metastatic spread from CRC include the peritoneal cavity and the lungs.[16]

1.1.3 Therapeutic approaches for CLM

Up to date the surgical removal of CLM represents the sole valid option for a possible cure.[17] However, because of the extent of the metastatic disease, due to tumor size, number and location of lesions or other poor prognostic factors, the majority of CRC patients (up to 85%) cannot directly receive surgery.[17] Hence, neoadjuvant chemotherapy (CHT) is generally administrated to these patients in order to reduce the metastatic disease and convert unresectable/potentially unresectable CLM into resectable ones[17] (**Figure 1.5**). This kind of neoadjuvant CHT is referred as "conversion CHT" and includes the use of classical anti-cancer drugs as a monotherapy or in combination with monoclonal antibodies (mAbs).[18] Because of its cytotoxic side effect, CHT is generally interrupted one month before the liver surgery.[18]

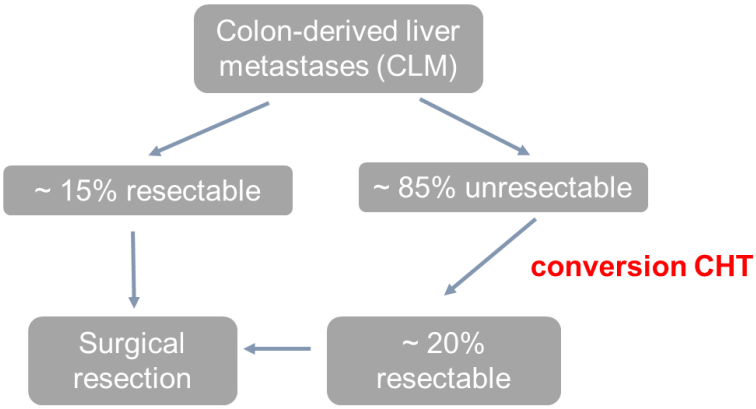

Figure 1.5. Clinical managing of CLM patients. *Schematic representation of the clinical management of resectable and unresectable liver metastases.*
CHT: chemotherapy

The two main standard CHT regimens for the treatment of advanced CRC include the combinations of folinic acid (leucovorin) and fluorouracil (5-FU) with either Oxaliplatin (FOLFOX regimen) or Irinotecan (FOLFIRI regimen).[18] FOLFOX and FOLFIRI regimens are generally combined with mAbs, also referred as target/biologic drugs, to improve the effectiveness of treatment.[18] The most recommended biologic drugs for CLM are anti-angiogenic drugs, which block the intratumoral neo-angiogenesis, and the epidermal growth factor receptor (EGFR) inhibitors.[19] These latter are effective only in the absence of *Kras* gene mutations, which have to be tested before starting the treatment.[19]

Bevacizumab was the first anti-angiogenic drug approved for cancer therapy with documented clinical benefit for metastatic CRC.[20] It is a humanized mAb directed against the vascular endothelial growth factor (VEGF), which is a central mediator of tumor angiogenesis.[21] In particular, it binds to all the isoforms of the VEGF-A molecule, which is the most relevant member of the VEGF family involved in tumor angiogenesis. This protein is secreted mainly by cancer cells and endothelial cells and upon binding with VEGF receptor (VEGFR)-1 and VEGFR-2, on endothelial cells, it promotes their proliferation, migration, survival and vascular permeability[21] (**Figure 1.6A**). For this reason, the overexpression of VEGF in the tumor microenvironment favors the development of new blood vessels with structural abnormalities and functional defects, which eventually support the tumor progression.[21] Several clinical trials have reported that bevacizumab-dependent blocking of this pro-tumor mechanism, in combination with standard anticancer drugs, increases the response rate as well as the overall and progression-free survival of CLM patients.[22]

Among EGFR-inhibitors, cetuximab is one of the biologic drugs with shown efficacy in CLM patients.[23] It is a chimeric immunoglobulin G1 (IgG1) mAb that specifically targets the extracellular domain of the EGFR.[24] The main mechanisms of action of cetuximab rely on its direct antiproliferative and proapoptotic effects on the tumor target due to the blocking of the ligand-induced receptor phosphorylation, which controls downstream signaling pathways and leads to cellular proliferation[24] (**Figure 1.6B**). However, somatic mutations in the *Kras* gene vanish the effect of cetuximab because of the constant activation of the EGFR even in the absence of its ligand.[23] Another agent possibly used in case of resistance to cetuximab is the panitumuab, which, similar to cetuximab, inhibits the interaction between the EGFR and its ligand EGF.[24] Both cetuximab and panitumumab are widely used in *wild-type* KRAS cases, in addition to FOLFOX or FOLFIRI, for the conversion of initially unresectable metastases into resectable and for the further potential curative resection.[18]

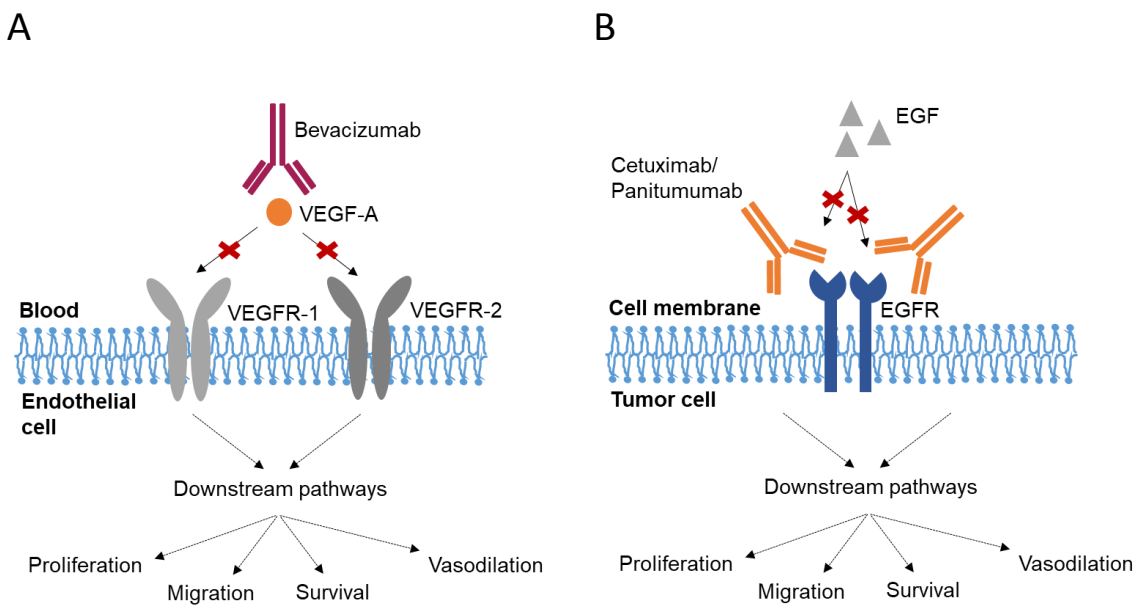

Figure 1.6. Mechanisms of action of mAb-based therapy for CLM patients. *(**A-B**) Illustration of the biologic mechanism of the anti-VEGF-A bevacizumab[21] (A) on an endothelial cell and the anti-EGFR drug cetuximab/panitumumab[24] (B) on a tumor cell. The intracellular pathways affected by the drugs are reported at the bottom of the figures. VEGF: Vascular Endothelial Growth Factor; EGF: Epithelial Growth Factor.*

All the therapeutic approaches described, when effective, allow the reduction in size of the liver metastases and their further removal in a meaningful number of patients.[18] However, surgery, even when combined with CHT, is curative only for few patients.[25] In fact, one out four CLM patients will experience disease recurrence, exclusively to the liver.[25]

1.1.4 The role of the immune system in CLM

The host immune system has been recently suggested as a major contributing factor in the prognosis of CLM patients.[15] Under physiological conditions, the majority of lymphocytes that populate the liver consists of Natural Killer (NK) cells, cytotoxic T cells (CTL) and gamma-delta (γδ) T cells, which contribute to the maintenance of liver homeostasis while favoring tumor immune surveillance.[15]

Within the myeloid lineage, liver-resident macrophages, also known as Kupffer cells, represent the most abundant immune population with fundamental role in the maintenance of tissue homeostasis through the clearance of damage associated molecular patterns (DAMPs) and pathogen associated molecular patterns (PAMPs).[26] Although not abundant, dendritic cells (DC) also populate the liver tissue and are essential for the antigen presentation and consequent activation of T lymphocytes.[27]

It has been reported that the local microenvironment of metastatic liver is characterized by higher levels of inflammatory cytokines and chemokine dysregulation that eventually can disrupt the normal immune cell milieu[28] (**Figure 1.7**). In fact, constant interactions between tumor cells and tissue-resident and infiltrating immune cells can directly control the evolution of cancer. In particular, the intratumor concentration and localization of specific subsets of immune cells have a major prognostic value.[15] Our group recently reported that higher intratumoral percentages of both T cells and NK cells are a positive prognostic factor in CLM patients.[29] Indeed, the density of these cells is associated with prolonged survival upon the removal of liver metastases.[29] The understanding of the mechanisms that regulate the infiltration of T cells and NK cells is a necessary step to estimate the clinical outcome of CLM patients and to improve current therapeutic approaches.

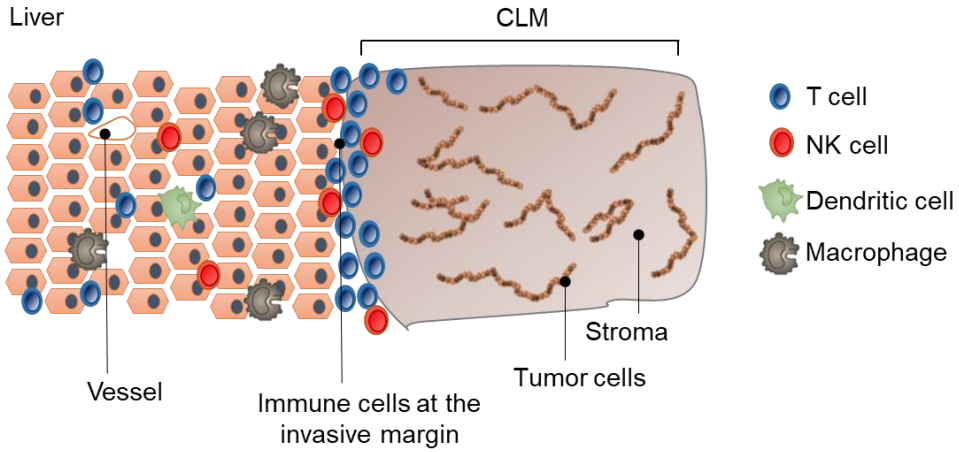

Figure 1.7. Composition of immune cells in CLM.[28] *Tissue distribution of T cells, Natural Killer (NK) cells, macrophages and dendritic cells within the "normal" liver parenchyma, the invasive margin and the intratumor compartments. Cytotoxic subsets, including T cells and NK cells, are preferentially located at the invasive margin right next to the liver metastatic stroma.*

In CRC, the presence of tumor-infiltrating immune cells has been linked with a higher survival rate.[30] More in detail, the density inside the tumor and at the invasive margin of cytotoxic $CD8^{pos}$ and memory $CD45RA^{pos}$ T cells can be used to assign an immunoscore.[30] This additional immune parameter in combination with the TNM staging system provides a further and more comprehensive criterion for the stratification and management of patients. The immunoscore can be further complemented by the immune profiling, which describes the immune signature of the host and is predictive of the patient's response to therapy.[31] This immune profile can be dynamically modified trough interactions between immune cells and tumor cells and it is a major determinant for the success of immunotherapeutic strategies.[31] The aim of these latter is to enhance the immune system response against tumor cells by targeting inhibitory receptors, known as checkpoint and generally expressed by cytotoxic T lymphocytes. The most relevant checkpoint inhibitors include the anti-Cytotoxic T-Lymphocyte Antigen 4 (CTLA4), the anti-Programmed cell death protein 1 (PD-1) and the anti-PD-1 ligand (PD1L). However, no evidence has been reported on the efficacy of these drugs for the treatment of CLM.

The use of target therapy as the anti-EGFR and the anti-VEGF can additionally modify the immunological setting of liver metastases. It is known that anti-EGFR mAbs enable the activation of immune cells and promote their migration to the site of the tumor.[32] Moreover, by the expression of CD16, which recognizes the Fcγ chain of IgG1 mAbs such as

cetuximab, NK cells and γδT cells can inhibit the tumor growth through antibody dependent cellular cytotoxicity (ADCC) further enhancing the efficacy of target therapies.[33]

In conclusion, each of the cells infiltrating the tumor tissue, including NK cells, αβT cells and γδT cells, contributes to the clinical heterogeneity of CLM patients and represents a potential target for the identification of new biomarkers, and the development of novel personalized immunotherapeutic approaches.

1.2 Gamma-delta (γδ) T lymphocytes

γδT lymphocytes are a unique T cell subpopulation expressing a T cell receptor (TCR) that is composed by a heterodimer of one TCRγ and one TCRδ chain[34](**Figure 1.8**). They were first identified in the late '80s as a distinctive T cell lineage that appears earlier than αβT cells during thymocyte maturation.[35,36]

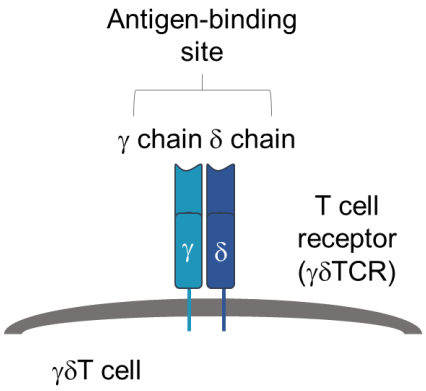

Figure 1.8. γδ T cell receptor (TCR). *Schematic representation of the γ and δ chains heterodimer composing the γδTCR.*

After birth, γδT cells constitute 1 to 5% of total human circulating T cells, which are mainly αβT lymphocytes.[37] However, they become more abundant in tissue compartments such as skin[38] (1 to 10%), liver[39] (5 to 20%) and intestinal mucosa[40] (5 to 30%), where they contribute to tissue homeostasis.[41] Similar, also mouse γδT cells are preferentially located at tissue barriers counting, for example, up to 20% of T resident gut intraepithelial lymphocytes (IELs)[42] and the 50% of skin epidermal γδT cells[43].

In human, the preferential tissue-tropism of γδT cells is mainly associated to the expression of a specific δ chain, although some γ chain combinations can be restricted to certain tissue sites (**Table 1.1**).[44] According to this classification, human γδT cell subsets include: Vδ1^{pos} T cells that constitute the predominant population in the gut, liver, thymus and skin, Vδ2^{pos} T cells, preferentially located in the peripheral blood and the Vδ3^{pos} T cell subset, which is more represented in the liver and poorly found in the circulation.[44] Differently, in mice, the tissue specialization is more linked

to the γ chain expression with no equivalents with the two main human subsets of Vγ9Vδ2 and Vδ1^{pos} T cells.[45]

Table 1.1. Subsets of human γδ T cells. *Preferential tissue distribution and Vγ-Vδ-paired combinations of human γδT cell subsets. Adapted from "human γδT cell subsets and their involvement in tumor immunity" by Wu et al. Cellular & Molecular Immunology, 2017.*

Species	Subset	Paired Vγ genes	Tissue localization
Human		Not defined	Liver, thymus, spleen
	Vδ1	Vγ4	Gut
		Vγ5	Skin
	Vδ2	Vγ9	Blood
	Vδ3	Not defined	Blood, liver

A unique property of γδT cells is their described ability to recognize antigens (Ags) in the absence of major histocompatibility complex (MHC) restriction.[46] This important feature allows the direct recognition of Ags without any prior processing and presentation through the MHC,[47] thus favouring the induction of rapid cytotoxic responses against infected or tumor-transformed cells.[46]

Upon target recognition, γδT cells can release cytotoxic granules, as granzyme and perforine and cytokines, including mainly interferon (IFN)-γ and tumor necrosis factor (TNF)-α.[41] In fact, it has been described that the frequency of blood circulating γδT cells can heavily increase (up to 60% of total T cells) during infections caused by both bacterial[48,49] and viral agents[50,51]. Moreover, considering their preferential tissue-localization within epithelial barriers, γδT cells can function as a first line of defence in response to tissue damage or during pathological conditions.[41] For instance, interleukin (IL)-17 sources, are provided by γδT cells without needing previous TCR activation for the physiological protection of mucosal barriers from bacterial infections.[52]

The current thesis work is mainly focused on the well-established γδT cells antitumor properties and on their potential role in cancer immunotherapy that will be discussed in detail in Paragraph 1.2.4 and 1.2.5, respectively.

1.2.1 TCR repertoire of γδ T cells

γδT cells are a distinct cell lineage[53] and the first subpopulation to appear during T cell differentiation[54].

In humans, the gene coding for the TCR γ-chain is located in the short arm of chromosome 7[55], while in mouse it is placed on chromosome 13[56]. The TCRδ-chain, instead, is located between the Vα and Jα gene segments of chromosome 14 in both human[57] and murine[36] genome. The generation of functional γ and δ genes is the result of complex gene rearrangement known as V(D)J recombination[58,59] (**Figure 1.9A**). This process takes place during T lymphocytes development in the thymus and defines the TCR repertoire of the T cell lineage.[58] It involves the rearrangement of variable (V), joining (J) and, sometimes, diversity (D) gene segments. The γ locus contains 4 Jγ genes in association with corresponding Cγ genes and 4-6 (based on the haplotype) functional Vγ genes.[55] The δ locus, placed within the TCRα locus, consist of 8 Vδ genes that rearrange to Dδ/Jδ-Cδ segments[57] (**Figure 1.9B**). Compare to αβT cells (>2000 possible V combinations), the number of V segments arrangements in γδT cells is limited.[60] Nevertheless, the potential diversity of the γδTCR repertoire is much higher (in the order of 10^{17}) of that of αβT cells, thanks to the use of distinct D segments of the TCRδ locus and the possible N-nucleotide addition between D-D as well as to V-D and D-J junctions.[61] This junctional diversity focussed the TCR variability in the complementarity determining region (CDR) that guides Ag-recognition. Moreover, structural studies on the V rearranged regions of the γδTCR demonstrated that they resemble the V regions of Abs rather than that of αβTCR,[62] consistent with the recognition of surface Ags rather than MHC-presented peptides[47].

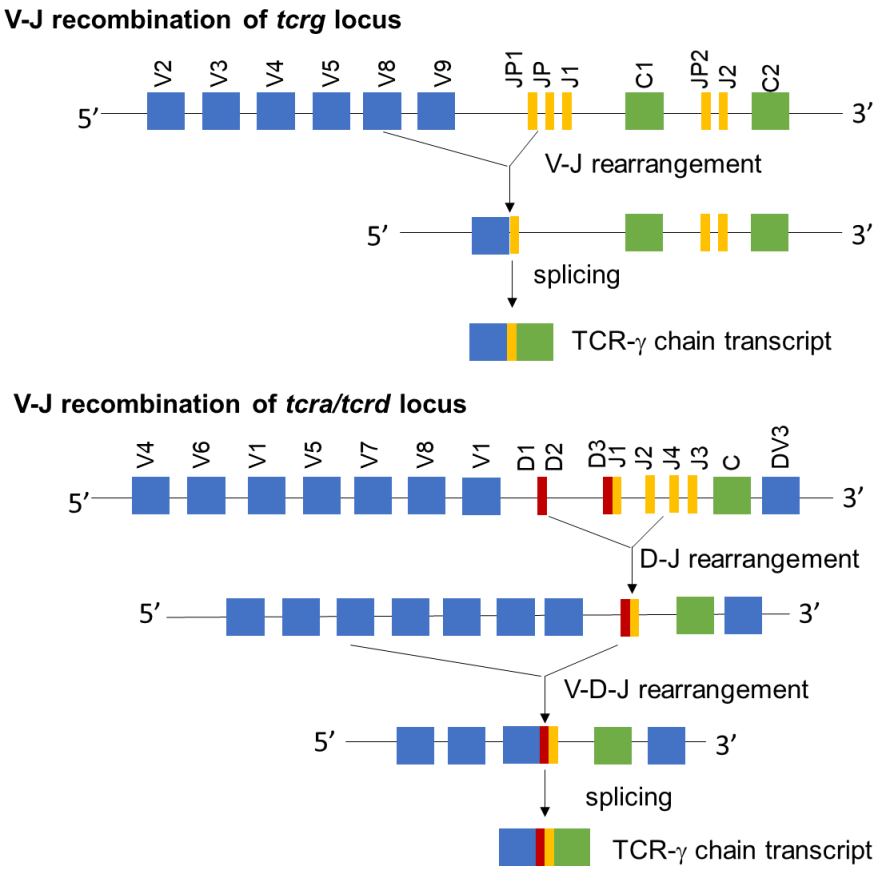

Figure 1.9. V(D)J recombination at the tcrg and tcra/tcrd gene loci*. Representation of the tcrg (upper panel) and tcrd (lower panel) chains loci. The TCR-γ chain is produced through a single V-J recombination, with N additions occurring at the V-J junction. The TCR-δ chain derives from a V-D-J recombination with the possible inclusion of either 2 or 3 D segments, which leads to the production of up to 4 N diversity regions. Only gene segments used for the TCR-δ chain formation are represented. The structure of the tcrg and tcra/tcrd loci was adapted from the IMGT database.*[59] *Only functional gene segments are shown. Adapted from "The promise of γδ T cells and the γδ T cell receptor for cancer immunotherapy" by Legut et al. Cellular & Molecular Immunology, 2015.*

The generation of a functional γδTCR is part of the maturation process that takes place in the thymus and it is known as thymic selection. During this process, which is divided into different stages, the result is the production of a proper Ag-specific TCR. Both αβ and γδ T cells derive from the same thymic progenitor, however, contrary to αβT cells, the process that drives γδT cell maturation, selection and peripheral localization are not well characterized since much of our knowledge in this field depends on mouse studies. In particular, in mice, γδT cells development is characterized by different waves of γ chain production. A first wave, during which the Vγ5 chain is expressed and the colonization of

the epidermis takes place, and a second wave when the Vγ6 chain is predominantly produced, corresponding to homing of the reproductive tract.[42] Vγ5 γδT cells originated from the first wave are referred as dendritic epidermal γδT cells (DETCs)[63] with no defined counterpart in human. Remarkably, about 90% of mouse DETCs express the invariant Vγ5Vδ1 TCR and their migration into the epidermis occurs early during embryonic development.[64]

Molecular analysis of human γδT cells revealed that the majority of adult circulating subsets are oligoclonal, have limited junctional diversity and use mainly Vγ9Vδ2 gene segments.[65] In addition, a conspicuous fraction of Vγ9Vδ2 T cells are shared between different individuals and are composed by similar Vγ9JγP variants. Interestingly, these variants are already present during prenatal development and expand in the first year after birth, probably as a result of microbial responses that consequently focus the Vγ9Vδ2 TCR repertoire of adults.[66]

Non-Vγ9Vδ2 T cells consist mainly of $V\delta1^{pos}$ rearrangements paired with different TCR-γ segments and hold high inter-individual heterogeneity.[67] For this reason, a more adaptive nature has been suggested for $V\delta1^{pos}$ T cells, compared to the more public $V\delta2^{pos}$ T cell subset.[68] For instance, substantial oligoclonal expansion of $V\delta1^{pos}$ T cells has been described in the presence of CMV infection.[69]

Even though, in human, correlations between a particular paired of VγVδ chains combination and its tissue localization is not as strictly defined as in mouse, the preferential expression of specific Vγ is found among gut intraepithelial lymphocytes (IELs). In fact, human IELs γδT cells are mainly Vγ4 restricted, similar to Vγ7 γδ T IELs in mice.[70] This organ-specific repertoire could depend on specific Ag-restriction and be associated with different migratory-capacity of γδT cells subsets.

1.2.2 Ligands recognition by the γδTCR

Since the discovery of γδT cells in the mid '80s, the putative ligands proposed or established for the γδTCR include compounds with extremely diverse molecular structures[71] (**Figure 1.10**). Among candidate molecules, stress-related ones are thought to be the main target of γδT cells.[72] Indeed, the majority of ligands identified so far correspond to self-molecules that are upregulated under cell stress, tumor transformation or upon bacterial and viral

infections.[73–75] Differently from peptides binding the αβTCR, this sort of molecules are not processed by the MHC complex but are lipid compounds usually deriving from metabolic pathways.[46] Among them, phosphoantigens (PAgs) have been one of the first ligands, not MHC-restricted, to be described for γδT cells.[41] PAgs are low molecular weights metabolites of the mevalonate pathway that are endogenously produced under physiological conditions. However, an intracellular accumulation of PAgs can originate from cell-stress, like tumor-transformation or during infections.[76] For example, high amount of isopentenylpyrophosphate (IPP) are induced in malignant cells and are efficiently recognized by Vγ9Vδ2 T cells.[77] On the contrary, homeostatic concentration of IPP does not stimulate the γδTCR allowing the discrimination of healthy cells.[78] An example of pathogens associated PAg is the hydroxyl-dimethyl-allylpyrophosphate (HDMAPP), which strongly induce Vγ9Vδ2 T cells cytotoxicity.[74]

Activation of Vδ2^{pos} T cells by PAgs is both TCR and contact-dependent, and recent observation suggested that B7-related butyrophilin (BTN) molecules CD277/BTN3A are directly involved in this mechanism.[79] More in detail, the BTN3A1 isoform has been identified as a mandatory molecule for the PAg-dependent activation of Vγ9Vδ2 T cells. In general, the recognition of PAgs by Vγ9Vδ2 T subset represents an efficient machinery for the sensing of cell stress and the rapid elimination of tumor-transformed or virus-infected cells that have dysregulated levels of PAgs.[76] Moreover, this innate-like mechanism of immunosurveillance has been widely explored for the expansion and the immunotherapeutic usage of Vδ2^{pos} T cells that will be further discuss in paragraph 1.2.5.

Other types of molecules capable to stimulate the γδTCR, in humans, are the stress-inducible receptor MICA and MICB that were firstly described as ligands for NKG2D, a typical NK cells activating receptor.[80] It has been demonstrated that the expression of MICA and MICB, which augments in tumor cells and damaged intestinal epithelial cells, drives Vδ1-TCR stimulation.[73]

Other ligands discovered in the last decade for the γδTCR include: the UL16-binding proteins 4 (ULBP4s), that is also recognized by human NK cells through the activating receptor NKG2D,[81] CD1c and CD1d molecules, recognized by Vδ1^{pos} T cells subset,[82,83] the endothelial protein C receptor (EPCR) induced during *Cytomegalovirus* infections,[84] the algae protein-phycoerythrin (PE),[85] the mitochondrial F1-ATPase expressed on tumor cells surface[86] and the histidyl-tRNA synthetase in patients affected by polymyositis[87].

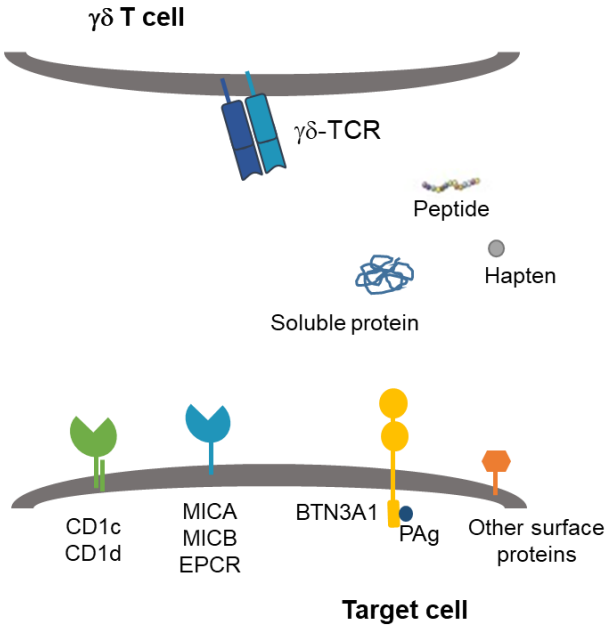

Figure 1.10. Putative and identified ligands recognized by the human γδTCR. *Different classes of γδT cell ligands, including: CD1 family member (CD1c, CD1d), MHC-related molecules (MICA, MICB), endothelial protein C receptor (EPCR) and butyrophilin-like molecule (BTN3A1) presenting phosphoantigens (PAgs). Other type of ligands include soluble protein, free peptides and haptens. Adapted from "γδ T cell responses: How many ligands will it take till we know?" by Vermijilen et al. Seminars in Cell & Developmental Biology, 2018.*

In conclusion, the exact role of γδT cells in both physiological and pathological conditions still remain enigmatic especially because of the lack of Ags identified so far.[88] Hopefully, TCR-sequencing technology in combination with mass spectrometry analysis will shed new light on ligand recognition by γδT cell subsets with direct implication for the clinical use of γδT cells.

1.2.3 Function of γδ T lymphocytes

γδT cells can execute a variety of functions depending on both tissue specialization and TCR restriction. A wide range of soluble factors, with regulatory or cytotoxic activity are secreted by γδT cells. Upon activation against pathogens, human circulating γδT cells can release a high quantity of inflammatory cytokines including IFN-γ and TNF-α.[89] γδT cells resident within the derma and the intestinal *lamina propria* naturally express IL-17, which has a protective role in case of bacterial and fungal infections and it is also important for cancer immunosurveillance and gut homeostasis.[52] For instance, IL-17 production by γδT cells is essential for the control of enteritidis caused by *Salmonella enterica* infections[90] or during *Mycobacterium tuberculosis* infection of the lung[91]. It has been reported that by IL-17-mediated recruitment of neutrophils, γδT cells could favor the removal of bacteria during *Listeria moncytogenes* liver infection and *Escherichia coli* intraperitoneal infection with $V\delta1^{pos}$ subset of γδT cells being the major source of IL-17.[52] The presence of IL-17-producing γδT cells was a feature also of some viral infections, including the one caused by

the *West Nile virus*[92] and the *Respiratory syncytial virus* (RSV)[93]. However, cytokine secretion by γδT cells is not only linked to cytotoxicity but it can also consist of regulatory functions. In mice, DETCs γδT cells not only produce IFN-γ and granzymes, but also secrete IL-13[94] or insulin like growth factor 1 (IGF1)[95] that ultimately regulate IgE production by B cells and stromal cells activity respectively. Always in mouse, γδT cells present in the liver or the spleen can secrete both IFN-γ and IL-4 which, similarly to IL-13, control the humoral response.[96]

The presence of a specific Vγ or Vδ chain can lead to different cellular responses. In mice, Vγ1 but not Vγ4 expression is associated with the clearance of *Listeria* infection while, in humans, the expression of the Vδ1^{pos} or Vδ2^{pos} chain, besides being associated with a distinct peripheral localization, is also involved in different responses.[73] Indeed, Vδ2^{pos} T cells can secrete many inflammatory cytokines such as IFN-γ, TNF-α, IL-17 and IL-12 as in response to virus-infections,[97] while Vδ1^{pos} T cells were recently found to be associated with antitumor activity[98].

γδT cells are also involved in wound healing due to their production of keratinocyte growth factor (KGF) which was reported in mice skin localized Vγ5Vδ1 cells.[99] Mice intestinal γδT cells also perform a protective role as it was demonstrated using a mouse model of IBD chemically induced with dextran sulphate sodium (DSS). These mice were more susceptible to chemical-induced epithelial cell damage when deprived of γδT cells if compared to wild type.[100]

Despite the many evidences that correlate the presence of a certain Vγ or Vδ chain with a specific function, the mechanisms responsible for this association remain unclear. Whether thymic selection give a specific function to the different γδT cell subsets or whether γδT cells acquire their phenotype once in the periphery according to tissue microenvironment, are still debated issues.

One of the main functions explicit by γδT cells, object of interest in the last decades, regards their antitumor activity, which will be discuss in more detail in Paragraph 1.2.4. Additionally, γδT cells are important during the resolution phase of infection thanks to their action as antigen presenting cells (APCs) and their recruitment of effector cells to the inflammatory site.[46]

Summarizing γδT cells do not have a single function but they participate in many ways during an immune response as schematically shown in **Figure 1.11.**

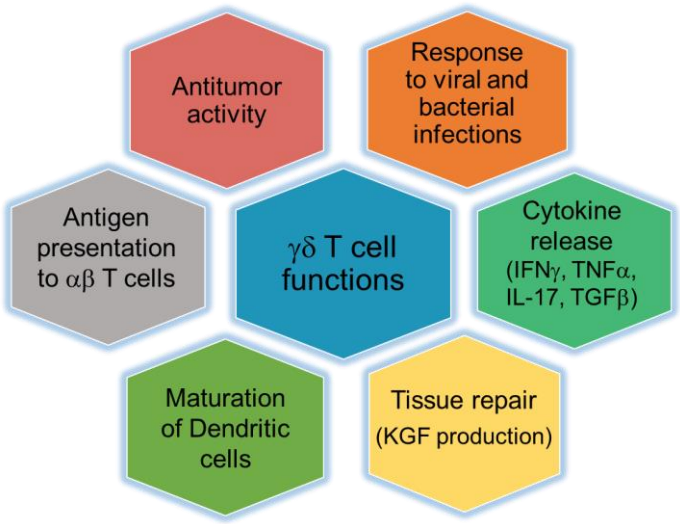

Figure 1.11. γδ T cells functions. *γδT cells participate to all phases of an immune response by: the production of inflammatory cytokines that are necessary for antitumor activity, the elimination of infected and stressed cells and neutrophil recruitment. Additionally γδ T cells regulates dendritic cells maturation, αβT cells activation and stromal cells activity. KGF: Keratinocyte Growth Factor*

1.2.4 γδ T cells in cancer

The described innate-like properties of γδT cells, mainly consisting in rapid and MHC-unrestricted cytotoxic-responses, define their role in cancer immunosurveillance. The first evidence of the antitumor protective role of γδT cells derived from a chemically-induced mouse model of skin cancer early in 2001.[101] Further studies confirmed the antitumor activity of γδT cells in different human cancer types, including both hematological malignancies, as lymphoma and leukemia[102], and solid tumors, as in the case of CRC[103], lung carcinoma[104], prostate cancer[105] and melanoma[106].

Different mechanisms are involved in the antitumor functions of γδT cells and they include both direct and indirect effects on the tumor growth. By the release of cytotoxic granules, including perforins and granzymes, γδT cells can directly induce the cytolysis of cancer cells.[44] The specific recognition of tumor-transformed cells can rely on the engagement of both the TCR as well as NK receptors (NKRs). One of the main NKR receptor expressed by γδT cells is NKG2D. This activating/antitumor receptor recognizes stress-induced molecules as IPP, MICA and MICB that are generally overexpressed on the surface of tumor cells thus inducing γδT effector functions.[107] For example, the production of inflammatory cytokines, IFN-γ and TNF-α, by γδT cells, not only drives the recruitment of other cytotoxic subsets but it also has a direct lytic effect on tumor target cells. In

particular, TNF-α can induce the apoptosis of target cells by binding to CD95 ligand and TNF-related apoptosis inducing ligand (TRAIL) expressed by tumor cells.[108] Whereas the secretion of IFN-γ by γδT cells, by enhancing MHC class I expression on tumor cells, further favor their recognition by cytotoxic $CD8^{pos}$ T lymphocytes. Recently it was also demonstrated that, once activated, γδT cells can increase the expression of CD16, which, by recognizing the Fc structure of IgGs (Fcγ), triggers ADCC against tumor targets.[108,109] In addition, γδT cells can favor the maturation of DCs thus promoting the development of Ag-specific responses mediated by αβT lymphocytes.[46]

In contrast to their antitumor activity, γδT cells also display protumor functions under specific circumstances.[110] For instance, it has been reported that the infiltration of γδT cells can promote the establishment of an inflammatory microenvironment associated with tumor progression. In fact, γδT cells are essential producers of IL-17 that strongly increases inflammation responses in tumor immunity and promotes angiogenesis.[111] For example, in a mouse model of metastatic breast cancer, it was shown that IL-17 secretion by γδT cells is responsible for the recruitment of immunosuppressive cells subsets as myeloid derived suppressor cells (MDSCs) that eventually support tumor growth by inducing neo-angiogenesis and by creating an immunosuppressive microenvironment.[112] In human CRC IL-17^{pos} γδT cells can induce a severe immunosuppressive milieu associated with high production of TNF-α and granulocyte- macrophage colony-stimulating factor (GM-CSF) which promote tumor growth.[113] Consequently, the infiltration of IL-17^{pos} γδT cells in human CRC positively correlates with tumor burden and worse prognosis. Moreover, γδT cells can contribute to immune-checkpoint inhibition of αβT cell, through the high expression of PDL1 as observed in a murine model of pancreatic ductal adenocarcinoma.[114]

In the last year, many studies focused on the specific subsets of γδT cells (defined by their TCR repertoire and functional differences) which may have diverse activity in antitumor immunity.[115] Indeed, the antitumor-activity of peripheral blood Vγ9Vδ2 T cells have been tested in different types of cell lines and primary tumors, including both leukemia and carcinoma cells.[116] The mechanism driving $V\delta2^{pos}$ T cells antitumor function is the TCR-mediated recognition of tumor-associated PAgs, mainly IPP. Other surface molecules, overexpressed on tumor cells, that are recognized by Vδ2-TCR include human MutS homologue 2 (hMSH2) and BTN3A1 which is essential for PAgs-mediated activation of

Vδ2^{pos} T cells. At the same time, the frequent expression of NKG2D related ligands on the surface of tumor cells, is a potent inducer of Vδ2^{pos} T cells antitumor cytotoxicity.[117]

Besides TCR-dependent mechanisms, an important role in the recognition and killing of tumor targets is played by CD16-mediated ADCC. Indeed, the upregulation of CD16 on activated Vδ2^{pos} T cells cause the binding of IgG-coated tumor cells during mAbs treatment, as it has been described for trastuzumab, which binds the human epidermal growth factor receptor 2 (HER2) and for the anti-CD20 mAb rituximab used for the treatment of B-lymphomas[118].

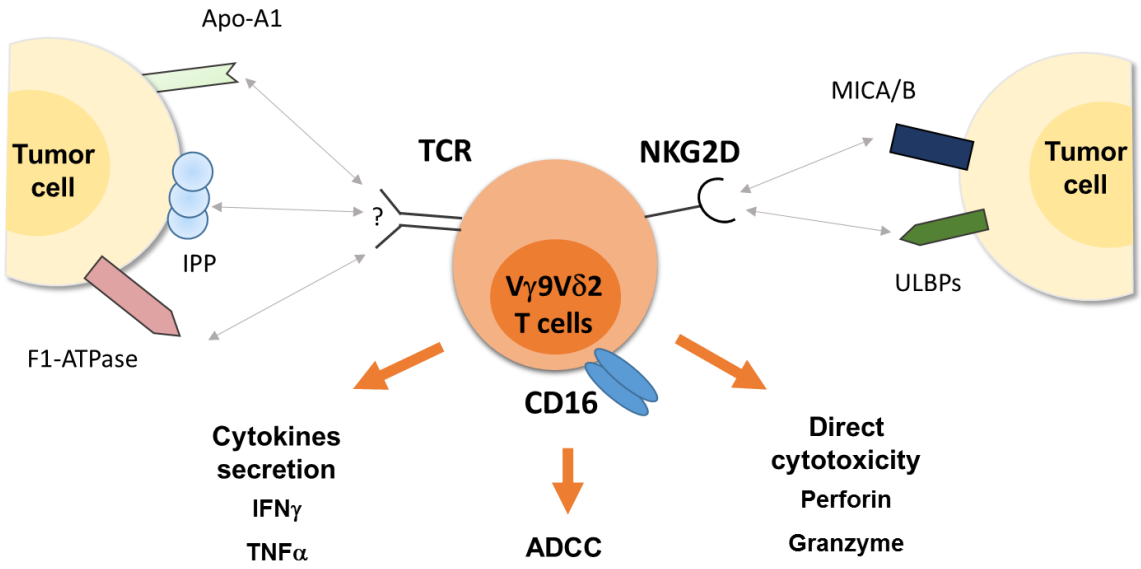

Figure 1.12. Main mechanisms of Vδ2^{pos} T cells antitumor response. *Interaction driving the recognition of tumor cells by Vδ2^{pos} T cell subsets are represented. Antitumor responses of Vδ2 include: direct cytotoxicity by the release of granzyme and perforin, proinflammatory cytokines production (IFN-γ and TNF-α) and CD16 mediated recognition of mAbs that activate the antibody dependent cellular cytotoxicity (ADCC). Known Ags recognized by Vδ2^{pos} T cells include MHC class I-related chain A/B (MICA/B); UL16-binding proteins (ULBs), isopentenyl pyrophosphate (IPP), Apo-A1 and F1-ATPase.*

Similar to the Vδ2^{pos} subset, the antitumor functions of Vδ1^{pos} T cells have been broadly investigated. For instance, we reported that cytokine and TCR-dependent *in vitro* stimulation of blood-circulating γδT cells, induces the expansion of natural cytotoxicity receptor (NCR)^{pos} Vδ1^{pos} T subset with high tumor-killing activity against leukemia cell lines.[119] However, tumor-ligands binding the Vδ1-TCR are still largely unknown. Till now the main mechanisms described to induce Vδ1^{pos} T cell antitumor response are based on the

expression of NKR, including NKG2D, NKp30 and NKp44.[120] Interestingly, it has been observed that MICA is directly recognized by the Vδ1-TCR and, together with NKG2D-mediated stimulation, induces an efficient antitumor activity mediated by increased levels of IFN-γ and perforins.[107] Analogously, high levels of ULBPs on tumor cells of hematological origin drive the cytotoxicity and/or cytokines production by Vδ1^{pos} subset even in the absence of TCR-involvement.[121] *In vitro*-expanded Vδ1^{pos} T cells from peripheral blood present enhanced antitumor activity against solid tumors. Recently, it has been shown that freshly isolated human peripheral Vδ1^{pos} T cells have increased killing activity against human colon cancer cell lines compared to Vδ2^{pos} T counterparts.[122]Moreover, CMV-induced Vδ1^{pos} T cells can inhibit not only the growth of primary CRC but also the occurrence of secondary tumor foci.[123] Tumor-Ags and corresponding receptors driving the recognition of tumor cells by Vδ2^{pos} and Vδ1^{pos} T cells subsets are represented in **Figure 1.12 and 1.13**, respectively.

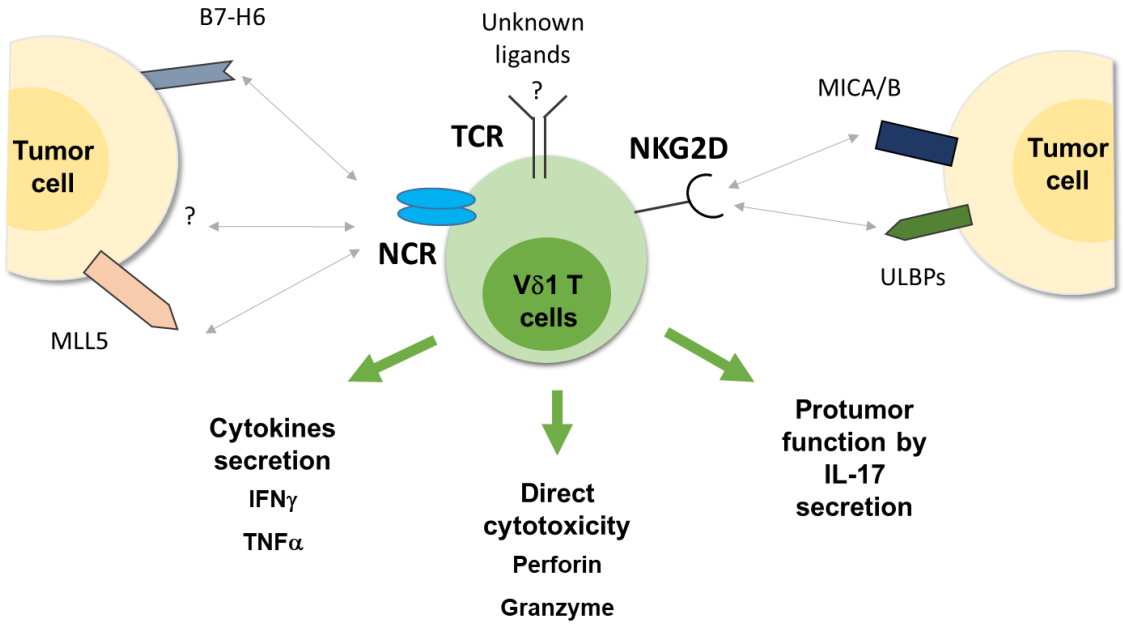

Figure 1.13. Tumor-Ags recognition by specific Vδ1^{pos} T cell subset. *Known and putative interactions driving the recognition of tumor cells by Vδ1^{pos} T cell subset are represented. They include NKG2D-mediated recognition of MHC class I-related chain A/B (MICA/B) and UL16-binding proteins (ULBPs) ligands and natural cytotoxicity receptors (NCRs)-dependent activation of Vδ1^{pos} T cells. Ligands specifically recognized by the Vδ1^{pos} TCR remain unknown. Moreover, protumor functions of Vδ1^{pos} T cells have been described trough the release of IL-17.*

In conclusion, our knowledge on the biology of tumor-associated γδT cells is progressively improving thanks to recent works that gave new insights on their interaction with tumor and other immune cells, underlining both the antitumor and protumor properties of γδT cells and the role of specific γδT cell subsets to cancer progression. All these evidences underline the great potential of γδT cells in cancer-immunotherapy, which will be discussed in the next paragraph.

1.2.5 Immunotherapeutic application of γδ T lymphocytes

The main goal of immunotherapy is to achieve durable and efficient antitumor responses using immune cells capable of releasing antitumor cytokines and successfully kill tumor targets. These properties are all intrinsic features of γδT cells that have a great potentiality for cancer immunotherapy.[124]

Currently strategies adopted for the manipulation of γδT cells involve both $V\delta1^{pos}$ and $V\delta2^{pos}$ T cell subsets. In case of $V\delta1^{pos}$ T lymphocytes, they include isolation and *in vitro* expansion from peripheral blood using a recently published approach known as Delta One T (DOT) protocol.[125] This strategy is based on TCR and cytokine-dependent stimulations and allows to obtain, after three weeks, NCR^{pos} $V\delta1^{pos}$ T cells endowed with high cytotoxic activity against both hematological malignancies and solid tumors.

On the other hand, Vδ2-based approaches rely on their *in vitro* or *in vivo* activation using chemical compounds that induce or resemble the expression of PAgs. (**Figure 1.14**). PAgs are intermediates of the mevalonate pathway, which is upregulated on tumor cells causing the accumulation of PAgs and consequent activation of $V\delta2^{pos}$ T cells.[74] For this reason, Vγ9Vδ2 T cells should efficiently and specifically target and kill cancer cells. In addition, it is possible to easily increase the levels of PAgs by the therapeutic administration of aminobiphosphonates (NBPs), including zoledronate or pamidronate. For this instance, zoledronate, by interfering with the mevalonate pathway, causes the increase of intracellular IPP, which is then presented on the surface of tumor cells and specifically recognized by the Vγ9Vδ2-TCR[126] (**Figure 1.14**). Another approach involves the generation of engineered γδT cells, known as TEGs that consist in the transfer of particular and high-affinity Vγ9Vδ2 TCRs gene into αβT cells.[127] These hybrid T cells are currently being tested in a phase I clinical trial in patients with hematological malignancies (Netherlands Trial Register. Trial NL6357).

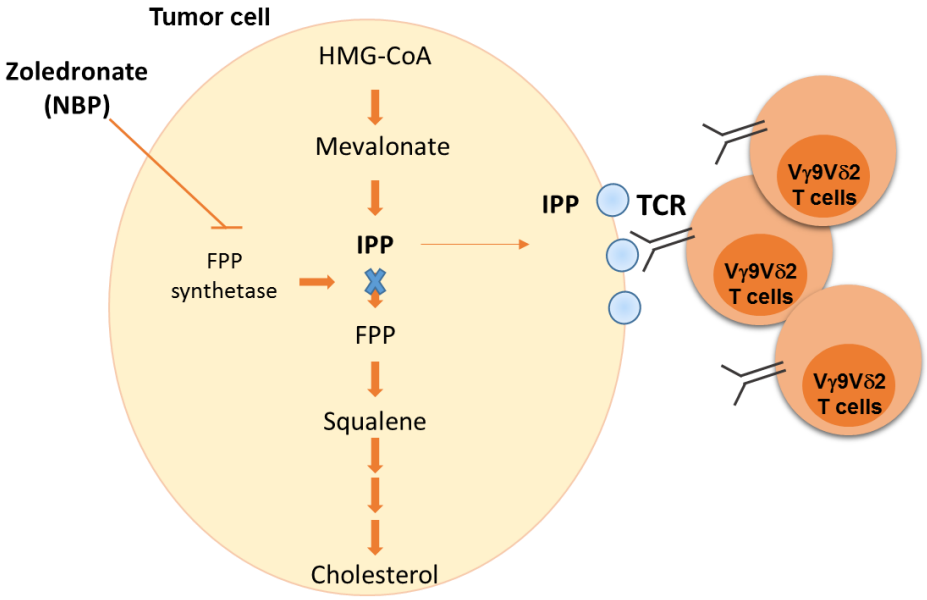

Figure 1.14. Vγ9Vδ2 T cells expansion by aminobiphosphonates (NBPs). *Isopentenyl pyrophosphate (IPP) is an intermediate metabolite of the mevalonate/cholesterol pathway that is exacerbated in tumor cells. NBPs administration by blocking the pyrophosphate (FPP) synthetase cause the accumulation of intracellular IPP levels. Endogenous IPP is then presented on the cell surface and recognized by the Vγ9Vδ2-TCR.*

To date, γδT cells have been tested in different clinical trials regarding both solid tumors, such as renal cell carcinoma (RCC)[128] and advanced lung cancer[129], and hematological malignancies, including multiple myeloma (MM) and acute myeloid leukemia (AML)[130]. All of them relied on the expansion of polyclonal Vγ9Vδ2 T cells, by either *in vitro* or *in vivo* stimulations and were based on the TCR-dependent recognition by Vγ9Vδ2 T cells of PAgs (**Table 1.2**). Interestingly, a complete remission of a patient affected by metastatic renal cell carcinoma has been reported, after 6 monthly cycles of peripheral autologous γδT injections, pre-activated and expanded *in vitro* with low dose of HMBPP and IL-2, combined with the infusion of zoledronate.[112] This response was specifically associated with a strong increase production of INF-γ by Vγ9Vδ2 T cells after the adoptive transfer. Even if clinical studies performed so far certainly proved the safety of using γδT cells in cancer immunotherapy, they also showed highly variable responses. This scarce efficacy can be explained by both quantitative and qualitative limitations of Vγ9Vδ2 T cells. Indeed, this subset is highly sensitive to activation-induced cell death and exhaustion deriving from chronic stimulation and precluding the full efficacy of this approach. To overcome this issue, new experimental approaches have been taken into consideration. For example, the use of checkpoint inhibitors against PD-1 or CTLA4, can overcome immune

suppression and exhaustion. For instance, the higher frequency of Vδ2^{pos} T cells in melanoma patients upon treatment with anti-CTLA4 mAb (ipilimumab) is associated with prolonged overall survival.[131] Combination approaches could also improve the functionality of autologous Vγ9Vδ2 T cells, as demonstrated by the potent antitumor activity of Vγ9Vδ2 T cells against chronic lymphocytic leukemia (CLL) cells obtained after coculture with monocyte-derived dendritic cells (moDC) together with ibrutinib administration.[132] This latter is a tyrosine kinase inhibitor approved for the therapy of CLL that has a direct effect on Vγ9Vδ2 T cells by promoting the production of IFN-γ. In addition, the production of bispecific Abs is under investigation in order to ameliorate Vγ9Vδ2 T cell cytotoxicity and specific targeting of the tumor as in the case of a nanobody-based construct recognizing both Vγ9Vδ2 T cells and the EGFR.[133] This bispecific Ab was tested in a xenograft model of CRC where it was found to induce high cytolytic capacity on Vγ9Vδ2-T cells with efficient killing of cancer cells. Lastly, the use of chimeric antigen receptors (CARs) represents another valid strategy in γδT cell-based immunotherapy since they combine the avid antigen recognition of Abs with TCR signaling, as shown for example with anti-CD19 specific CAR.[134]

Table 1.2. Clinical trials using γδ T cell-based cancer immunotherapies*. CBR=Clinical Benefit Rate= (complete response+ partial response+ stable disease)/n. of evaluable patients. Adapted from Godfrey DI et al. Immunity Review, 2018*

Cell type	Disease	Cell source	N. of patients	Phase of clinical trial	Outcome CBR (%)	References
Vγ9Vδ2 T	Prostate cancer	PBMC	18	I	73	*Dieli et al. (2007)*
Vγ9Vδ2 T	Renal cell carcinoma	*In vivo* expansion	10	I	100	*Bennouna et al. (2008)*
γδT	Lung carcinoma	PBMC	10	I	38	*Nakajima et al. (2010)*
Vγ9Vδ2 T	Lung carcinoma	PBMC	15	I	50	*Sakamoto et al. (2011)*
γδT	Renal cell carcinoma	PBMC	11	I/II	55	*Lang et al. (2011)*
αβT, γδT, NK	Renal cancer, MM, AML	*In vivo* expansion	21	I/II	40	*Kunzman et al. (2012)*
Vγ9Vδ2 T	CRC	PBMC	6	I	100	*Izumi et al. (2013)*
γδT	Lung carcinoma	PBMC	15	I	50	*Kakimi et al. (2014)*

The therapeutic efficacy of γδT cells against human tumors is still undervalued and so far constrained to autologous settings. However, the use of γδT cells is particularly relevant for allogenic strategies, giving their MHC-unrestriction that largely abolishes graft versus host reactivity. Identification of new molecules directing γδT cell functions in the tumor microenvironment and of other ligands binding the γδTCR or other NKRs is necessary to take advantage of the pan-cancer antitumor potential of γδT cell-based cancer immunotherapy.

Liver immune-biology

The liver constitutes the largest tissue of our body and is characterized by unique physiology and functions. By receiving blood supply from both the hepatic artery and the portal vein, the liver organ constantly drains fluids from the gut. For this reason, it is continuously exposed to potentially harmful bacterial products and Ags as well as non-pathogenic stimuli, including for example, food-derived and self-Ags, which have to be finely tolerated.[135]

External insults such as drugs or toxins, and viral infections can break liver immune-tolerance and result in acute liver disease. If the insult is not removed and persists in time, the outcome is a chronic liver condition characterized by fibrosis, at first, and the development of cirrhosis and/or hepatocellular carcinoma (HCC) in the ultimate stages. Infections by hepatitis C virus (HCV) and hepatitis B virus (HBV) represent the main causes of chronic liver disease. Other pathological conditions, associated with liver inflammation and fibrosis, include alcoholic liver disease and autoimmune disorders, as primary biliary cholangitis (PBC).[136]

It is widely recognized that specialized immune cell populations reside in the liver tissue providing local immunosurveillance. For instance, liver sinusoids, are enriched of sentinels and antigen presenting cells (including liver sinusoidal endothelial cells, Kupffer cells, and hepatic stellate cells), which are important for the initiation and recruitment of immune responses. In general, activation of the intrahepatic immune system can play a dual role contributing to both host defence, as well as to liver inflammation and chronic disease.

The protective nature of intrahepatic immune responses is evident during viral hepatitis, in which the spontaneous control of HCV replication is linked with the activation of intrahepatic cellular immunity. Whereas high production of IFN-γ and TNF-α can contribute to the inhibition of HBV replication and results in HBV-clearance in the majority of cases.

In humans, the most relevant lymphocyte populations resident in the liver, include NK cells, αβ and γδ T cells, whose role will be discussed in the next paragraph.

1.3.1 Liver-associated γδ T lymphocytes

Liver γδT cells are particularly abundant in the liver tissue, especially if compared to peripheral blood.[39] Among intrahepatic γδT cells, Vδ1^{pos} T cells represent the predominant cell subset, while Vδ2^{pos} and Vδ3^{pos} are found at lower amount.[39]

Considering the high proportion of liver-resident γδT lymphocytes, which count up to 20% of total T cells[39], understating their contribution to liver physiopathology is extremely relevant. During chronic HCV infection an increased liver-infiltration of γδT cells was found in patients.[137] *Agrati* and colleagues observed a specific increase of Vδ1^{pos} γδT cells in HCV-infected liver, reaching up to 9% of CD3^{pos} lymphocytes.[138] Moreover, Vδ2^{pos} T cells were able to control HCV replication *in vitro*, through the secretion of IFN-γ.[138] Studies in mice suggest the contribution of γδT cells to liver inflammation. For example, in the presence of adenovirus infection, IL-17 secretion by γδT cells was associated with increased liver injury as well as with the recruitment of cytotoxic T cells.[139] However, analogous subpopulations of Th17-like γδT cells have not been yet identified in humans. A decreased intratumoral infiltration of γδT cells has been observed in HCC patients.[140] In this setting, the lower antitumor capacity of γδT cells was attributed to the immunosuppressive microenvironment, associated with Tregs infiltration. Differently, in a mouse model of CRC, Vδ1^{pos} T cells displayed important anti-metastatic effector functions.[123] In another study, the production of IL-17 by γδT cells favored the accumulation MDSCs in human CRC tissue specimen, thus contributing to tumor progression.[113]

Finally, recent TCR-sequencing analysis revealed the existence of liver-resident Vδ1^{pos} T cell subpopulation with unique clonal diversity.[141] This study revealed that liver-resident Vδ1^{pos} T cells are mainly T_{EMRA} and T_{EM}. However, only T_{EM} Vδ1^{pos} cells constitute the actual liver-resident subset as same clones of T_{EMRA} subset were identified in the blood, suggesting the recirculation of Vδ1^{pos} T_{EMRA} subpopulation between liver tissue and blood.[141] Further studies are needed to clarify the functional role of recirculating Vδ1^{pos} T_{EMRA} in both physiological and pathological conditions

2. Aim and rationale

The liver is the most common metastatic site in colon-rectal cancer (CRC) patients. In fact, more than 50% of patients with primary CRC develop liver metastasis (CLM) within one or two years after the primary tumor diagnosis. Up to date surgical resection of CLM is the only option for potential cure, and even when combined with chemotherapy, it is curative in only 20% of cases. Thus, there is crucial need of finding novel prognostic markers and effective therapeutic approaches.

Gamma-delta (γδ) T cells are innate-like lymphocytes with an important role in cancer immunosurveillance. Given to their broad array of antitumor functions, including potent cytotoxicity and cytokines production, they can limit cancer progression. Based on the TCR-δ chain expression, two main subsets of human γδT cells are distinguished, $V\delta1^{pos}$ and $V\delta2^{pos}$, which preferentially localize in mucosa/epithelial tissues and peripheral blood (PB) respectively. Functional and tissue-distribution diversity of $V\delta1^{pos}$ and $V\delta2^{pos}$ T cells reflect their distinctive TCR features, as recently demonstrated by transcriptomic and T cell receptor (TCR)-repertoire sequencing analysis. In particular, $V\delta2^{pos}$ T cells are characterized by less clone heterogeneity and more innate-like properties, while $V\delta1^{pos}$ T cell subsets consist mainly of adaptive and private TCR repertoire with the ability to undergo clonal/oligoclonal expansion. In the human liver tissue γδT cells represent up to 20% of total T lymphocytes. Nevertheless, their specific behavior during metastatic spreading remains largely unexplored. Therefore, a comprehensive phenotypical characterization of the specific subsets of human $V\delta1^{pos}$ and $V\delta2^{pos}$ T cells will help to elucidate their impact on CRC progression and possibly clarify their immunotherapeutic potential.

To this aim, we studied the frequency, maturation and activation status as well as the effector functions of human $V\delta1^{pos}$ and $V\delta2^{pos}$ T cell subsets in patients with CLM. In collaboration with The Liver Surgery Unit of Humanitas Research Hospital (HRH), Milan, Italy, we obtained biological specimens from the PB, tumor-free and intratumor tissue compartments of CLM patients. By high dimensional flow cytometry analysis, we were able to deeply characterize, at a single cell level, the exclusive phenotypic signatures of both PB and liver tissue-associated/resident γδT cell subpopulations linked to the CLM pathological condition. Finally, our experimental findings were correlated to the clinical outcome of CLM patients with a particular focus on their prognosis and therapy.

3

Material and Methods

3.1 Ethic statement

Research use of clinical samples was in accordance with the Declaration of Helsinki. The Institutional Review Board (IRB) of Humanitas Research Hospital (HRH), Rozzano, Milan, Italy, approved all clinical and experimental procedures (Approval N.168/18). Each patient signed a consent form approved by the above IRB, which clarifies that the donation of specimens for this research project did not affect in any way the diagnosis, the therapies and the prognosis of the disease.

3.2 Clinical features of patients

We recruited patients undergoing surgical resection for colon-derived liver metastases (CLM) at the Hepatobiliary Surgery Unit of HRH in Milan, from 2014 to 2019. From each patient we collected fresh peripheral blood, tumor-free (from 0.2 to 1 cm far from the tumor lesion) and intratumor tissues. In total, 97 CLM patients were analyzed and followed post-surgery for the occurrence of relevant clinical outcomes such as recurrence of metastasis and overall survival. The vast majority of patients was represented by elderly (mean age of 64 years old) males (58%) with advanced TNM staging of the primary CRC (positive N status in 76% of cases). The number of CLM was highly variable, ranging from 1 to 30 metastatic foci with a median number of 4 concomitant lesions, which in the 71% of cases appeared in less than 1 year from the primary colon surgery (early CLM). Before surgical resection of CLM, the majority (75%) of patients underwent neoadjuvant chemotherapy (CHT) that consisted in different number of chemotherapy cycles, ranging from 1 to 34. Due to the toxic effect of CHT, surgery was performed on the average of 6 weeks after the completion of the last CHT cycle. CHT administration included CHT-monotherapy (14% of cases) or combined with mAbs including anti-VEGF (41%) and/or anti-EGFR agents (19%).
All the main features of patients are reported in **Table 3.1.**

Table 3.1. Characteristics of CLM patients.

Feature	Variable	Patients (N=97)
Age - mean (range)		64 (30-83)
Sex – no. (%)	Male	54 (58)
	Female	39 (42)
N status of primary tumor - no. (%)	Negative	22 (24)
	Positive	68 (76)
K-RAS status - no. (%)	Wild type	40 (50)
	Mutated	40 (50)
Liver metastases - no. (%) (Median = 4; range: 1-30)	Early (<12 month)	67 (71)
	Late (>12 month)	29 (29)
Adjuvant CHT - no. (%) (Courses median = 8; range: 1-34)		73 (75)
	Monotherapy (FOLFOX/FOLFIRI)	36 (14)
	Ass. with anti-VEGF (Bevacixumab or Aflibercept)	39 (41)
	Ass. with anti-EGFR (Cetuximab or Panitumumab)	18 (19)
	No CHT	24 (25)
Recurrence – no. (%)		61 (63)
	Only liver	32 (33)
	Only lung	7 (7)
	Liver and lung	11 (11)
	Others	11 (11)

3.3 Blood absolute count

Absolute cell count was performed on 100 µL of freshly collected and undiluted blood samples that were stained with anti-human mAbs from BioLegend (San Diego, CA, USA): CD3 (SK7; BV605) and CD45 (H130; AF700), from Beckman Coulter (Brea, CA, USA) Vδ2 (IMMU-389; FITC). Then, 1.0 ml of *BD FACS*™ lysing solution (BD Bioscience, New Jersey, NJ, USA) was added and after 10 min of incubation, a fixed volume of 25 µl of *CountBright*™ Absolute Counting Beads (Invitrogen, Carlsbad, California, USA) was added to the sample prior to evaluation using *FACS Symphony*™ flow cytometer (BD Bioscience). By flow cytometry analysis we assessed the number of $V\delta1^{pos}$, $V\delta2^{pos}$ and $CD3^{pos}$ T cells per µL of blood.

3.4 Isolation of peripheral blood mononuclear cells (PBMCs)

Blood samples were obtained from CLM patients (N= 76), prior to surgical resection of CLM and healthy volunteers (N=55). PBMCs were isolated by using *Lympholyte*® Cell Separation density gradient solution (Cederlane Laboratories, Burlington, Canada). Briefly, 10 to 15 mL of fresh blood were first diluted in a 1:1 ratio with sodium chloride physiological solution. Diluted blood was added to the *Lympholyte*® solution in a volume ratio of 1:3 and centrifuged for 30 minutes at 400 rcf at room temperature (RT) without brake. The interphase ring containing mononuclear cells was collected, washed with Hank's Balanced Salt Solution without calcium and magnesium (HBSS-/-) (Lonza, Basel, Switzerland Basel, Switzerland) and centrifuged two times for 10 minutes at 200 rcf in order to remove platelets cells. After isolation, PBMCs were frozen in cryovials (Globe Scientific INC., Paramus New Jersey, USA) in a final volume of 1mL of Fetal Bovine Serum (FBS) (Lonza) with 10% of cryoprotective Dimethyl Sulfoxide (DMSO) (Sigma Aldrich, St. Louis, Missouri, USA). All flow cytometry experiments were then performed in batch on frozen samples to minimize technical variability.

3.5 *Ex-vivo* isolation of human lymphocytes from tumor-free and intratumor tissues

Human tumor-free and intratumor tissue samples were obtained from patients affected by liver metastatic disease from primary CRC who underwent a surgical resection of CLM by the Hepatobiliary Surgery Unit at HRH. Tissue samples were conserved in Roswell Park Memorial Institute (RPMI)-1640 medium supplemented with 10% FBS, 1% UltraGlutamine (Lonza, Basel, Switzerland), 2% Hydroxyethylpiperazine-Ethanesulfonic Acid (HEPES) buffer 1M (Lonza), 1% Penicillin-Streptomycin-Amphotericin (Lonza), 0.1% geneticin (Sigma-Aldrich), until use. After removal of sutures and occasional adipose tissue, samples were weighted and cut in smaller pieces of 2-3 mm to favour the digestion. Tissue dissociation was obtained by mechanical dissection using *gentleMACS*™ Dissociator (Miltenyi, Bergisch Gladbach, Germany) and enzymatic digestion with 2 mg/mL of collagenase D (Roche Diagnostic; Indianapolis, IN, USA) in HEPES buffer for 45 minutes at 37°C/5% CO_2 under rotation. 5ml of enzymatic solution were used for each gram of tissue and up to 2g were placed in *GentleMACS*™ C-Tubes (Miltenyi). After enzymatic incubation, obtained cells were filtered using 100 μm and 70 μm cell strainers, washed in HBSS-/- and lymphocytes were separated using 30% and 70% Percoll gradient. After isolation, lymphocytes from the tumor-free and intratumor compartments were counted and preserved with the same procedure described for PBMCs.

3.6 High-dimensional flow cytometry analysis

3.6.1 Technical principles

Flow cytometry is a widely used technology for the analysis of surface markers expression and intracellular molecules at a single cell level allowing the characterization of different subpopulations within a heterogeneous group of cells.

The staining protocol is based on the incubation of a single-cell-suspension with specific fluorescent probes or fluorochrome-conjugated monoclonal antibodies (mAbs) followed by the acquisition at the flow cytometer. During the acquisition, cells are excited by different laser beams to investigate the size (Forward-scatter, FSC), the intracellular-complexity of the cell (Side-scatter, SSC) and the fluorescence emitted by fluorescent molecules and/or mAbs used.

Nowadays, many fluorochromes are available, each of them characterized by specific wavelengths of excitation and emission, thus allowing the combination of several mAbs labelled with different fluorochromes for the simultaneous detection of a large spectrum of molecules.

For an accurate flow cytometer analysis, cells have to pass uniformly through the bright centre of the focused laser beams and be excited by the same amount of laser-light. Thanks to the fluidic part of the cytometer cells are hydrodynamically focused through a small nozzle to cross one by one through the laser beams (**Figure 3.1**). Then, the optical system of the cytometer, which includes the lasers that illuminate the particles and optical filters, will split the forward and side scattered light and all fluorescences from stained cells into defined wavelengths. The various filters will direct photons of the correct wavelength to each detector, limiting the range of wavelength measured by a specific detector. However, spectral overlap can occur when two or more fluorochromes emitting at similar wavelength are used causing that the light emitted from one fluorochrome is collected also by a detector optimized for a different fluorochrome. This phenomenon is called *spillover* and can be corrected by using compensation approaches (detailed in paragraph 3.6.3).

Finally, the electronic part of the cytometer includes the detectors that convert the fluorescence into proportional electrical pulses and are divided into: i) photomultiplier tubes (PMTs), usually used to detect the SSC and the signals generated by all fluorescence channels; ii) photodiodes, less sensitive to light signals compared to PMTs and appropriate for the detection of the FSC signal; iii) software for the conversion of voltage pulses into digitized values, visualized on a computer.

For this project all data were acquired on a *FACSymphony*™ (BD Biosciences) flow cytometer that is equipped with five lasers (blue, red, violet, ultraviolet and yellow-green) and allows the simultaneous measurement of up to 28 different parameters on a single cell.

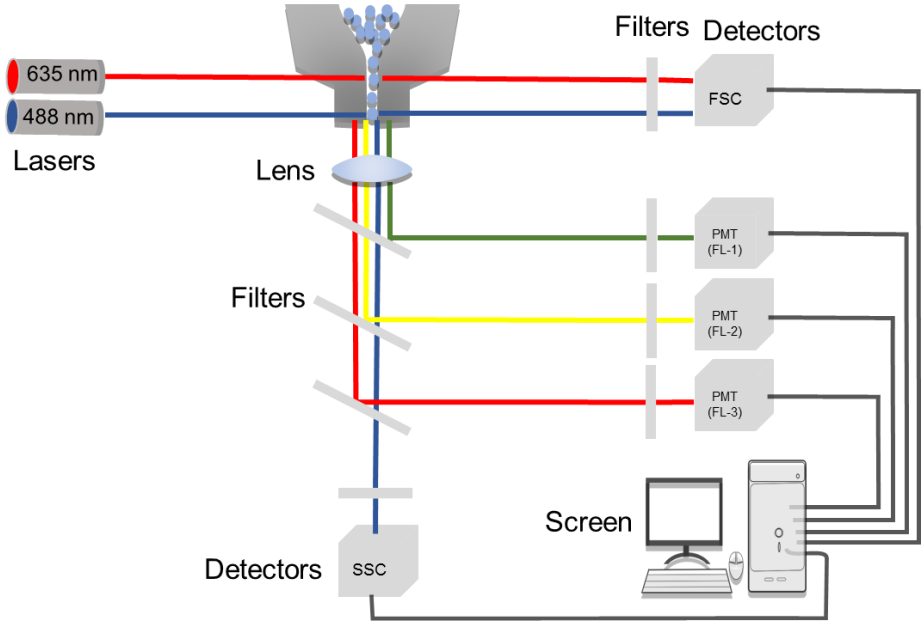

Figure 3.1. Schematic representation of the components in a flow cytometry system. *A flow cytometer is composed by three main systems: fluidics, optics, and electronics. The fluidics system is necessary to transport particles in a stream to the laser beam for interrogation while the optic system includes the lasers that illuminate the particles and optical filters that direct the resulting light signals to detectors (photomultipliers) where the signal is converted into proportional electronic input by the electronics system.*

3.6.2 Polychromatic Flow Cytometry staining

Polychromatic Flow Cytometry (PFC) panels were developed both for phenotypical (extracellular staining) and functional analysis (extracellular and intracellular staining) of γδ T cells in CLM patients and healthy donors (**Table 3.2**). All stainings were performed in dark in order to preserve fluorochromes stability. For the identification and phenotypical characterization of γδT lymphocytes, we included Abs against specific lineage marker (CD3, CD45, Vδ1 and Vδ2 TCR) and extracellular molecules (CD45RA, CD27, CD28, CCR7, CD57, CD8, CD16, CD56, CD69, CD161, PD-1, CTLA4, NKG2A, NKG2D, CXCR3, and CD86). Whereas, the functional evaluation was assessed by the expression of lysosomal-associated membrane protein 1 (LAMP-1), also known as CD107a (BD Biosciences) conjugated with PE for the study of γδT cells cytotoxicity, as described in Paragraph 3.7, and of intracellular cytokines TNF-α (Mab11; BV786), IFN-γ (B27; PE-Cy7) and IL-17 (BL168, BV570) according to the procedure described in paragraph 3.8.

The mAbs used in our panel were purchased from the following companies: BioLegend (St. Diego, California, USA), BD Biosciences (San Jose, California, USA), eBioscence (St. Diego, California, USA), and Miltenyi (Bergisch Gladbach, Germany).

Additionally, to design our PFC panel, Abs titrations, optimal combination between antigen and fluorochrome, spectral overlapping and grade of compensation between channels (further described in 3.6.3 and 3.6.4), have all been carefully considered.

Table 3.2. List of mAbs used for multiparameter flow cytometry analysis. *In the list are indicated all Abs used in the panel, conjugated-fluorochrome, clone, company and type of staining (extracellular/intracellular).*

Marker	Fluorochrome	Clone	Company	Staining
NKG2A	VioBright-FITC	REA110	Miltenyi	Extracellular
CD27	APC eFluor780	0323	eBioscience	Extracellular
CCR7	AF700	150503	BD	Extracellular
CXCR3	APC	1C6	BD	Extracellular
NKG2D	BV780	1D11	BD	Extracellular
PD-1	BV711	EH12.1	BD	Extracellular
CD86	BV650	2331 (FUN-1)	BD	Extracellular
CD69	BV605	FN50	BioLegend	Extracellular
CD161	BV421	HP-3G10	BioLegend	Extracellular
CD8	BUV805	SK1	BD	Extracellular
CD45RA	BUV737	HI100	BD	Extracellular
CD3	BUV661	UCHT1	BD	Extracellular
CD56	BUV563	NCAM16.2	BD	Extracellular
CD16	BUV496	348	BD	Extracellular
Vδ2	BUV395	B6	BD	Extracellular
CD28	PE-CY7	CD28.2	BioLegend	Extracellular
CD152/CTLA4	PC5	BNI3	BD	Extracellular
CD57	PE-Vio615	REA769	Miltenyi	Extracellular
Vδ1	PE	REA173	Miltenyi	Extracellular
CD107	PE	H4A3	BD	Extracellular
IFN-γ	PE-Cy7	B27	BD	Intracellular
TNF-α	BV786	MAb11	BioLegend	Intracellular
IL-17	BV570	BL168	BioLegend	Intracellular

3.6.2.1 Extracellular staining

Frozen PBMCs, tumor-free and intratumor lymphocytes were thawed in medium (RPMI-1640 supplemented with 10% FBS, 1% penicillin-streptomycin and 1% UltraGlutamine) and washed in HBSS-/-.

After pelleting cells by centrifugation for 5 min at 400 rcf, they were immediately stained for live/dead discrimination with *Zombie Aqua*™ fixable viability kit (Invitrogen, Carlsbad, California, USA), in a final volume of 100 µl for 15 min at RT, for a maximum of 10 x 10^6 cells. The Aqua mix was freshly prepared diluting: 0.5 µl of the *Zombie Aqua*™ Fixable viability kit (Invitrogen) with 19.5 µl of sterile water and 380 µl of HBSS -/-.

The *Zombie Aqua*™ is a fluorescent reactive dye that permeates into cells with compromised membranes (i.e. dead or necrotic cells) and reacts with amines located intracellularly in death cells, resulting in a bright positive fluorescent signal. On the contrary, in viable cells having intact cell membrane *Zombie Aqua*™ dye only reacts with cell-surface amines, resulting in a dim fluorescence signal. Hence, the use of the *Zombie Aqua*™ kit allows the identification of dead cells and their consequent exclusion from the analysis, avoiding unspecific binding and false positive events possibly due to dead cells auto-fluorescence.

At the end of incubation, cells were washed with 1 ml of FACS Buffer (HBSS -/- with 2% FBS) and centrifuged for 5 min, at 400 rcf. Then, pelleted cells were incubated with the appropriate combination of anti-human mAbs chosen for the extracellular staining, for 20 min at RT, prepared in FACS Buffer, in a final volume of 100 µL (for a maximum of 10 x 10^6 cells). Finally, cells were washed with 1 ml of FACS Buffer and fixed in 1% paraformaldehyde (PFA; Santa Cruz Biotechnology, Dallas, TX, USA).

3.6.2.2 Intracellular staining

Intracellular staining was done using *Cytofix/Cytoperm*™ and *Perm/Wash*™ kits (BD Biosciences) according to the manufacturer's instructions. After the extracellular mix incubation, cells were washed with 1 mL of FACS Buffer and centrifuged for 5 min, at 400 rcf. Pelleted cells were resuspended in 150 µl of *Cytofix/Cytoperm*™ (BD Bioscences) and incubated for 30 minutes at 4°C. *Cytofix/Cytoperm*™ simultaneously fixes and permeabilizes cells, allowing the following intracellular staining.

At the end of incubation, cells were washed with 1 mL of saponin-containing *Perm/Wash*™ Buffer 1X (BD Bioscence) and centrifuged for 5 min, at 450 rcf. The use of *Perm/Wash*™ Buffer (BD Bioscence) is particularly important since saponin-mediated cell permeabilization is a reversible process, thus cells need to be kept in solution with saponin during all the successive passages of the intracellular staining.

Pelleted cells were incubated for 30 minutes at 4°C with the *Perm/Wash*™ Buffer (BD Bioscence) containing the mix of antibodies chosen for the intracellular staining, in a final volume of 100 µL (for a maximum of 10 x 10^6 cells).

Finally, samples were washed with 1 mL of *Perm/Wash*™ Buffer (BD Bioscence), centrifuged for 5 min, at 450 rcf and resuspended in an appropriate volume (100-150 µl) of *Perm/Wash*™ Buffer (BD Bioscience) for the further acquisition at the flow cytometer.

3.6.3. Compensation

As already mentioned, when two or more fluorochromes are detected simultaneously, spectral overlap can occur, especially if they emit at similar wavelengths, causing what is known as spillover. Compensation allows to mathematically correct spillover. In order to obtain a proper compensation, every fluorochrome used during staining procedure should have a paired single-stained control. Additionally, the following precautions should be followed:

1. Single-stained control samples have to be at least as bright as the test staining, since dimmer controls will lead to overcompensated or undercompensated data.
2. Each compensation control must have a paired negative control of the same source, since autofluorescence can vary depending on the type of source (cells vs beads).
3. If the conjugate is a tandem, the same antibody-fluorochrome conjugate used during the staining has to be used for single stained controls. Indeed, fluorochrome:protein molar ratio can vary between different batches of reagents thus affecting compensation.

The higher is the number of parameters analyzed simultaneously in a polychromatic experiment the more compensation procedure is complex due to the higher amount of possible pair wise combinations between fluorochromes and the increased chance of operator-driven mistake. To avoid manual compensation errors is harshly recommended to use Software-assisted compensation. For our experiments, all samples were compensated with *Comp-Beads*™ (BD Biosciences). These beads are conjugated with an antibody

specific for the Kappa light chain of Immunoglobulins (Ig), from mouse, rat, or rat/hamster. For probes like AQUA live/dead (Invitrogen) we used The ArC Amine Reactive Compensation Bead Kit (Molecular Probes Invitrogen, Eugene, Oregon, USA), that includes two types of specially modified polystyrene microspheres for the compensation of the LIVE/DEAD fixable stains: the ArC reactive beads which bind any of the amine-reactive dyes, and the ArC negative beads.

3.6.4 Antibody Titration

Manufactures' recommended concentration of the fluorochrome-conjugated mAb not always allow optimal detection of the antigen in a specific experimental setting. Therefore, to choose the right amount of reagent to use in a flow cytometry experiment, titration is necessary. During a titration experiment two parameters must be considered. The first one is separation between negative vs positive signal and the second one is the background due to unspecific binding of mAb. The correct titer should give the highest separation between negative and positive events and it can be calculated by dividing the median of fluorescence intensity (MFI) of positive and negative events. The optimal separation corresponds to the highest ratio. The background that results from unspecific binding is determined by considering the negative population. Usually a maximum of 10 x 10^6 cells in a final volume of 100μL are stained with the chosen titer of mAb.

The main aspects to consider when performing a titration experiment are antigen level of expression (bright or dim), type of cell population expressing the antigen (cell specific or ubiquitous) and dead cells exclusion to avoid unspecific binding and false positive events due to dead cells autofluorescence.

In this study mAb titrations were performed using cryopreserved PBMCs isolated from blood of healthy donors. After thawing, PBMCs were stained firstly with the probe AQUA live/dead (Invitrogen), to exclude dead cells contamination, and then marked with 2-fold serial dilutions of the mAb of interest (1:2 1:4, 1:8, etc.). An example of titration experiment is shown in **Figure 4.1**.

3.7 CD107a degranulation assay

CD107a, also known as LAMP-1 is a type I transmembrane glycoprotein usually located across lysosomal membranes which can be used as a degranulation marker for lymphocytes because it is exposed on the exterior membrane layer upon cellular exocytosis.

In order to test the cytotoxic activity of human *ex-vivo* isolated lymphocytes from blood, tumor-free and intratumor compartments, total cells were plated in a 96 well plate at a concentration of 2 x 10^6 cells/mL and incubated over-night (O/N) in RMPI-1640 complete supplemented with IL-15 (Peprotech, Rocky Hill, NJ, USA) 10 ng/ml. The day after, cells were stimulated with 10 ng/ml Phorbol-Myristate-Acetate (PMA) and 0.5 μg/ml Ionomycin (both from Sigma-Aldrich) and cell cytotoxic activity was assessed by CD107a flow cytometry-based assay using 8 μg/mL of PE-conjugated anti-CD107a Ab (H4A3; BD Biosciences). After 4 hours of incubation at 37°C with 5% CO_2 cells were collected, washed with HBSS and stained for extracellular markers as described above.

3.8 Cytokine detection by flow cytometry

Freshly isolated PBMCs and tumor-free and intratumor-derived lymphocytes were plated in U-bottom 96-well plates (2 x 10^6 cells/mL) in RPMI-1640 supplemented with IL-15 (Peprotech) 10 ng/mL. The day after, for intracellular IFN-γ, TNF-α and IL-17 accumulation cells were stimulated or not with PMA (0.5 μg/mL) and Ionomycin (0.1 μg/mL) (both from Sigma Aldrich) in the presence of 1μg/mL of Golgi Plug (BD Biosciences) for 4 hours. Intracellular staining was done using *Cytofix/Cytoperm*™ and *Perm/Wash*™ kits (BD Biosciences) as described (Paragraph 3.6.2.2) and using specific anti-human Abs (BD Biosciences) for TNF-α (Mab11; BV786), IFN-γ (B27; PE-Cy7) and IL-17 (BL168, BV570).

3.9 Hematoxylin and Eosin (H&E) staining

Formalin-fixed paraffin-embedded (FFPE) metastatic liver specimens, were sectioned with a microtome HM310 Microm (GMI, MN, USA) at 2-4 μm thickness and mounted onto charged glass slides Superfrost+ (Thermo Fisher Scientific). Then slides were stained for H&E using a standard protocol. Briefly, after two changes of xylenes, rehydration in an ethanol/water gradient (100%, 90%, 70%), followed by washing in water, slides were stained with in Mayer's Hematoxylin solution (Dako, CA; USA) for 18 min, differentiated under running tap water for 10 min, then stained with 1% aqueous solution of Y Eosin (Dako) for 8 min, followed by three washes with 100% ethanol, and three washes with xylenes. Lastly, H&E stained slides were mounted with Eukitt (Sigma Aldrich) and dried before acquisition on imaging Microscope BX51 (Olympus, Tokyo, Japan).

3.10 TCR-repertoire analysis

3.10.1 Cell sorting

PBMCs and tumor-free lymphocytes of CLM patients were stained with following mAbs: anti-CD45 (H130; AF700; BioLegend), anti-CD3 (SK7; BV650; BD Bioscience), anti-Vδ1 (REA173; PE; Miltenyi), anti-Vδ2 (IMMU 389; FITC; Beckman Coulter) and anti-CD69 (FN50; BV605; BioLegend). $CD69^{pos}$ and $CD69^{neg}$ $V\delta1^{pos}$ T cells from PB and total $V\delta1^{pos}$ T cells from tumor-free tissue were sorted on a FACSAria cell sorter (BD Biosciences).

3.10.2 TCR-sequencing

CDR3 regions of either the γ-chain or δ-chain were amplified from flow cytometry-sorted $CD69^{pos}$ and $CD69^{neg}$ $V\delta1^{pos}$ T cells from PB and total $V\delta1^{pos}$ T cells from tumor-free tissue of CLM patients, via a previously described mRNA-based multiplex PCR amplification method (**ref: PMID ID 28218745**). PCR amplicons were indexed with the Illumina Nextera Index Kit, purified with Agencourt AMPure beads, equally pooled with 96-samples and sequenced at the Illumina MiSeq platform (paired-end, 500 cycles, high-output) as recommended by Illumina guidelines, while 20% PhIX was used as a spike-in control. The obtained Fastq files of read1 were annotated with MiXCR software (**PMID: 25924071**) using default parameters and further analyzed with the R package TCR (**PMID: 26017500**) and VDJtools (**PMID: 26606115**). For TRD repertoires only $V\delta1^{pos}$ sequences were processed after MiXCR annotation.

3.11 Immunohistochemistry

Immunohistochemical analysis was performed on 5 mm-thick FFPE sections of metastatic liver specimen. Slides were heated for Ag retrieval in 10 mM sodium citrate (pH 6.0). After rinsing in distilled H_2O, inhibition of endogenous peroxidase was performed with 3% H_2O_2 for 5 min. After two washes in Tris-Buffered Saline (TBS) solution, slides were incubated with 10% human serum for 20 min to block unspecific staining. Following elimination of excess serum, sections were exposed to specific Abs against anti-human γδTCR (mouse monoclonal, BD Pharmingen) or anti-CD3 (mouse monoclonal, Dako) or isotype-matched controls at appropriate dilutions, overnight at 4° C. Then sections were washed in TBS and incubated with biotinylated anti-mouse antibody for 30 min at RT and treated with streptavidin-peroxidase (LSAB2 Kit, Dako).

Antigen detection was performed by using 3,3-diaminobenzidine (DAB chromogen) and counter-staining of nuclei was performed with hematoxylin. Images were obtained with optical microscopy (Olympus BX53). The immune-reactivity to $CD3^{pos}$ and $\gamma\delta TCR^{pos}$ T cell was evaluated in three different areas for each case of CLM: a) intra-tumor, b) invasive margin and c) tumor-free liver parenchyma. For each area (a,b,c), we determined the frequency of $CD3^{pos}$ and $\gamma\delta TCR^{pos}$ T cell in 10 consecutive 40x microscopic fields (HPF) after having pre-analytically evaluated the homogenous distribution of all immune reactive cells in all areas. The choice of the first field was arbitrarily. 10 HPF correspond circa to 1 cm^2 that is the size of the lesions sampled by surgeons for pathological analysis. Hence, the number of examined HPF fields covered approximately the entire sampled tumor area of the majority of CLM specimens. By manual count we determined the percentages of $\gamma\delta TCR^{pos}$ T among $CD3^{pos}$T cells.

3.12 Data analysis

3.12.1 Flow-Jo

Flow Cytometry Standard (FCS) 3.0 files, obtained from FACS Symphony flow cytometer, were analyzed using FlowJo software (TreeStar Inc, Ashland, Oregon, USA), versions 9.9.6 and 10.2.0. Flow cytometry data analysis based on t-stochastic neighbor embedding (t-SNE) algorithm were performed using FlowJo 9.6 software.

3.12.1.1 High-dimensional cytometry data

The analysis of high-dimensional cytometry data was performed by manual single gating strategy. After their generation, raw data were pre-processed using FlowJo software version 9.9.6. In particular, FCS file were firstly compensated by using single stained controls (*Paragraph 3.6.3*) and analyzed in order to remove debris, dead cells, doublets and other cell populations and identify $V\delta1^{pos}$ and $V\delta2^{pos}$ T cells. In addition to single gating, an unbiased computational approach was applied to combine all marker information at the same time and to assess cell similarity. This approach was based on t-SNE algorithm that enables the identification of novel cell subpopulation or biomarkers, which would be hardly detected by manual analysis.

3.12.1.2 Cluster visualization with t-SNE

Data from each sample, were randomly subsampled for Vδ1 or Vδ2 T cells and concatenated in a single matrix to perform the t-SNE algorithm. This algorithm is based on non-linear

dimensionality reduction analysis, which allows to visualize high-dimensional data into a two-dimensional scatter plot (t-SNE map), named t-SNE1 and t-SNE2. On the t-SNE map, cells that are phenotypically similar are located closely together, and correspond to different cellular cluster.

3.12.2 Statistical analysis

Statistical analysis was performed using GraphPad PRISM (version 7.0, La Jolla, California, USA) software. The significance of the data was assessed by parametric (Student's *t*-test) and non-parametric approaches such as the unpaired Mann-Whitney test, or the Wilcoxon matched-pair test. Results are represented as a mean ±Standard Deviation (SD). The number of experiments is specified in the Figure legends. For correlation analysis Pearson's coefficient was applied. Statistically significant P values were represented with GraphPad style and summarized with following number of asterisks (*): *P≤0.05; **P≤0.01; ***P≤0.001; ****P≤0.0001.

3.12.3 Survival analysis

Overall survival (OS) was examined from date of metastatic disease to date of death or last available follow-up. Recurrence Free survival (RFS) was examined from date of liver surgery to the diagnosis of recurrent metastatic disease in the liver or other organs. Kaplan-Meier survival curves were generated and compared using the log-rank test.

4

Results

4.1 Optimization of the high-dimensional flow cytometry panel for the analysis of γδ T cells

For the high-dimensional flow cytometry analysis of γδT cells in CLM patients, we designed a multiparameter flow cytometry panel in order to identify both Vδ1^{pos} and Vδ2^{pos} γδT cell subsets and analyze several markers known to be associated with the γδT cell immune-maturation, migration, regulatory activation and inhibition as well as antitumor response. Overall, the panel shown in Table 3.2 allowed the examination of 22 different markers/parameters. The gating strategy adopted for the identification of Vδ1^{pos} and Vδ2^{pos} γδT cell subsets is shown in **Figure 4.1**. First of all, we gated on single cell events by using a forward scatter-area (FSC-A) versus a forward scatter-height (FSC-H) plot in order to exclude from the analysis doublet events. Then, on *Zombie^{neg}* live cells we selected the lymphocytes population based on cell dimension (FSC) and intracellular complexity (SSC). Finally, the specific subsets of Vδ1^{pos} and Vδ2^{pos} γδ T cells were identified on total CD3^{pos} T cells. On each of the two γδ T cell subpopulations, phenotypical (CD45RA, CD27, CD28, CCR7, CD57, CD8, CD16, CD56, CD69, CD161, PD-1, CTLA4, NKG2A, NKG2D, CXCR3, CD86) and functional (CD107a, TNF-α, IFN-γ and IL-17) markers were analyzed.

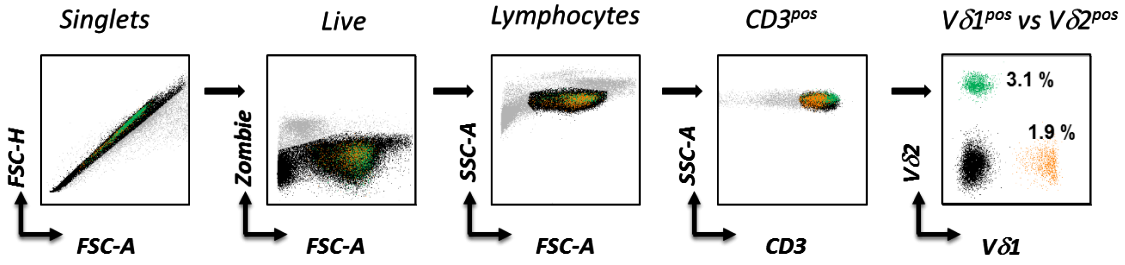

Figure 4.1. Gating strategy adopted for the identification of Vδ1^{pos} and Vδ2^{pos} T cell subsets in CLM patients. *Representative dot plots showing Vδ1^{pos} (orange dots) and Vδ2^{pos} (green dots) γδT cell subsets on peripheral blood mononuclear cells (PBMCs) of a healthy donor. The two cell subpopulations were identified among CD3^{pos} live lymphocytes after doublet events exclusion.*

Technical and analytical issues might be the consequence of spillover of fluorochromes and/or spreading, thus, we optimized the panel by choosing the most favorable combination between marker and fluorochrome, by antibody titration and by applying automatic compensation, as described in the *Material and Methods* section (**Paragraph 3.6.3 and 3.6.4**). According to the general level of expression of surface

markers included in the panel, we combined brightest fluorochromes with molecules of "dim" expression, such as CD57 or CD69, and less "bright" dye with highly represented receptors, such as CD8 or CD16 lineage markers. Every combination was first tested on peripheral blood mononuclear cells (PBMCs) of healthy donors or tissue samples of CLM patients, accordingly to the preferential distribution of the marker. For instance, the expression of CD57 receptor on peripheral blood (PB) lymphocytes resulted in lower background signal and high brightness when the anti-CD57 monoclonal antibody (mAb) was combined with the PE-Vio615 tandem dye rather than the BV605 (**Figure 4.2A**). Similar, better separation of CD69 positive signal on tissue-associated lymphocytes, was obtained when conjugated with BV605 fluorochrome rather than BV421 (**Figure 4.2B**). In order to validate the specificity of a certain mAb and to obtain the optimal concentration to be used in the panel, each fluorochrome-conjugated mAb was previously titrated on positive controls by using different mAb concentrations and unstained cells were used as the negative control. Representative examples of titration experiments are shown for the anti-Vδ1 and the anti-Vδ2 mAbs conjugated with PE and BUV395 fluorochromes respectively (**Figure 4.2C-D**). The titer with the highest median fluorescence index (MFI) ratio between positive and negative populations was chosen for the further validation of the panel.

Once the concentration of mAbs was optimized, we tested the panel on PBMCs of a healthy donor. In parallel, single-stained positive control beads and negative beads were acquired for the automatic calculation of the compensation matrix by *FlowJo* 10 software (**Table 4.1**). After examining the N-by-N view of plots (**Figure 4.3**), which shows all the possible combinations between acquisition channels, the compensation matrix was accurately applied to the sample to further proceed with the manual gating analysis. Only few combinations of parameters needed major compensation and mainly derived from the Brilliant Violet and Brilliant Ultraviolet lasers as in the case of BUV737 spillover into BUV805-derived signal.

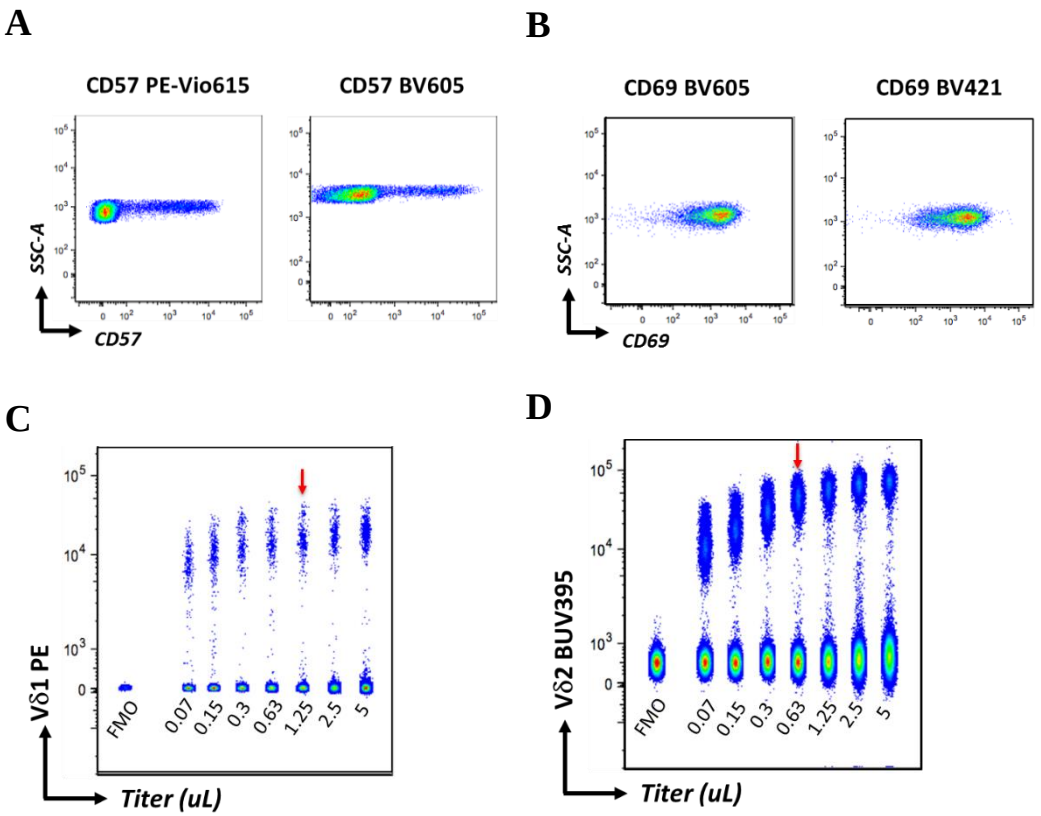

Titer anti-Vδ1 PE	MFI^{pos}/MFI^{neg}
5	545
2.5	903
1.25	1244
0.63	1138
0.3	1077
0.15	1154
0.07	1108

Titer anti-Vδ2 BUV395	MFI^{pos}/MFI^{neg}
5	131
2.5	155
1.25	161
0.63	142
0.3	105
0.15	63
0.07	35

Figure 4.2. Optimization of the high-dimensional flow-cytometry panel for the phenotypical analysis of γδ T cells in CLM patients. (A-B) *Flow cytometry plots showing the expression of CD57 (A) and CD69 (B) receptors on PB lymphocytes using different combinations of fluorochromes.* ***(C-D)*** *Data corresponding to different concentration of the anti-Vδ1 mAb in PE (C) and the anti-Vδ2 mAb in BUV395 (D) concatenated in a single file. Decreasing concentrations of Ab were used, starting from recommended titer (ranging from 5.00 µL to 0.07 µL in a total volume of 100 uL). The last plot represents the negative control, indicated as fluorescence minus one (FMO), and corresponding to unstained for the specific tested mAb cells. Red arrows correspond to the established titer. Under the graph, tables of the median fluorescence index (MFI) ratio between positive (MFI^{pos}) and negative (MFI^{pos}) events.*

Table 4.1. Compensation matrix of spillover values automatically calculated by FlowJo 10 software. *The color scale from white to yellow/orange is proportional to spillover values, with darker boxes corresponding to higher values.*

	FITC	APC	AF700	APC-H7	BV421	BV510	BV605	BV650	BV711	BV786	BUV395	BUV496	BUV563	BUV661	BUV737	BUV805	PE	PE-Vio615	PE-Cy5	PE-Cy7
FITC	100	0	0,0225	0	0,0238	2,3486	0,8643	0,1686	0,0745	0,0077	0,8669	3,1137	1,697	0,2334	0,032	0	0	0	0	0
APC	0,0005	100	67,7389	14,6476	0,0004	0,0066	0,0764	13,6985	3,8759	2,4412	0,1224	0,0203	0,0155	19,1573	2,9724	1,9692	0,0077	0,2399	46,9909	8,1118
AF700	0,0434	2,9289	100	21,8173	0	0,0384	0,0274	0,3189	6,838	5,367	0,2046	0,0435	0,0401	0,3035	3,6429	2,5967	0	0,0477	0,4228	7,2083
APC-H7	0,0134	11,9321	20,0697	100	0,01	0,0343	0,0356	1,4836	0,468	23,6635	0,0953	0,0262	0,0261	1,9164	1,5669	16,3262	0	0,0322	5,1071	50,0918
BV421	0,1286	0	0,108	0,0384	100	34,7647	4,5318	1,0017	0,7367	0,6173	0,6173	17,2706	3,0187	0,3853	0,1047	0,0769	0	0,0094	0	0
BV510	0,9406	0,4803	0,9446	0,0433	2,6081	100	49,4923	9,4478	3,5536	1,9733	5,2394	43,9002	28,3371	3,967	0,5459	0,3703	1,9431	0,3061	0,2816	0,1376
BV605	0,0002	0,0592	0,0495	0,0097	0,5704	0,2405	100	45,8216	18,5601	10,7184	0,0227	0,0727	8,5541	18,1089	2,9588	2,4055	12,5938	19,1274	16,7681	3,766
BV650	0,0141	10,5491	7,9388	1,6198	0,7688	0,4732	10,537	100	44,4683	19,0287	0,0814	0,1421	0,19	37,2945	5,6657	3,9667	0,0733	0,9661	11,29	2,2916
BV711	0,0129	3,2876	44,6153	11,6278	0,9746	0,4566	0,251	10,1371	100	74,6526	0,0646	0,139	0,0751	4,234	18,3542	17,4911	0,0004	0,0072	0,3303	2,4903
BV786	0,0352	0,2684	0,6387	2,5822	0,6637	0,5375	0,4354	0,5431	0,6606	100	1,5814	0,5706	0,4077	0,3634	1,9388	20,3119	0	0,0521	0	0,6134
BUV395	0,001	0,0031	0,0044	0	0,0101	0,0157	0,0132	0	0,0033	0	100	1,8915	0,3448	0,1135	0,0408	0,0678	0	0,0016	0	0
BUV496	4,0415	0,0081	0,0033	0,0185	0,0747	10,6542	3,4724	0,8349	0,3312	0,0946	78,7664	100	36,4095	5,4452	0,8134	0,7018	0,0123	0,0316	0	0
BUV563	2,0983	0,0068	0,0112	0	0,0123	0,0571	2,0246	0,4135	0,1688	0	21,9849	0,8608	100	13,874	1,5586	1,1418	21,1961	11,7742	4,9828	0,805
BUV661	0,0074	41,6164	31,2048	6,3496	0,0024	0,0107	0,0813	6,3451	2,5997	1,215	8,7666	0,2014	0,098	100	15,7072	10,6088	0,0113	0,2037	15,8305	3,1844
BUV737	0,021	0,767	72,3814	28,3958	0,0153	0,0936	0,0608	0,0966	4,3224	12,1481	20,303	0,5836	0,3101	2,3037	100	98,7199	0	0	0,0198	5,1469
BUV805	0,0073	0	0,0979	4,6066	0,0061	0,0158	0,0175	0	0,0002	6,4989	19,1211	0,4691	0,1955	0,0965	0,3439	100	0,0016	0,0142	0	1,0795
PE	1,2326	0,0071	0,0108	0	0,0014	0,011	12,6197	2,8741	1,1524	0,4026	0,0443	0,0115	24,713	2,7968	0,3087	0,209	100	46,6955	20,7769	3,2105
PE-Vio615	0,2258	0,0913	0,0627	0,0104	0,0022	0,015	20,6433	7,9582	2,9194	1,241	0,0663	0,0221	2,6828	8,1143	0,9766	0,6976	26,6287	100	58,7432	10,8078
PE-Cy5	0,0561	28,3778	18,67	4,2703	0,0056	0,0203	0,0947	10,9543	3,3891	1,7161	0,0613	0,0271	0,1368	10,6568	1,5091	0,921	0,9051	0,5101	100	20,615
PE-Cy7	0,0691	0,0307	0,4253	3,5112	0,0079	0,0326	0,0713	0,0242	0,0356	13,4855	0,1419	0,0228	0,1026	0,0362	0,4615	6,6092	0,6268	0,332	0,2569	100

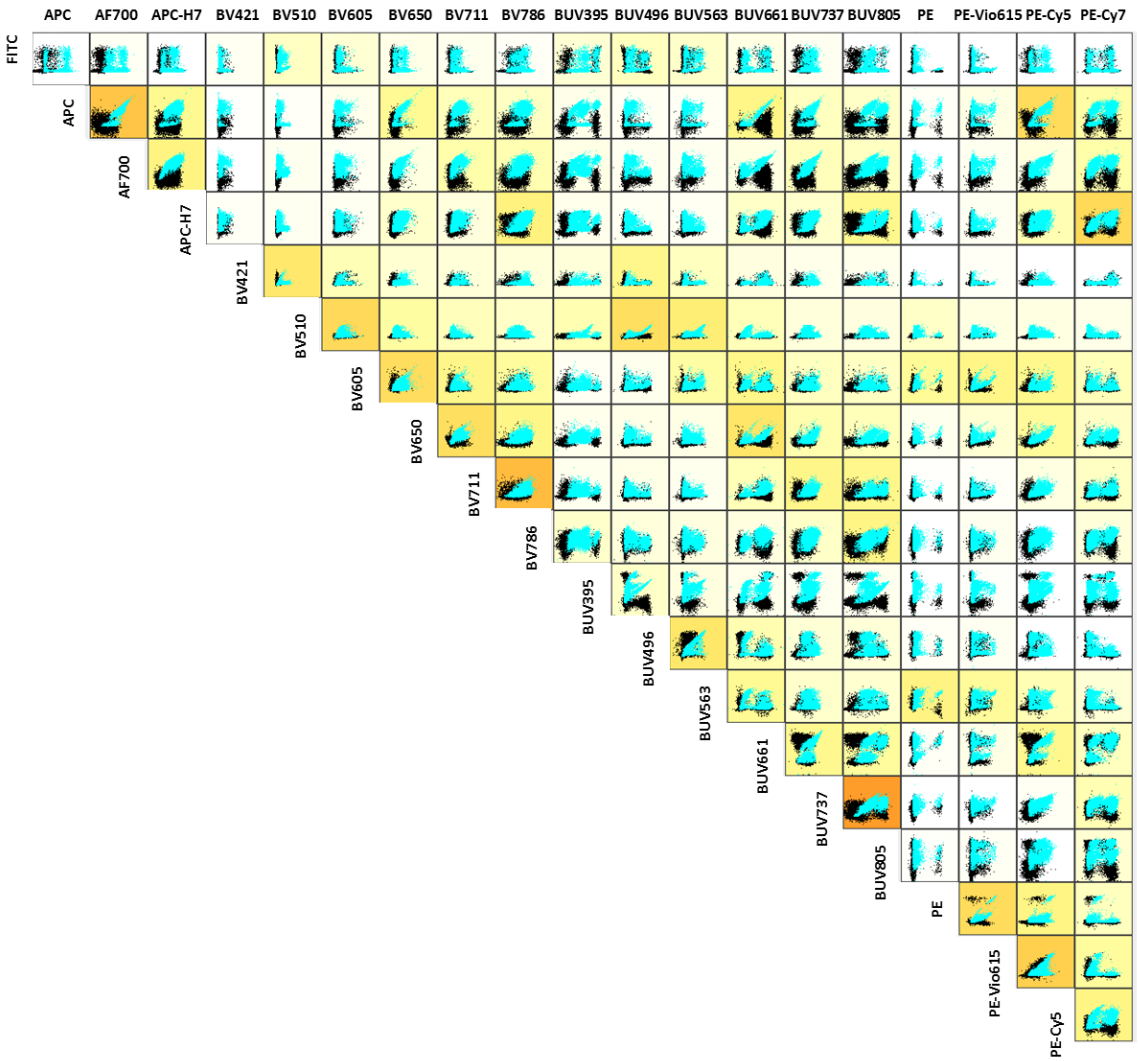

Figure 4.3. N by N view of the 22-parameter flow cytometry panel on PBMCs of a healthy donor. *N by N plots view showing every combination between acquisition channels on the lymphocyte population. Light blue events correspond to the uncompensated sample. Darker yellow/orange plots refer to the more compensated channels accordingly to the compensation matrix shown in Table 4.1.*

4.2 Phenotypical evaluation of γδ T cells in CLM patients

In collaboration with The Liver Surgery Unit of Humanitas Research Hospital (HRH), we recruited a cohort of 94 patients with late stage CRC, who developed CLM either before (early metastases) or after (late metastases) one year from the primary colon tumor surgery. On the day of hepatic operation, from each patient the peripheral blood (PB), the tumor-free tissue and the intratumor samples were collected (**Figure 4.4A**). Tumor-free tissues were located from few millimeters up to 1 cm distant from the tumor lesion and corresponded to a physiologically preserved liver parenchyma both in color and consistency, with no macroscopic evidence of metastatic disease as analyzed by the surgeons (**Figure 4.4B**). In the presence of multiple metastases, only one metastasis of the highest dimension was selected for the flow cytometry analysis. Lymphocytes from each of the three compartments, PB, tumor-free and intratumor tissues, were freshly isolated as described in the *Material and Methods* section (**Paragraph 3.4 and 3.5**) and stocked in liquid nitrogen for the further simultaneous study. Globally, we applied high-dimensional flow cytometry analysis for the comprehensive phenotypical characterization of γδ T cells on 76 PBMCs, 82 tumor-free and 40 intratumor tissue samples.

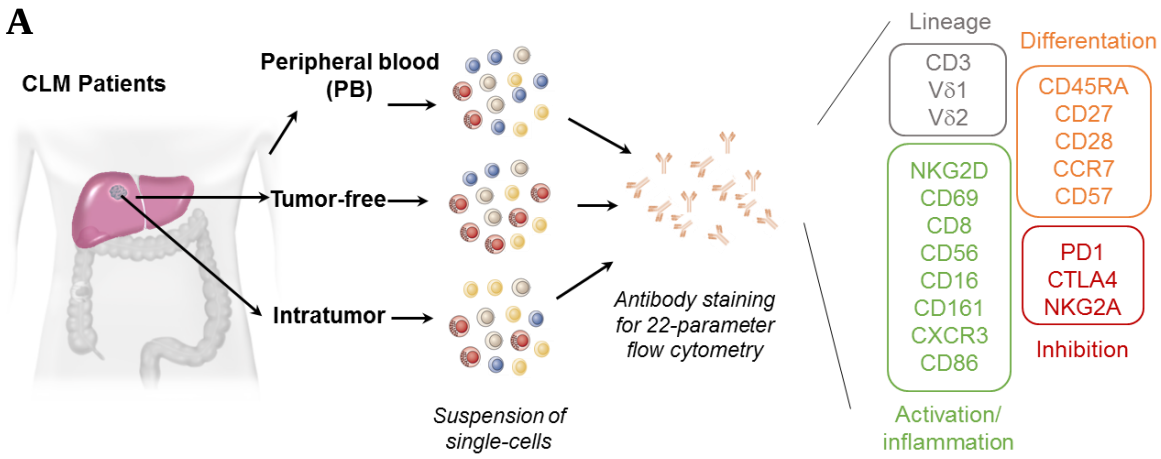

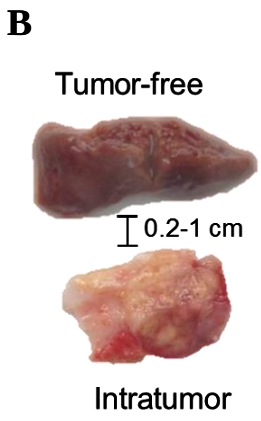

Figure 4.4. Scheme of the study design for the phenotypical investigation of γδ T cells in CLM patients. (A) *Experimental workflow. From each CLM patient we collected blood, tumor-free and intratumor tissue samples. Obtained single-cell suspensions were used for multiparameter flow cytometry analysis, which included several phenotypical markers indicated inside the colored boxes.* ***(B)*** *Picture of the tumor-free tissue (upper photograph) and the intratumor lesion (bottom photograph) after surgical removal.*

4.2.1 Study of the frequency and the differentiation status of γδ T cells in CLM patients

4.2.1.2 Analysis on peripheral blood (PB)

Firstly, we investigated the frequency and the absolute number of two major subsets, $V\delta1^{pos}$ and $V\delta2^{pos}$, of human γδT cells in the PB of both healthy donors and CLM patients. In physiological condition, as expected[65], $V\delta2^{pos}$ T cells constitute the predominant subpopulation of circulating γδT lymphocytes with the mean of 2.6% ±2.8 on total T lymphocytes. Instead, a lower percentage of $V\delta1^{pos}$ T cell counterpart that reached the average of 1.4% ±1.3 was observed (**Figure 4.5A**). Diversely, similar frequencies of $V\delta1^{pos}$ (3% ±3.7) and $V\delta2^{pos}$ (4.2% ±6.5) T cell subsets were found in CLM patients (**Figure 4.5A**). Indeed, a statistically significant increase in the frequency of $V\delta1^{pos}$ T cells was observed in CLM patients compared to healthy controls (**Figure 4.5A**). Whereas no variation was found in the frequency of PB $V\delta2^{pos}$ T cells between CLM patients and healthy individuals (**Figure 4.5A**).

Observed higher proportion of $V\delta1^{pos}$ T cells in the PB of CLM patients was not associated with increase in their absolute number (**Figure 4.5B**). Indeed, the absolute count of $V\delta1^{pos}$ T cells per 1 μL of whole-blood was similar between CLM patients and healthy controls (**Figure 4.5B**). On the other hand, respect to physiological conditions, significant lower counts of PB $V\delta2^{pos}$ and total $CD3^{pos}$ T cells were found in the blood of CLM patients (**Figure 4.5B**).

To evaluate additional phenotypical changes possibly affecting the maturation status of circulating γδT cells in CLM patients, we examined the cellular membrane expression of CD45RA and CD27 receptors, which identify four T cell subpopulations: T_{NAIVE} ($CD45RA^{pos}CD27^{pos}$), T_{CM} (central memory, $CD45RA^{neg}CD27^{pos}$), T_{EM} (effector memory, $CD45RA^{neg}CD27^{neg}$) and T_{EMRA} (terminally differentiated effector memory, $CD45RA^{pos}CD27^{neg}$) that represents the most differentiated effector subset[142,143]. In both healthy donors and CLM patients, T_{EMRA}, and T_{NAIVE} are the most represented subpopulations of $V\delta1^{pos}$ T cell subset among PBMCs (**Figure 4.5C**). Diversely, $V\delta2^{pos}$ T cells mainly consist of T_{EM} and T_{CM} without significant variations in these two subpopulations between pathological and physiological conditions (**Figure 4.5D**). Notably, CLM patients were characterized by a major increase of T_{EMRA} $V\delta1^{pos}$ T cells, with the mean increased from 51.9% ±25.6 to 68.4% ±23.5 (**Figure 4.5C**). Similar, but at lower extent,

higher proportion of T_{EMRA} $V\delta2^{pos}$ T subpopulation, which changed from 17.9% ±15.1 to 25.3% ±23.7, was observed (**Figure 4.5D**). The increase of T_{EMRA} subset, among $V\delta1^{pos}$ and $V\delta2^{pos}$ T lymphocytes, was associated with a decrease of the less mature T_{NAIVE} subpopulation (**Figure 4.5C-D**). On the other hand, T_{CM} and T_{EM} subpopulations were poorly represented among $V\delta1^{pos}$ T lymphocytes in both CLM patients and controls and their relative proportion remained similar between the two groups (**Figure 4.5C-D**).

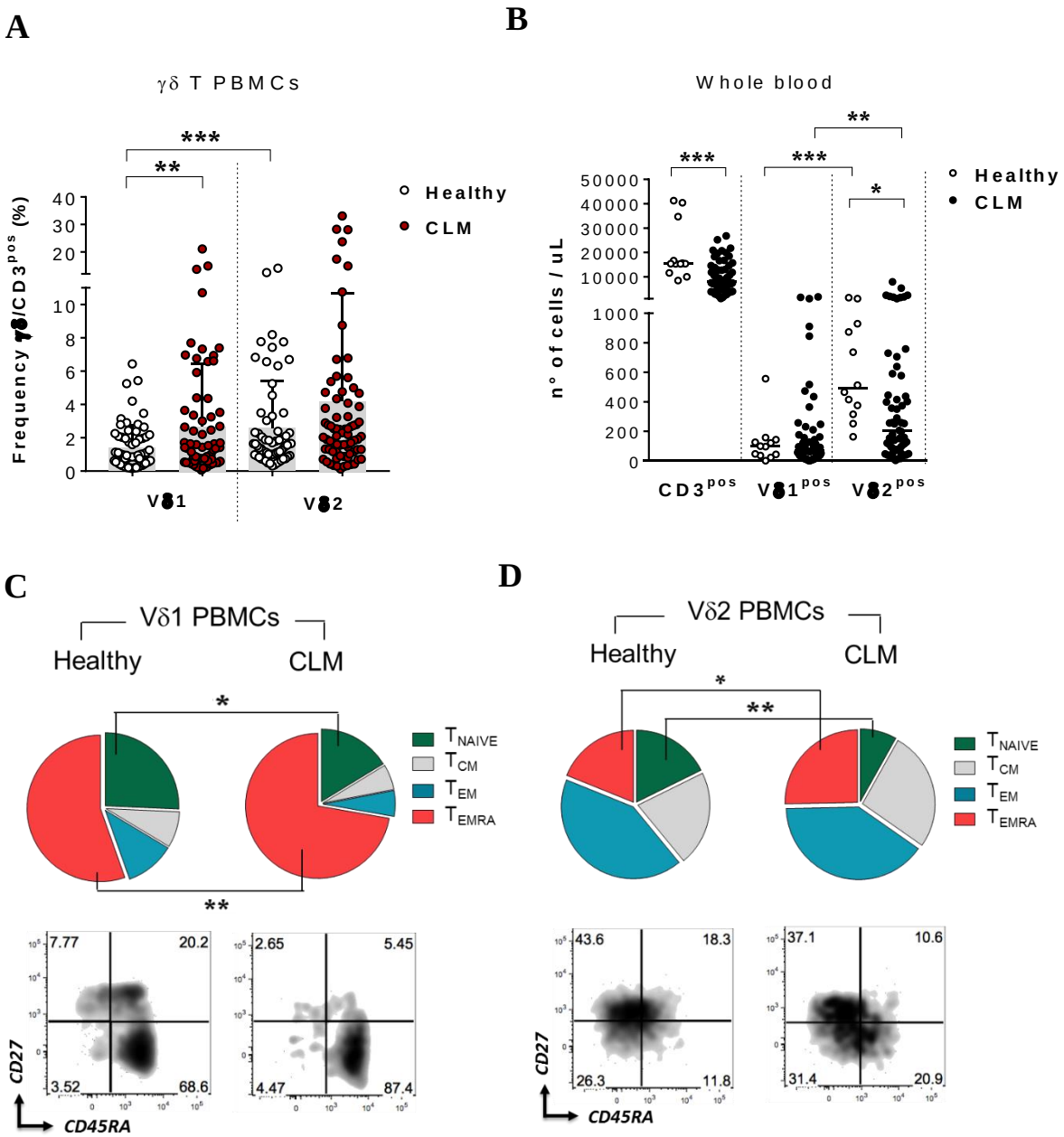

Figure 4.5. Frequency and differentiation status of Vδ1^{pos} and Vδ2^{pos} γδ T cell subsets in PBMCs of healthy donors and CLM patients. *(**A**) Frequency (%) of Vδ1^{pos} and Vδ2^{pos} T cell subsets in PBMCs of CLM patients (red circles, N=76) and healthy donors (white circles, N=66). (**B**) Absolute counting (n°) of cells per 1 μL of whole-blood of CD3^{pos} T cells, Vδ1^{pos} and Vδ2^{pos} T subsets in CLM patients (black circles N=59) and healthy individuals (white circles, N=12). (**C-D**) Pie-chart of T_{EMRA}, T_{NAIVE}, T_{CM} and T_{EM} mean distribution on Vδ1^{pos} (**C**) and Vδ2^{pos} (**D**) γδT lymphocytes in PBMCs of CLM patients (N=50) and healthy controls (N=33). Below, representative flow cytometry dot plot of CD45RA and CD27 expression. Results are shown as a mean ±SD (A) or median (B). Statistical significance was calculated with two-way, unpaired or paired t-test (A, C, D) and Mann-Whitney, unpaired test (B). *P ≤ 0.05; **P ≤ 0.01; ***P ≤ 0.001; ****P ≤ 0.0001*

All these data indicate that in CLM patients the frequency and the maturation status of PB γδT cells resulted to be altered respect to physiological conditions. In particular, CLM patients are characterized by an increased percentage of Vδ1^{pos} T cells probably due to decrease of the absolute amount of total T lymphocytes and Vδ2^{pos} T cells in the blood. Importantly, the increase percentage of Vδ1^{pos} T lymphocytes, in CLM patients, is associated with the higher abundance of T_{EMRA} subpopulation.

4.2.1.3 Analysis of tissue-associated γδ T cell subsets

As predictable[39,141], in the liver tissue, Vδ1^{pos} T cells are the predominant subset in the tumor-free region (8.1% ±8.8) reaching up to 40% of total T cells (**Figure 4.6A-B**). However, in the intratumor tissue Vδ1^{pos} T lymphocytes were drastically decreased, counting the average less than 1.9% ±2.0 (**Figure 4.6B**). Compared to the Vδ1^{pos} T subset, Vδ2^{pos} T lymphocytes where less abundant in the tumor-free tissue (2.7% ±2.5) (**Figure 4.6B**). In addition, similar frequency of Vδ2^{pos} T cells was observed in the intratumor region. Indeed, the percentage of Vδ2^{pos} T lymphocytes did not change between the tumor-free and the intratumor areas (**Figure 4.6B**).

Concerning the differentiation status of tissue-associated γδT cell subsets, T_{EMRA} and T_{EM} were the most represented subpopulations of Vδ1^{pos} T lymphocytes in both tumor-free and intratumor compartments (**Figure 4.6C**). However, the intratumor tissue was characterized by a higher occurrence of T_{CM} and T_{NAIVE} Vδ1^{pos} subpopulations and a lower concentration of T_{EMRA} Vδ1^{pos} cells (**Figure 4.6C**). The frequency of T_{EM} Vδ1^{pos} cells did not change between the two tissue-regions (**Figure 4.6C**). On the other hand, Vδ2^{pos} T lymphocytes in the tumor-free area were mainly T_{EM} (74.6% ±15.8) (**Figure 4.6D**). This

latter subpopulation was decreased in the intratumor lesion (56.4% ±19.6), while T_{CM} $V\delta2^{pos}$ cells were increased from the mean of 13.6% ±9.0 to 30.6% ±16.1 (**Figure 4.6D**). On the contrary, the relative proportions of T_{EMRA} and T_{NAIVE} $V\delta2^{pos}$ cells were similar among tumor-free and intratumor tissues (**Figure 4.6D**).

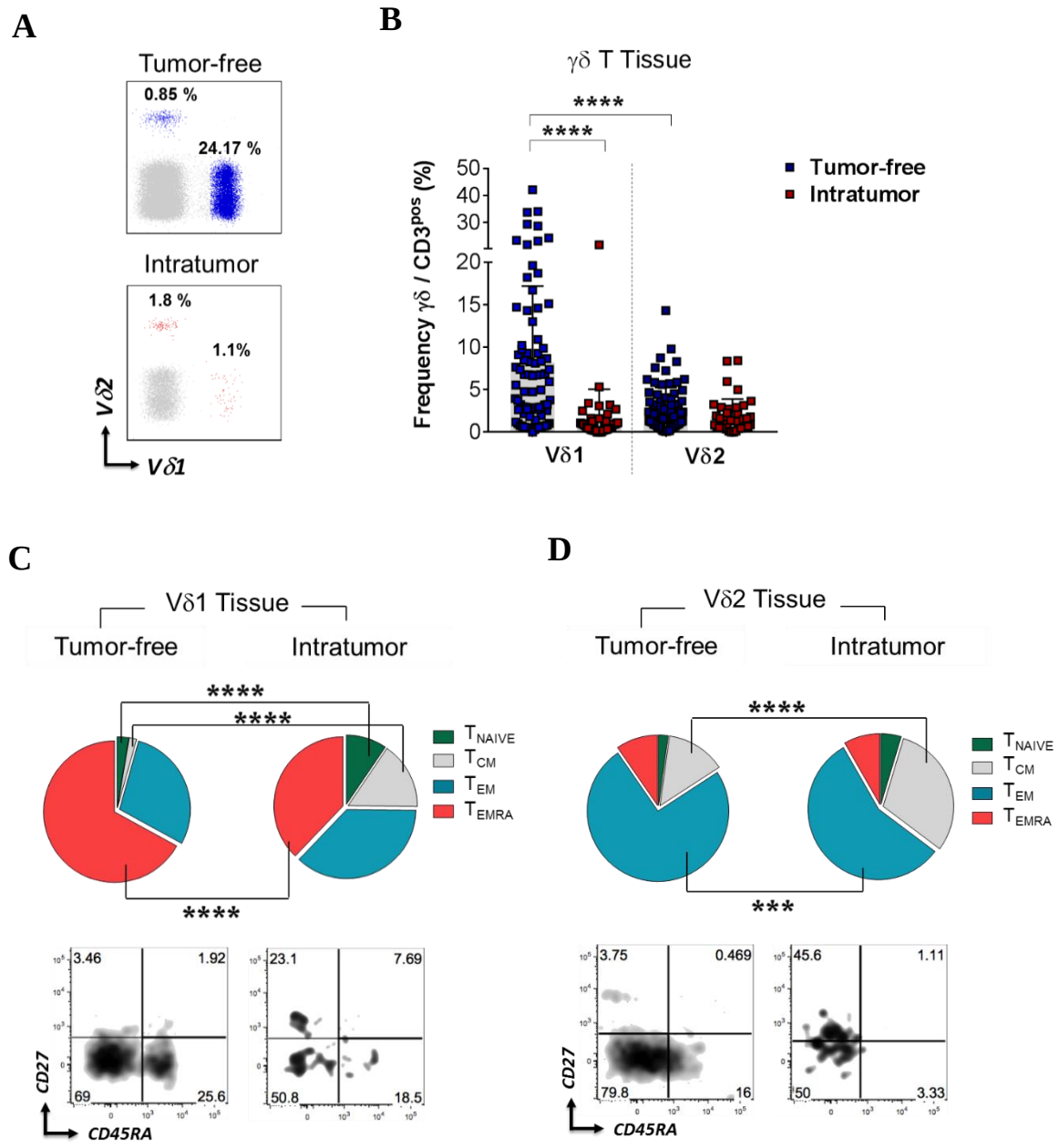

Figure 4.6. Frequency of γδ T cell subsets from tissue of CLM patients. (A) *Representative dot plots showing the frequency of Vδ1 ^{pos} and Vδ2 ^{pos} γδT cell subsets from tumor-free (upper panel) and intratumor tissues (bottom panel).* ***(B)*** *Frequency (%) of $V\delta1^{pos}$ and $V\delta2^{pos}$ T cell subsets in the tumor-free (blue squares; N=82) and the intratumor (red squares; N=40) tissues of CLM patients.* ***(C-D)*** *Pie-chart of T_{EMRA}, T_{NAIVE}, T_{CM} and T_{EM} mean distribution on $V\delta1^{pos}$ (C) and $V\delta2^{pos}$ (D) γδT lymphocytes from tumor-free (N=50) and intratumor tissues (N=15). Below, representative flow cytometry dot plot of CD45RA and CD27 expression.*

To determine the spatial distribution of γδT cells within the tumor-free and the intratumor parenchyma of CLM patients we performed an immunohistochemistry (IHC) staining of formaldehyde-fixed and paraffin-embedded (FFPE) liver specimen routinely prepared for the histopathological evaluation as described in the *Material and Methods* section (Paragraph 3.11). For the IHC analysis, histological sections were divided into three distinct tissue regions: intratumor (IT), invasive margin (IM) surrounding the tumor, and normal liver (NL) parenchyma located distantly from the IT region (**Figure 4.7A**). Consistently with our flow-cytometry data, the majority of $CD3^{pos}$ $\gamma\delta TCR^{pos}$ cells localized within the IM and the NL tissue, which corresponded to the tumor-free samples analyzed by flow cytometry (**Figure 4.7B**). In contrast, fewer γδT cells were detectable in the IT stroma (**Figure 4.7B)**, in accordance with our previous results (**Figure 4.6A**). Indeed, the percentage of $\gamma\delta TCR^{pos}$ cells was lower in the IT compartment compared to both the IM and the NL tissues (**Figure 4.7B**). On the other hand, no differences were observed in the frequency of γδT cells between the IM and NL areas (**Figure 4.7B**).

Unfortunately, IHC analysis on separate $V\delta1^{pos}$ and $V\delta2^{pos}$ γδT cell subsets was technically unfeasible due to the absence of specific Abs suitable for IHC staining.

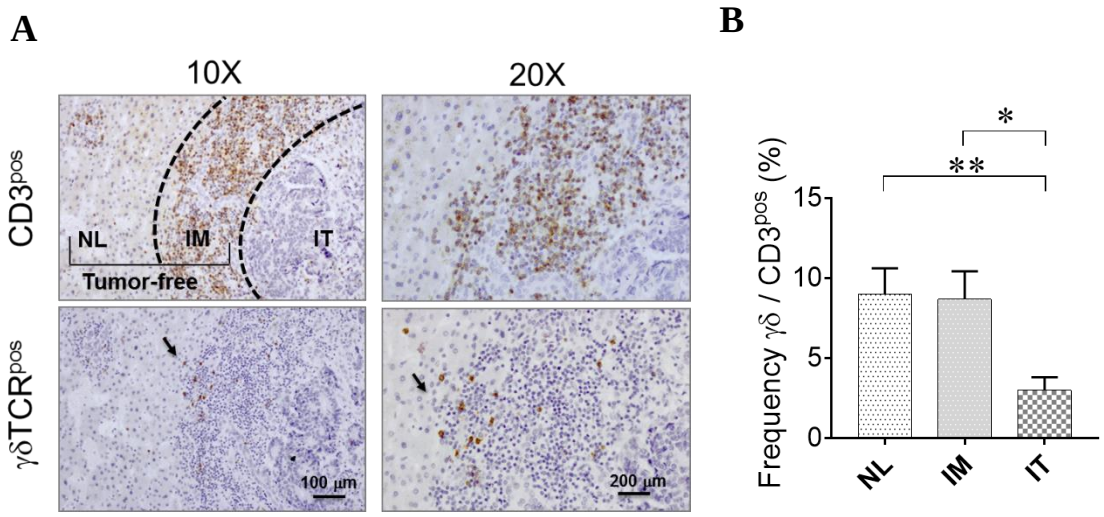

Figure 4.7. IHC staining of γδ T cells in liver specimen of CLM patients. (A) *Representative IHC staining for $CD3^{pos}$ (upper panel) and $\gamma\delta TCR^{pos}$ (lower panel) cells on sequential FFPE sections from the liver specimen of a CLM patient viewed at 10X (left) and 20X (right) magnification obtained with optical microscopy. Black arrows indicate $CD3^{pos}$ $\gamma\delta TCR^{pos}$ cells* ***(B)*** *Statistical representation of the frequency (%) of $\gamma\delta TCR^{pos}$ cells, measured by IHC in the normal liver (NL), invasive margin (IM) and intratumor (IT) regions of FFPE liver section of CLM patients (N=9). Results are shown as a mean ±SD. Statistical significance was calculated with two-way paired t-test. *P ≤ 0.05; **P ≤ 0.01; ***P ≤ 0.001; ****P ≤ 0.0001*

All these results indicate that the distribution and frequency of γδT cells is largely different between the tumor-free area and the intratumor stroma in metastatic lesions. This latter is characterized by a three-fold lower proportion of $V\delta1^{pos}$ T cells with higher frequency of less mature/differentiated subpopulations of T_{CM} and $T_{NAÏVE}$ cells. Concerning $V\delta2^{pos}$ T cells, besides that their global frequency is similar between the intratumor lesion and the tumor-free area, their maturation status changes. Indeed, the percentage of the specific intratumor T_{EM} $V\delta2^{pos}$ subpopulation is lower compared to the tumor-free tissue. Additionally, T_{CM} $V\delta2^{pos}$ cells represent the second major subpopulation of the tumor-free anatomical site.

All found differences, in the frequencies and maturation of γδT cells, within tumor-free and intratumor tissue regions, might be the consequence of intrinsic factors of γδT lymphocytes biology and/or effects of the tumor microenvironment. For this instance, intratumor $V\delta1^{pos}$ and $V\delta2^{pos}$ T cell subsets might be endowed with a different migration capacity or a diverse activation status, which could be further affected by the toxic and/or suppressive mechanisms carried out by tumor cells.

4.2.2 Effect of chemotherapy on the frequency and maturation status of γδ T cells in CLM patients

Chemoterapy (CHT) is generally administrated to CLM patients before surgery to convert unresectable metastases into resectable and to improve the overall clinical outcome.[18] In our cohort, 75% of all patients received CHT, which corresponded in the administration of monotherapy CHT (14% of all cases), generally based on FOLFOX/FOLFIRI regimens, or combined-CHT (82% of CHT-treated patients) with either an anti-VEGF and/or an anti-EGFR mAb (**Figure 4.8)**. The remaining 25% of CLM patients directly underwent liver surgery without receiving any prior treatment (NO CHT) (**Figure 4.8**).

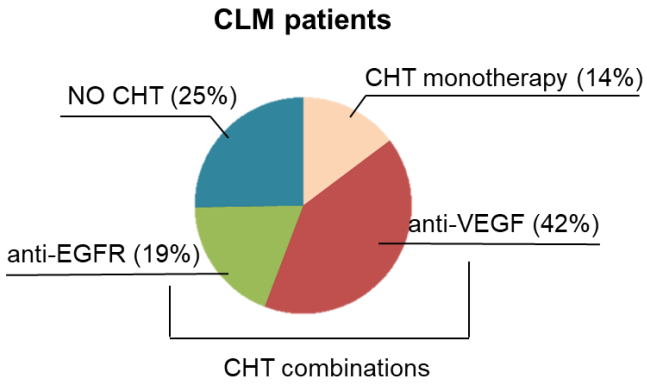

Figure 4.8. Distribution of CLM patients according to CHT. *Pie-chart showing the distribution of CLM patients who received CHT monotherapy or CHT combination with the anti-EGFR mAb and/or the anti-VEGF. All treatments are considered prior to the liver surgery.*

Since conventional chemotherapeutics, by acting on highly proliferating cells, not only affect the tumor growth but can also lead to immunological consequences[144], we evaluated the effect of CHT on the proportion and differentiation status of γδT cells in PBMCs, tumor-free and intratumor tissues of CLM patients.

To assess the potential outcome of CHT-treatment on the rate of γδT lymphocytes, we compared patients that received CHT, either in combination with targeted agents or as a monotherapy, with untreated ones (NO CHT). We observed that the frequency of $V\delta1^{pos}$ T lymphocytes was affected by CHT administration (**Figure 4.9A**). Indeed, CHT-treated patients had a higher proportion of $V\delta1^{pos}$ T cells compared to the NO CHT group. (**Figure 4.9A**). On the contrary, CHT administration did not affect the frequency of $V\delta2^{pos}$ T cells since similar percentage was observed in both CHT and NO CHT cohorts of CLM patients (**Figure 4.9B**).

The administration of CHT and mAbs might affect the ratio of lymphocytes, not only in the PB, but also in the tissue compartments. In particular, the use of targeted drugs can have either a direct or indirect effect on the tumor growth. In fact, anti-EGFR agents binds the EGF receptor expressed on the surface of tumor cells to inhibit their proliferation, while anti-VEGF mAbs inhibit the intratumoral neovascularization, thus affecting indirectly the progression of the tumor. Therefore, we evaluated the possible differences in the frequency of $V\delta1^{pos}$ and $V\delta2^{pos}$ T cell subsets in the tumor-free and the intratumor tissue areas according to CHT.

Diversely from the blood, similar proportion of tissue-associated $V\delta1^{pos}$ and $V\delta2^{pos}$ T cells were observed between CHT and NO CHT groups in both the tumor-free and intratumor tissue (**Figure 4.9C-D**).

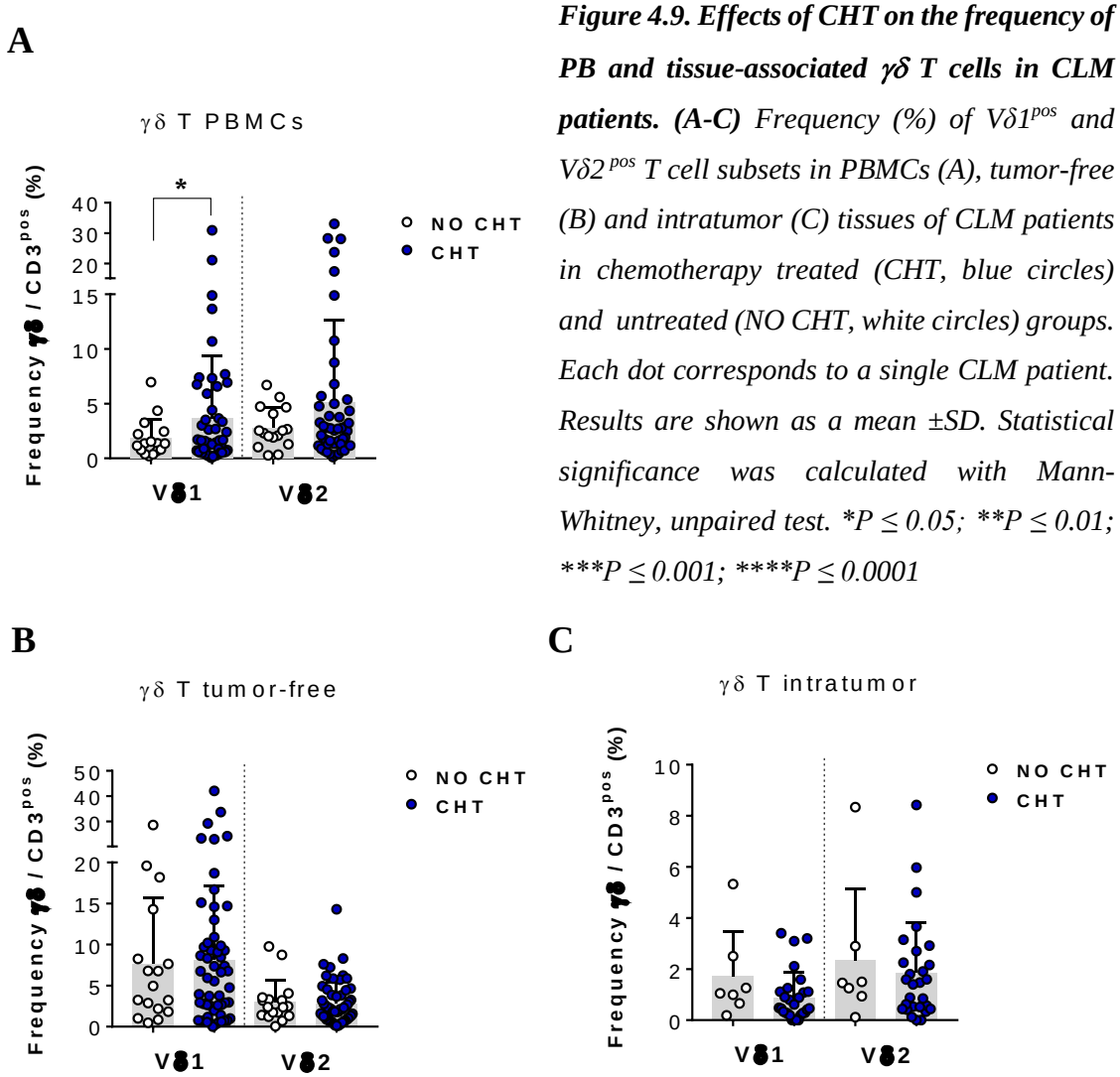

Figure 4.9. Effects of CHT on the frequency of PB and tissue-associated γδ T cells in CLM patients. (A-C) *Frequency (%) of Vδ1^{pos} and Vδ2^{pos} T cell subsets in PBMCs (A), tumor-free (B) and intratumor (C) tissues of CLM patients in chemotherapy treated (CHT, blue circles) and untreated (NO CHT, white circles) groups. Each dot corresponds to a single CLM patient. Results are shown as a mean ±SD. Statistical significance was calculated with Mann-Whitney, unpaired test. *P ≤ 0.05; **P ≤ 0.01; ***P ≤ 0.001; ****P ≤ 0.0001*

The diverse effect of CHT on the proportion γδT lymphocytes from PB compartments might also be influenced by the status of maturation of cells. In particular, knowing that the proliferation capacity of γδT cells depends on the stage of differentiation [145] we then considered the effect of anti-cancer therapy on the frequency of T_{EMRA}, T_{CM}, T_{EM} and $T_{NAÏVE}$ in both Vδ1^{pos} and Vδ2^{pos} T lymphocytes. From the analysis of Vδ1^{pos} T cells in PBMCs, we observed a similar distribution of all four subpopulations between CHT and NO CHT groups (**Figure 4.10A upper graph**) indicating that the increase of blood-circulating Vδ1^{pos} T_{EMRA} cells (**Figure 4.5C**) is independent of the CHT-treatment. Diversely, major differences emerged from the examination of PB Vδ2^{pos} T cells. Indeed, CHT-treated patients had a higher proportion of the T_{EMRA} subpopulation and a lower abundance of T_{CM} compared to the untreated ones (**Figure 4.10A lower graph**). In accordance, the increase of T_{EMRA} Vδ2^{pos} cells was a feature of only CHT-treated patients (**Figure 4.10B**). No

differences were observed in the frequency of T_{EM} and T_{NAIVE} $V\delta2^{pos}$ cells between these two groups (**Figure 4.10A**). We then assessed whether the frequency of the specific T_{EMRA} $V\delta2^{pos}$ cell subset depended on the number of CHT cycles. We observed that the number of DNA-damaging CHT cycles (8.0 ±5.3) did not correlate with the frequency of $V\delta2^{pos}$ T_{EMRA} subpopulation (**Figure 4.10C**) but, it was inversely associated to the frequency of $V\delta2^{pos}$ T_{CM} cells (**Figure 4.10D**). This difference might be due to the increased frequency of non-dividing cells among T_{EMRA} $V\delta2^{pos}$ cells in contrast to proliferating T_{CM} cells, which are directly affected by CHT toxicity.

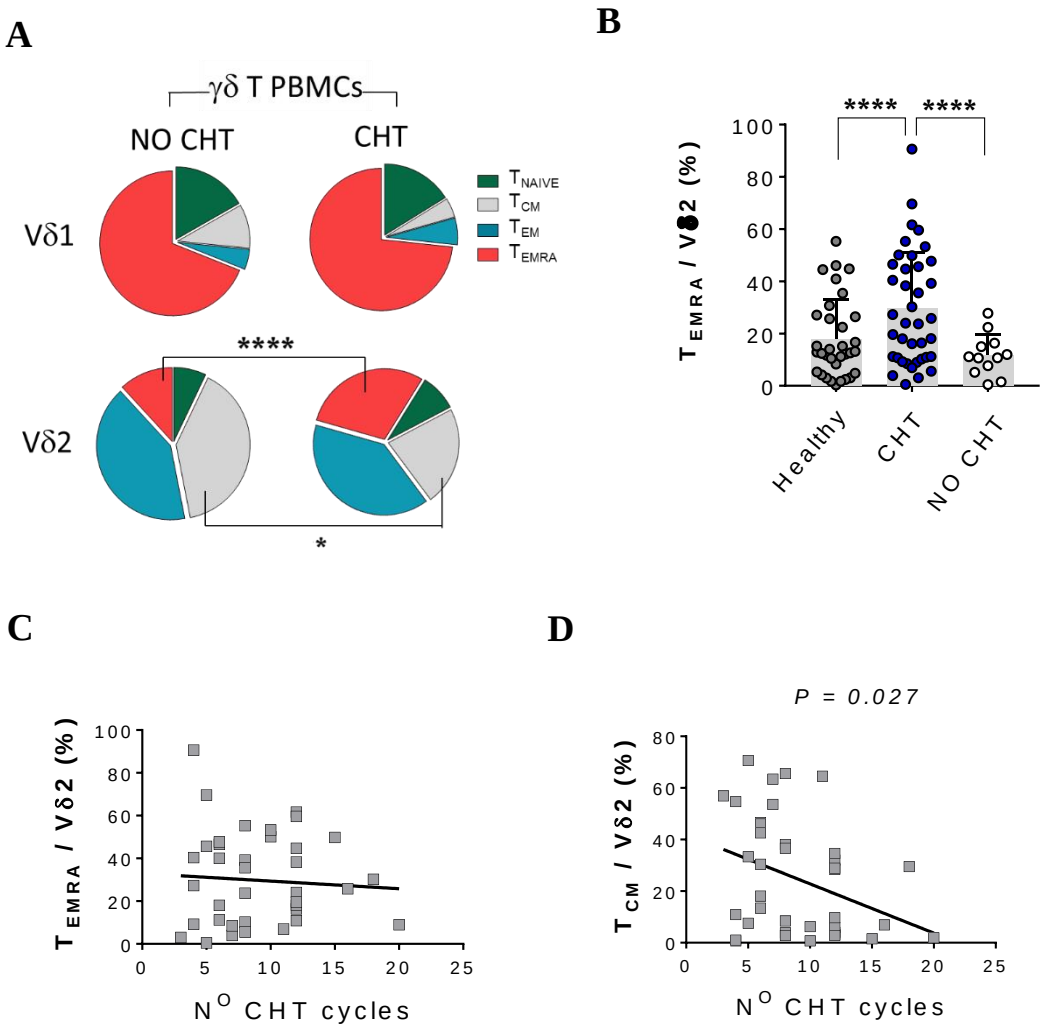

Figure 4.10. Effects of CHT on the maturation stage of γδ T cells in PBMCs of CLM patients. *(**A**) Pie-chart of the mean distribution of T_{EMRA}, T_{NAIVE}, T_{CM} and T_{EM} on $V\delta1^{pos}$ (upper panel) and $V\delta2^{pos}$ (lower panel) γδT lymphocytes in PBMCs of CHT-treated (right graph; N=39) and NO-CHT (left graph; N=12) CLM patients. (**B**) Statistical representation of the frequency (%) of T_{EMRA} $V\delta2^{pos}$ cells in PBMCs of healthy controls (grey; N=33) and CLM patients divided into NO CHT (white circles; N=12) and CHT (blue circles; N=39). (**C-D**) Statistical analysis showing the correlations between the frequency of either T_{EMRA} (C) or T_{CM} (D) $V\delta2^{pos}$ T cells and the number (n°) of CHT cycles administered to patients affected by CLM (n=40). Results are shown as a mean ±SD. Statistical significance was calculated with two-way, unpaired t-test or Mann-Whitney, unpaired test. *P ≤ 0.05; **P ≤ 0.01; ***P ≤ 0.001; ****P ≤ 0.0001. For correlation analysis Pearson's coefficient was applied.*

Finally, analysis of T_{EMRA}, T_{CM}, T_{EM} and $T_{NAÏVE}$ subpopulatios in the tumor-free tissue did not reveal any difference in CLM patients associated to CHT, neither in the $V\delta1^{pos}$ nor in the $V\delta2^{pos}$ T cell subsets (**Figure 4.11**). Owing to the small number of untreated patients, as well as, low number of isolated cells, it was not possible to perform similar analysis on intratumural γδ T cell subsets.

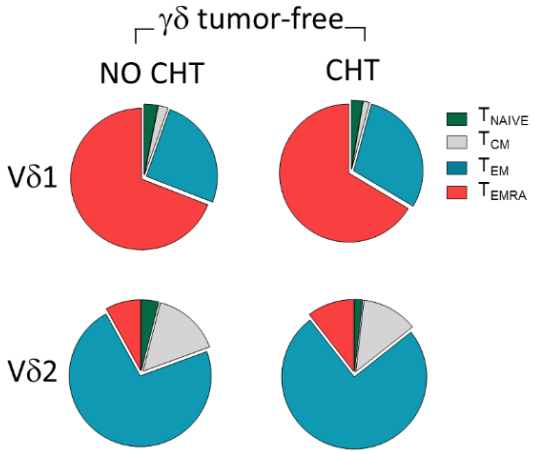

Figure 4.11. Effects of CHT on the maturation stage of γδ T cells in the tumor-free tissue of CLM patients. *Pie-chart of the mean distribution of T_{EMRA}, T_{NAIVE}, T_{CM} and T_{EM} subsets on $V\delta1^{pos}$ (upper panel) and $V\delta2^{pos}$ (lower panel) γδT lymphocytes from tumor-free tissue of CHT-treated (right graph; N=39) and NO-CHT (left graph, N=12) CLM patients.*

Above results suggest that the observed increase of total PB $V\delta1^{pos}$ T cells in CLM patients (**Figure 4.6A**) is associated with CHT treatment. On the other hand, the proportion of T_{EMRA} $V\delta1^{pos}$ in the circulation is similar and independent from CHT. Diversely, circulating T_{EMRA} $V\delta2^{pos}$ cells might be positively selected by CHT therapy since their frequency is much higher in treated rather than untreated patients. One explanation of this data is that increased frequency of PB $V\delta1^{pos}$ T cells in CHT patients is due to the higher sensitivity to CHT of less differentiated and more proliferating $V\delta2^{pos}$ T cells, as well as other, $CD4^{pos}$ and $CD8^{pos}$, T lymphocytes. Indeed, as shown in Figure 4.5A, we observed a

significant drop in the absolute count of total $CD3^{pos}$ and $V\delta2^{pos}$ T cells but not in $V\delta1^{pos}$ T cells. On the other hand, at the liver site CHT has no appreciable influence on neither the frequency nor the differentiation status of tissue-associated γδT cells. Thus the systemic outcome of therapy that results in the higher abundance of total $V\delta1^{pos}$ T cells and the specific increase of T_{EMRA} $V\delta2^{pos}$ cell subset is consequence of their distinct/intrinsic differentiation status and immuno-recostitution after CHT treatment.

4.2.3 Identification of the tumor-related cluster of $CD69^{pos}V\delta1^{pos}$ T_{EMRA} in PBMCs of CLM patients

We took advantage of high-dimensional flow cytometry analysis for the phenotypical evaluation of $V\delta1^{pos}$ T cells from PBMCs of 54 CLM patients in comparison to 44 healthy donors. Consistently with the higher abundance of circulating T_{EMRA} $V\delta1^{pos}$ subpopulation in CLM patients compared to healthy donors (**Figure 4.5C**), we found that $V\delta1^{pos}$ T cells from CLM patients expressed lower levels of CD28 receptor, a well-characterized costimulatory molecule for T cells[146], with non-redundant function in the proliferation and survival of both $CD27^{pos}$ and $CD27^{neg}$ γδT cells[147] (**Figure 4.12**). No significant variations were observed in regard to other markers associated with γδT cells differentiation, including CD57 and CD16, which are induced upon maturation[145,148]. Additionally, low and not different expression level was observed for CCR7, generally lost at higher stages of differentiation[149] (**Figure 4.12**). The analysis of different activating receptor associated with γδT cells effector functions, revealed a more cytotoxic-related phenotype of $V\delta1^{pos}$ T lymphocytes in CLM patients compared to healthy individuals. In particular, PB $V\delta1^{pos}$ T cells of CLM patients were characterized by increasing levels of CD69, CD161 and NKG2D receptors (**Figure 4.12**). Notably, CD69, defines early stages of T cell activation[150] and thus it is poorly expressed at steady conditions (6.8% ±5.2) (**Figure 4.12**).

We observed a higher average expression (24.4% ±18.8) of CD69 protein on total $V\delta1^{pos}$ T lymphocytes of CLM patients that could reach up to 80% of total cells (**Figure 4.12**). Similarly, CD161 molecule, which cellular membrane expression is associated with different functions of γδT cells, including liver-homing[151] and cytokines production[152], reaches high levels of expression in CLM patients (**Figure 4.12**). While NKG2D receptor, a well-established antitumor-receptor for γδT cells[107], constitutively expressed on the

majority of Vδ1^{pos} T cells at physiological setting (53.5% ±26.7), showed a further increase with the average expression of 77% ±28.3 **(Figure 4.12)**.

For a more comprehensive view of the activation status of Vδ1^{pos} T cells we also evaluated the presence of CTLA4 and PD-1, the two main checkpoint inhibitors commonly expressed after T lymphocytes activation[153,154]. Remarkably, the expression of CTLA4 raised up from the mean of 7.9% ±8.8 to 18.3% ±17.6. This increase of CTLA4 was in line with lower expression of CD28 molecule, which shares with CTLA4 the same, CD80 and CD86, ligands[155] (**Figure 4.12**). On the other hand, PD-1 levels were similar between healthy controls and CLM patients with the average of 10.9% ±9.5 and 12.2% ±13.4, respectively. Lastly, the costimulatory molecule CD86 and the chemokine receptor CXCR3 were poorly represented on the cellular membrane of Vδ1^{pos} T cells in both physiological conditions and CLM patients, although some statistically significant changes were observed in the expression of CD86 (**Figure 4.12**).

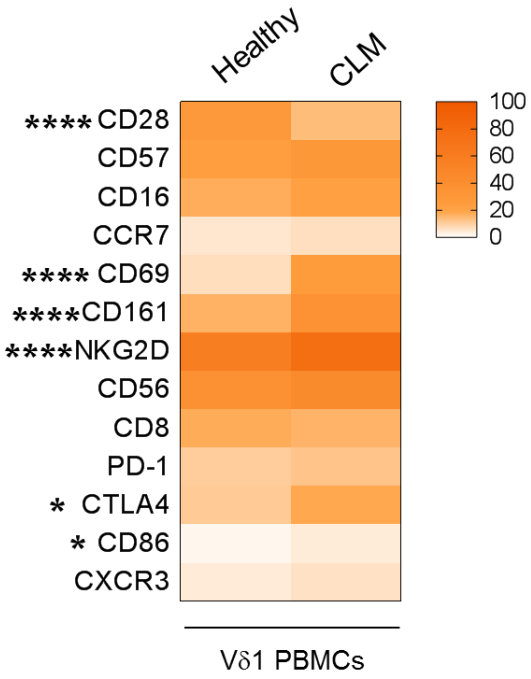

Figure 4.12. Phenotype of Vδ1^{pos} T cells in PBMCs of CLM patients compared to healthy donors. (A) *Heatmap of the mean of expression (%) of different surface markers measured by flow cytometry on PB Vδ1 ^{pos} T cells from healthy individuals (N=44) and CLM patients (N=58). Color-scale is depicted at the top right side. Results are shown as mean ±SD. Statistical significance was calculated with two-way Mann-Whitney unpaired test. *P ≤ 0.05; **P ≤ 0.01; ***P ≤ 0.001; ****P ≤ 0.0001*

Importantly, no differences in the expression of the main cellular activating markers including, CD69, CD161 and NKG2D was observed between Vδ1^{pos} T cells of the two CHT and NO CHT groups (**Figure 4.13**). Higher, CHT-independent expression of CD69, CD161 and NKG2D markers in CLM patients compared to healthy controls, indicates a tumor-related, rather than therapy-associated, activating phenotype of Vδ1^{pos} T cells (**Figure 4.13A-C**).

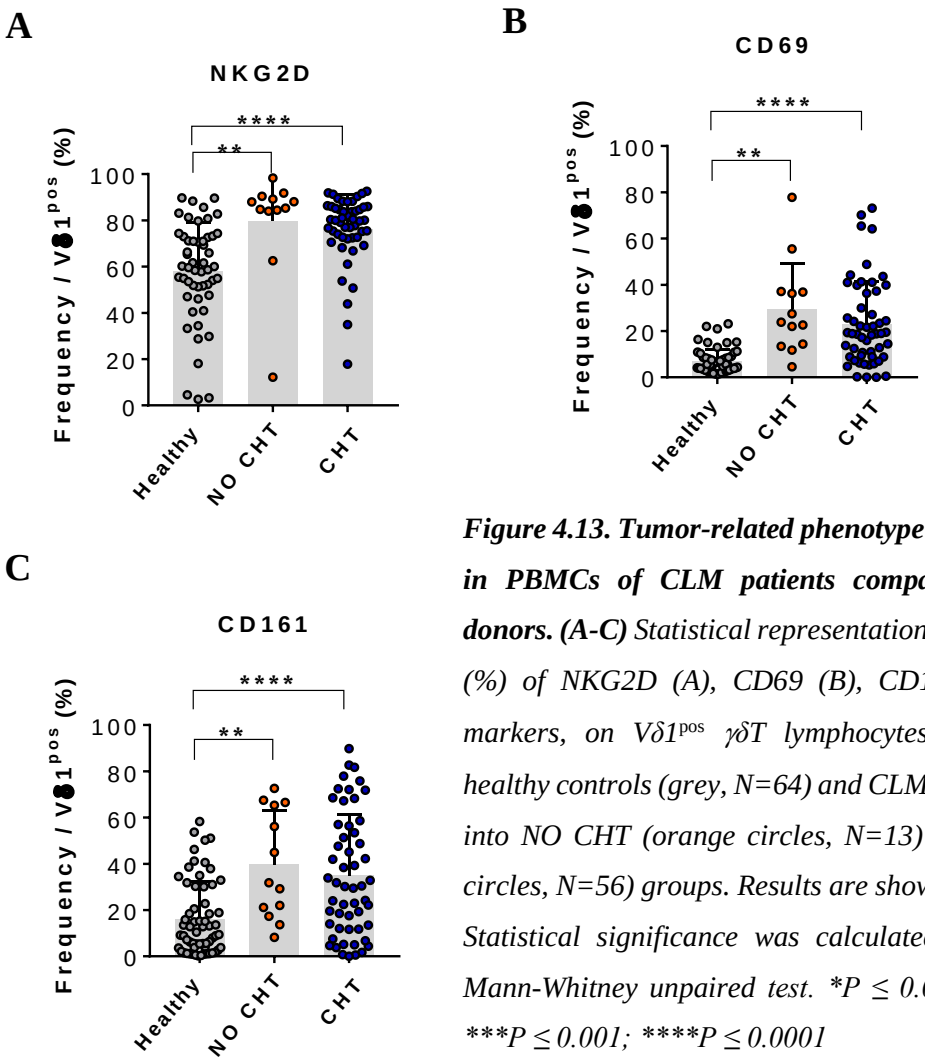

Figure 4.13. Tumor-related phenotype of Vδ1^{pos} T cells in PBMCs of CLM patients compared to healthy donors. (A-C) *Statistical representation of the frequency (%) of NKG2D (A), CD69 (B), CD161 (C) surface markers, on Vδ1^{pos} γδT lymphocytes in PBMCs of healthy controls (grey, N=64) and CLM patients divided into NO CHT (orange circles, N=13) and CHT (blue circles, N=56) groups. Results are shown as mean ±SD. Statistical significance was calculated with two-way Mann-Whitney unpaired test. *P ≤ 0.05; **P ≤ 0.01; ***P ≤ 0.001; ****P ≤ 0.0001*

For a more complete and unbiased phenotypical analysis, we performed the t-SNE algorithm on the global flow cytometry results collected on Vδ1^{pos} T cells from PBMCs of CLM patients and healthy individuals. This algorithm enables the visualization of complex high-dimensional flow cytometry data into a two-dimensional map, in which cells with a similar cytometric signature are placed in the same region of the graph.[156]

The t-SNE analysis revealed a different distribution of Vδ1^{pos} T cells between CLM patients and healthy controls, indicating important changes happening in this subset, not only in the frequency but also in the distribution of different immunological markers (**Figure 4.14A**). Thus, we looked at the spatial localization of all analyzed receptors on the t-SNE plots obtained from healthy donor and CLM patients. We noticed that the expression of CD69 was largely different in terms of both frequency and spatial distribution between the two t-SNE maps (**Figure 4.14B**). Indeed, the CLM t-SNE plot was characterized by a well-

defined cluster of CD69^{pos} Vδ1^{pos} T cells that was poorly represented and quite disperse in the t-SNE map of healthy individuals (**Figure 4.14B)**. A more detailed analysis of the CD69^{pos} cluster revealed that the 91% of Vδ1^{pos} T cells in CLM patients corresponded to the T_{EMRA} subset, defined as CD45RA^{pos}CD27^{neg} (**Figure 4.14C)**. Moreover, the CLM-associated CD69^{pos} Vδ1^{pos} cluster was characterized by high co-expression of CD161 and NKG2D receptors (**Figure 4.14C)**, which were statistically increased in CLM patients (**Figure 4.11**). Finally, the vast majority of CD69^{pos} Vδ1^{pos} T cells of CLM patients were negative for CD28, further confirming the prevalence, within the cluster, of highly differentiated and effector cells (**Figure 4.14C**).

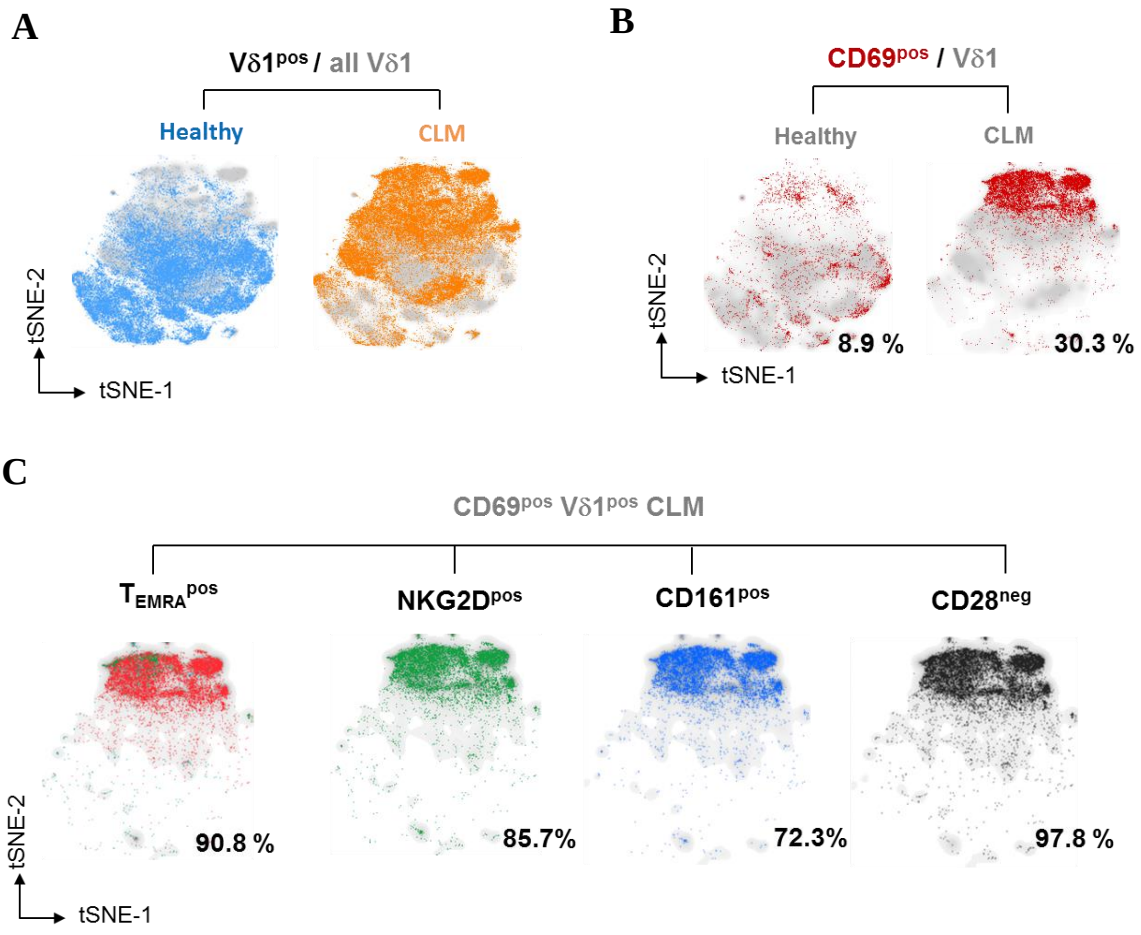

Figure 4.14. Tumor-related cluster of CD69^{pos} Vδ1^{pos} T_{EMRA} cells from PBMCs of CLM patients. ***(A-B)*** *t-SNE graphs showing the spatial distribution of Vδ1^{pos} T cells (A) and CD69 (B) in healthy individuals (N=22) and CLM patients (N=26).* ***(C)*** *t-SNE graphs showing the frequency of T_{EMRA}, NKG2D, CD161 and CD28 on CD69^{pos} Vδ1^{pos} cluster in CLM patients. t-SNE analysis was performed on concatenated Vδ1^{pos} T cells for a total of 100.000 events including both donor and CLM patients.*

Remarkably, the cluster of CD69^{pos}CD161^{pos}NKG2D^{pos}CD28^{neg} Vδ1^{pos} T_{EMRA} cells counted for only about 2% in healthy individuals while it appeared on about 20% of total Vδ1^{pos} T cells in CLM patients (**Figure 4.15A-B**) suggesting its relevance in the presence of liver metastatic disease.

Expression and cluster-distribution of additional markers relevant for the γδT cells immune response on the CLM-associated cluster of CD69^{pos}CD161^{pos}NKG2D^{pos}CD28^{neg} Vδ1^{pos} T_{EMRA} cells are shown in **Figure 4.15C**.

In conclusion, the overall t-SNE analysis on PB Vδ1^{pos} T lymphocytes allowed the identification of the **activating and tumor-related CD69^{pos} Vδ1^{pos} T cells cluster** preferentially associated with the T_{EMRA} subset and distinguished from the healthy counterpart by higher expression of NKG2D receptor and CD161 molecule (**Figure 4.14C)**.

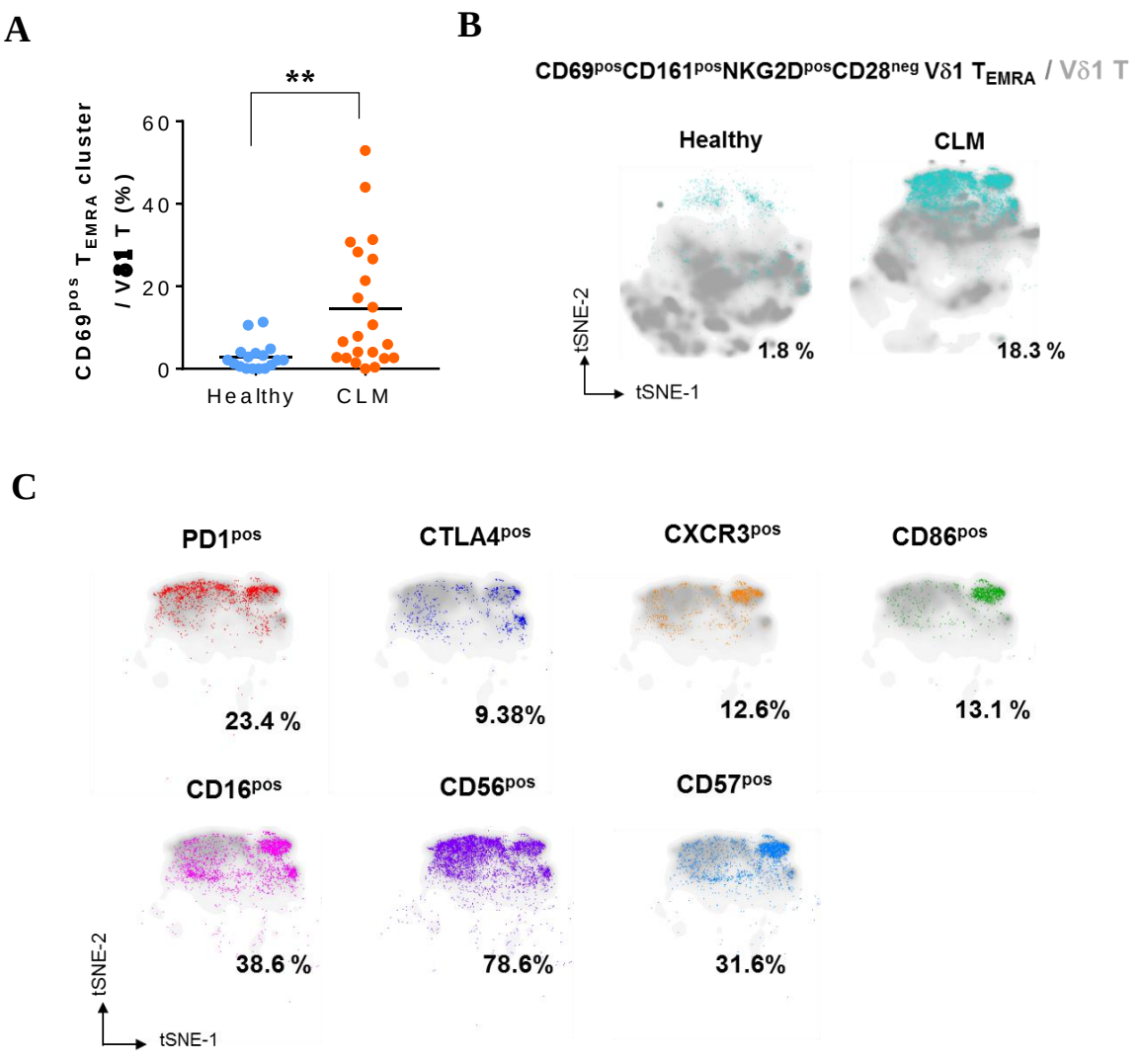

Figure 4.15. Frequency and phenotype of the cluster of CD69^{pos}CD161^{pos}NKG2D^{pos}CD28^{neg} Vδ1^{pos} T$_{EMRA}$ cells in PBMCs of CLM patients. *(**A-B**) Statistical chart (A) and related t-SNE graphs (B) showing the frequency of the tumor-related CD69^{pos}CD161^{pos}NKG2D^{pos}T$_{EMRA}$ Vδ1^{pos} T cells cluster between healthy controls (N=17) and CLM patients (N=22). (**B**) Expression and distribution of PD-1, CTLA4, CXCR3, CD86, CD16, CD56 and CD57 receptors on the tumor-related cluster shown in Figure 4B. Results are shown as mean. Statistical significance was calculated with two-way, unpaired t-test. *P ≤ 0.05; **P ≤ 0.01; ***P ≤ 0.001; ****P ≤ 0.0001.*

4.2.4 Chemotherapy related changes of PB Vδ2^{pos} T cell in CLM patients

The same panel of markers studied on PB Vδ1^{pos} T cells was applied for the phenotypical evaluation of Vδ2^{pos} T cells from PBMCs of CLM patients. Similar to Vδ1^{pos} T cells, Vδ2^{pos} T lymphocytes of CLM patients had lower levels of CD28 molecule compared to healthy donors (**Figure 4.16**). This result, was in line with the observed decrease percentage of T$_{NAIVE}$ Vδ2^{pos} cells in CLM patients (**Figure 4.5D**). On the other hand, in accordance with the increased proportion of PB Vδ2^{pos} T$_{EMRA}$ cells (**Figure 4.45D**), CD57 and CD16 molecules, whose expression is associated with γδT cells maturation and senescence[145,148], were upregulated in CLM patients (**Figure 4.16**). In particular, the level of CD57 receptor growth up from the average of 3.9% ±6.2, at physiological conditions, to 14.9% ±16.7 in CLM patients. Although, expression of CD16 receptor, relevant for the antibody dependent cellular cytotoxicity (ADCC) response, presented variable expression in normal adults (21.5% ±21.9), however, it was higher in CLM patients (31.6% ±27.3) (**Figure 4.16**). Moreover, no variations were observed in the poorly expressed chemokine receptor CCR7, normally associated with the migration of T cells to lymph nodes[149] (**Figure 4.16**).

Regarding activating receptors, Vδ2^{pos} T cells of CLM patients presented several differences compared to healthy controls. In particular, we observed higher expression of activating CD56 marker and NKG2D receptor, which has critical role on the antitumor effector functions of Vδ2^{pos} T cells[81] (**Figure 4.16**). Interestingly, the increased CHT-independent occurrence of NKG2D molecule was observed in both Vδ1^{pos} and Vδ2^{pos} T cells in PBMCs of CLM patients (**Figure 4.16 and Figure 4.12**). Diversely, the expression of CD69 and CD161 receptors, which increased in the PB Vδ1^{pos} T cells of CLM patients (**Figure 4.12**), in case of Vδ2^{pos} T lymphocytes, did not change (**Figure 4.16**), thus suggesting different tumor-related impact on the activation of Vδ2^{pos} T cells. On the other hand, similar to Vδ1^{pos} T cells (**Figure 4.12**), we found a slight increase in the expression of

CTLA4 receptor, while PD-1 levels remained unchanged between controls and CLM patients. Similar, in both CLM patients and healthy controls more than 50% of Vδ2^{pos} T cells were positive for NKG2A (**Figure 4.16**). Since antigen-presenting function have been described for Vδ2^{pos} T cells[157], we evaluated the expression of CD86 molecule, usually present on the cellular surface of antigen presenting cells (APCs). However, a very low expression of this molecule was found in both groups (**Figure 4.16**). Finally, CXCR3, which is poorly represented on Vδ2 ^{pos} T cells of healthy individuals, maintained its low expression levels in CLM patients as well (**Figure 4.16**).

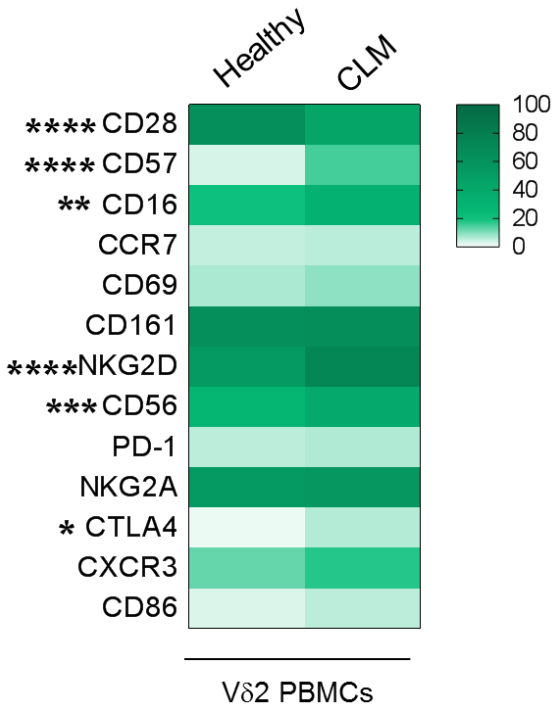

Figure 4.16. Effect of CHT on the phenotype of Vδ2^{pos} T cells from PBMCs of CLM patients. *Heatmap of the mean of expression (%) of different surface markers measured by flow cytometry on PB Vδ2^{pos} T cells from healthy individuals (N=44) and CLM patients (N=58). Color-scale is depicted at the top right side. Statistical significance was calculated with two-way Mann-Whitney unpaired test. *P ≤ 0.05; **P ≤ 0.01; ***P ≤ 0.001; ****P ≤ 0.0001*

Overall, the analysis of the PB Vδ2^{pos} T cells revealed substantial phenotypical changes between CLM patients and healthy controls, which mainly resulted in the increase of maturation-related markers, CD57 and CD16, activating receptors CD56 and NKG2D and the checkpoint inhibitor CTLA4.

We observed that the increase of T_{EMRA} Vδ2^{pos} cells in the PB was associated with CHT-treatment (**Figure 4.5A**), thus we looked for others phenotypical CHT-related differences in the Vδ2^{pos} T cell subset. Interestingly, only CHT-treated patients, compared to untreated ones, were characterized by higher expression of CD57, strictly induced on senescent T cells[145]. Similar, increased expression of CD16, which identify terminally differentiated subset of Vδ2^{pos} T cells[148], was also associated with CHT treatment (**Figure**

4.17A-B). On the other hand, the expression level of NKG2D receptor was similar in both groups, regardless of CHT (**Figure 4.17C**).

These results further confirmed a major susceptibly of the blood-circulating Vδ2^{pos} T cells to the toxic effect of CHT-therapy, which result not only in the higher proportion of Vδ2^{pos} T_{EMRA} subset compared to the less mature subpopulation but also in the induction of a highly-differentiated and senescent-like phenotype.

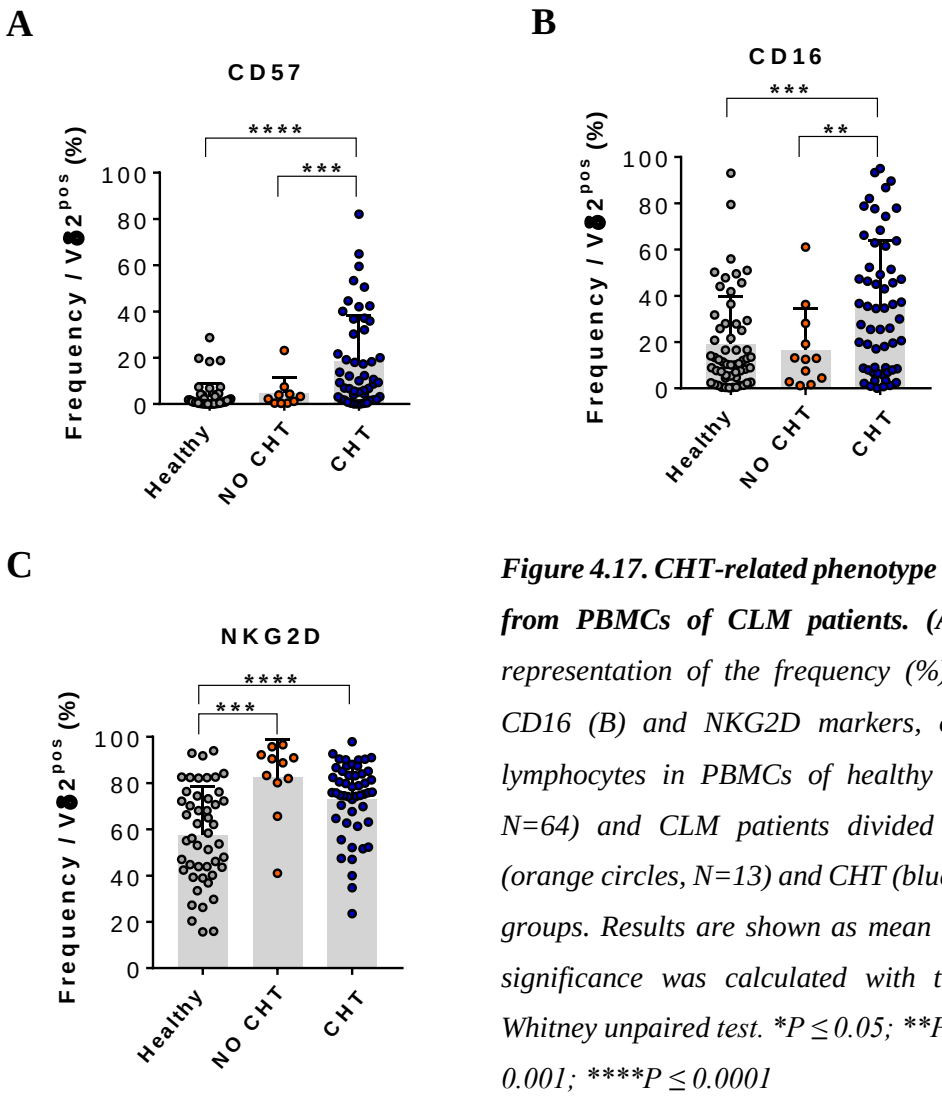

Figure 4.17. CHT-related phenotype of Vδ2^{pos} T cells from PBMCs of CLM patients. (A-D) *Statistical representation of the frequency (%) of CD57 (A), CD16 (B) and NKG2D markers, on Vδ2 ^{pos} γδT lymphocytes in PBMCs of healthy controls (grey, N=64) and CLM patients divided into NO CHT (orange circles, N=13) and CHT (blue circles, N=56) groups. Results are shown as mean ±SD. Statistical significance was calculated with two-way Mann-Whitney unpaired test. *P ≤ 0.05; **P ≤ 0.01; ***P ≤ 0.001; ****P ≤ 0.0001*

The use of t-SNE algorithm allowed a better characterization of the cluster of CD57^{pos} Vδ2^{pos} T cells found in PBMCs of CLM patients. Remarkably, 95% of CD57^{pos} Vδ2^{pos} T cells coexpressed CD16 receptor and was 99% negative for CD28 molecule (**Figure 4.18A**). For instance, the majority of CD57^{pos} Vδ2^{pos} T cells belonged to the T_{EMRA}

subpopulation (**Figure 4.18A**). The freqeuncy of the specific $CD57^{pos}CD16^{pos}CD28^{neg}$ T_{EMRA} $V\delta2^{pos}$ cell cluster (**Figure 4.18B**) was statistically higher in CHT patients compared to the NO CHT group of patients and to the healthy counterpart (**Figure 4.18C-D**).

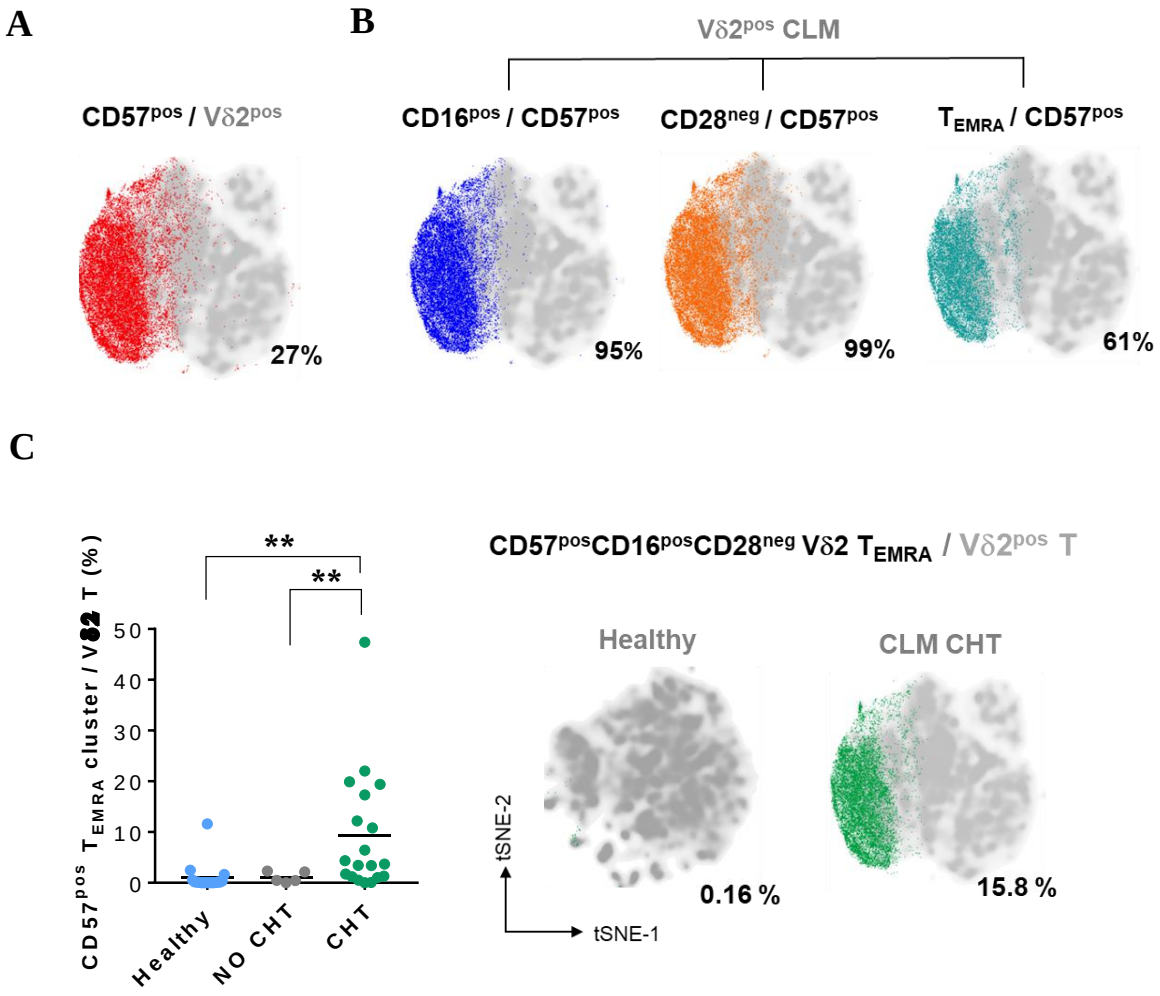

Figure 4.18. t-SNE analysis of the specific CHT-dependent $CD57^{pos}CD28^{neg}CD16^{pos}T_{EMRA}$ $V\delta2^{pos}$ T cell cluster. (A) *t-SNE analysis plots in CHT treated CLM patients (n=16) showing $CD57^{pos}$ cells cluster on total $V\delta2^{pos}$ T cell subset.* ***(B)*** *Expression of CD16, CD28 and T_{EMRA} cells on $CD57^{pos}V\delta2^{pos\ T}$ cells;* ***(C)*** *t-SNE analysis plots (right plots) and statistical chart (left graph) of the CHT-mediated changes in the frequency (%) of $CD57^{pos}CD16^{pos}CD28^{neg}$ T_{EMRA} $V\delta2^{pos}$ T cell cluster between healthy controls (N=17), and CHT treated (CHT; N=22) and not treated (NO CHT; N=) CLM patients. Results are shown as mean. Statistical significance was calculated with two-way Mann-Whitney unpaired test. *P ≤ 0.05; **P ≤ 0.01; ***P ≤ 0.001; ****P ≤ 0.0001*

The comparison of phenotypical changes observed on γδT cells from PBMCs of CLM patients highlights the different features and impact of CHT treatment on Vδ1^{pos} and Vδ2^{pos} T cell subsets. In general, major differences existing between these two subpopulations in healthy donors were maintained in CLM patients (**Figure 4.19A-B**). Of notice, two markers, including CD69, which identified the tumor-related cluster of Vδ1^{pos} T cells (**Figure 4.14**) and CD57, which together with CD16 discerned the CHT-associated cluster of Vδ2^{pos} T lymphocytes (**Figure 4.18**), were differentially expressed on Vδ1^{pos} and Vδ2^{pos} T cells in CLM patients (**Figure 4.19B**). Interestingly, the expression of CD69 receptor on Vδ2^{pos} T lymphocytes remained very low in both controls and CLM patients (**Figure 4.19A-B**) indicating that the induction of CD69 expression in CLM patients is a specific feature of Vδ1^{pos} T cells (**Figure 4.19B**).

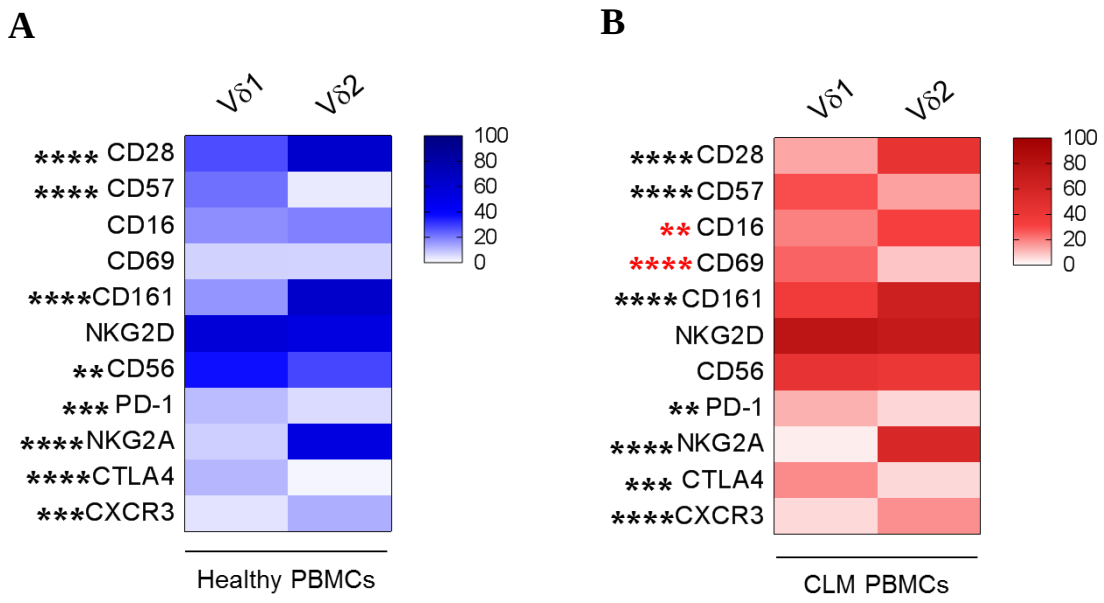

Figure 4.19. Phenotypical differences of γδ T subsets from the PBMCs of healthy donors and CLM patients. (A-B) *Heatmap of the mean of expression (%) of different surface markers measured by flow cytometry on Vδ1^{pos} and Vδ2^{pos} T cells from healthy donor PBMCs (N=48) (A) and CLM patients (N=65) (B). Red stars indicate the marker differentially expressed on Vδ1 and Vδ2 in CLM patients and not in healthy controls. Statistical significance was calculated with two-way, paired t-test. *P ≤ 0.05; **P ≤ 0.01; ***P ≤ 0.001; ****P ≤ 0.0001.*

4.2.5 Immunophenotyping of γδ T lymphocytes from tumor-free and intratumor tissues of CLM patients

To evaluate the tissue-associated γδT cell subsets in patients with CLM we performed a phenotypical analysis of the main relevant markers for Vδ1^{pos} and Vδ2^{pos} T subpopulations derived from the intratumor lesion and the surrounding tumor-free tissue. Both γδT subsets were largely different between these two tissue compartments. For this instance, higher prevalence of less differentiated Vδ1^{pos} T cells inside the tumor (**Figure 4.6C**) was accentuated by the increase expression of CD28 molecule compared to the tumor-free region (**Figure 4.21A**). As expected[141], the tissue-associated phenotype of γδT cells was deductible by high expression of CD69 molecule on both Vδ1^{pos} and Vδ2^{pos} T cell subsets. In particular, the expression of this receptor recently has been linked to the liver-resident Vδ1^{pos} T cell subsets.[141] Indeed, *Davey et. al.* demonstrated that human CD69^{pos} Vδ1 liver-resident cells include two T_{EM} and T_{EMRA} cell subpopulations.[141] The T_{EM} subsets is characterized by a unique TCR-clonality/repertoire, specifically found in the liver and not among PB Vδ1^{pos} T cells while, on the contrary, T_{EMRA} Vδ1^{pos} T cells can recirculate from the liver to the PB, as similar clones were found within both anatomical compartments.[141] To prove the existence, at a clonal level, of recirculating liver-derived Vδ1^{pos} T cells within the increased CD69^{pos} Vδ1^{pos} T cell subset (**Figure 4.14B**) in CLM we performed TCR-sequencing analysis. Obtained result on one CLM patient revealed that specific Vδ1-TCR clones in the PB are shared with the tumor-free tissue and are associated with CD69 expression (**Figure 4.20**). Indeed, 3 out of the 20 majorly represented clones are specifically shared between PB CD69^{pos} Vδ1^{pos} T cells and liver-derived Vδ1^{pos} T cells of the tumor-free tissue (**Figure 4.20**). The same 3 clones are absent in PB CD69^{neg} Vδ1^{pos} T cells, although some other clones are shared between liver and blood independently of CD69 expression (**Figure 4.20**). Further TCR-sequencing analysis on additional CLM patients will clarify if an expansion of liver-derived clones is indeed associated with CD69 expression on PB Vδ1^{pos} T cells of CLM patients.

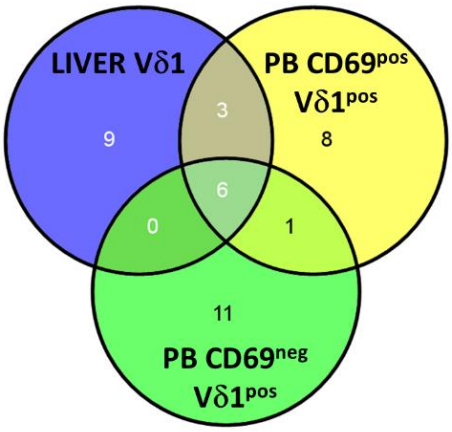

Figure 4.20. TCR-sequencing analysis of PB and liver tumor-free Vδ1 ^{pos} T cells. *Venn diagram showing the number (in white) of liver tumor-free Vδ1-TCR clones shared with CD69^{pos} and/or CD69^{neg} Vδ1^{pos} T cells from PB of one CLM patients. In black, number of shared clones between CD69^{pos} and CD69^{neg} PB Vδ1^{pos} T cells.*

In accordance to literature evidence on the immunosuppressive tumor microenvironment typical of CLM[158,159], we found that intratumor γδT lymphocytes displayed a less effector and cytotoxic phenotype resulting in lower expression levels of activating NKG2D and CD161 receptors in both Vδ1^{pos} and Vδ2^{pos} T cell subsets (**Figure 4.21A-B**). Moreover, intratumor Vδ2^{pos} T lymphocytes expressed lower amount of CD56 further confirming their lower activating profile (**Figure 4.21B**). Whereas higher frequency of PD-1 were observed in intratumor Vδ1^{pos} T cells compared to the tumor-free counterpart, further suggesting a more inhibitory rather than cytotoxic behavior (**Figure 4.21A**). Likewise, higher levels of checkpoint inhibitor CTLA4, were found on Vδ1^{pos} T cells residing the tumor-free region (**Figure 4.21A**).

In line with the low abundance of T_{EMRA} Vδ2^{pos} T cells in the liver tissue (**Figure 4.6D**), both CD57 and CD16 were little expressed in both tumor-free and intratumor compartments (**Figure 4.21B**). Finally, CXCR3 which is involved in the recruitment of T cells to the liver tissue[160], was found at higher levels on both Vδ1^{pos} and Vδ2^{pos} T cell subsets of the tumor-free area compared to the intratumor site, which might explained the lower abundance of γδT cells in this latter compartment (**Figure 4.21A-B**).

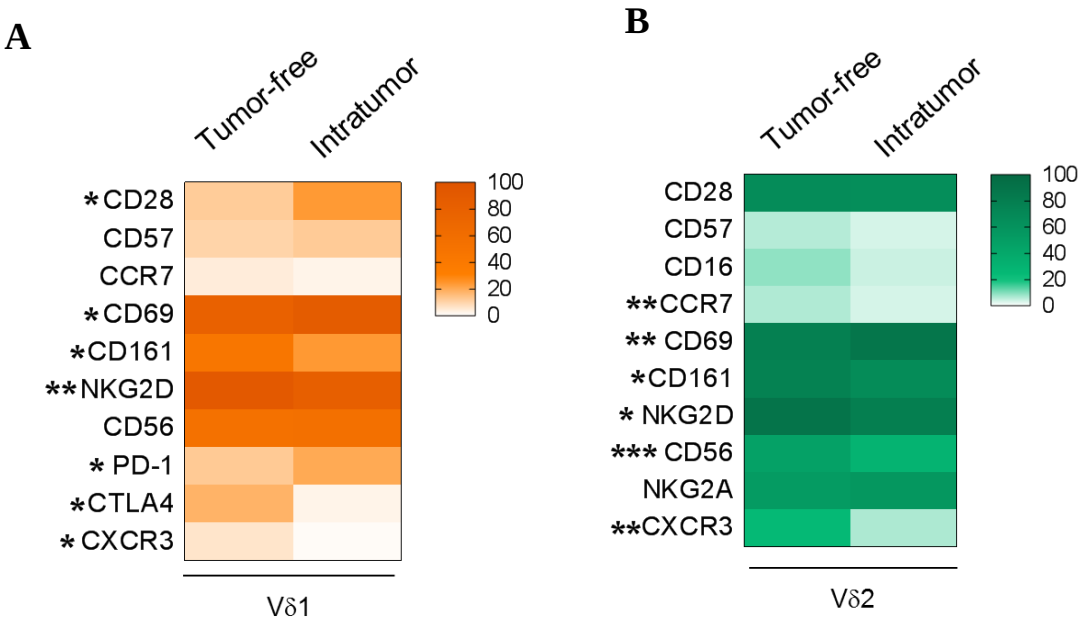

Figure 4.21. Phenotypical differences of γδT cell subsets from the tumor-free and intratumor tissues of CLM patients. (A-B) *Heatmap of the mean of expression (%) of phenotypical markers measured by flow cytometry on Vδ1^{pos} (A) and Vδ2 ^{pos} (B) T cells from tumor-free (N=68) and intratumor tissues (N=21) of CLM patients. Statistical significance was calculated with two-way, Mann-Whitney unpaired test. *P ≤ 0.05; **P ≤ 0.01; ***P ≤ 0.001; ****P ≤ 0.0001.*

Altogether, the phenotypical analysis of the tissue-associated γδT cells suggests an important impact of the tumor microenvironment on the maturation status and the cytotoxic potential of both Vδ1^{pos} and Vδ2^{pos} T cell subsets resulting in the selection of poorly differentiated and less effector populations.

4.3 Clinical relevance of γδ T cell subsets identified in CLM patients

By high-dimensional flow cytometry analysis we identified in the PB of CLM patients two distinct subpopulation of Vδ1^{pos} and Vδ2^{pos} T cells. In this paragraph the clinical relevance of the cluster of the tumor-related CD69^{pos} T_{EMRA} Vδ1^{pos} cells and the CHT-dependent CD57^{pos}CD16^{pos} T_{EMRA} Vδ2^{pos} cells will be assessed separately.

4.3.1 Expression of CD69 on Vδ1^{pos} T cells is associated with better prognosis in CLM patients

CD69 receptor besides being an early marker of activation it is also associated with the tissue- residency of T cells.[161] In addition, in αβ T lymphocytes CD69 identifies the subset of tissue-resident memory (TRM) cells.[162] We found that CD69 molecule is highly expressed by Vδ1^{pos} T cells of both tumor-free and intratumor tissue-regions (**Figure 4.21 and Figure 4.22A**). Moreover, in the blood of CLM patients, CD69 expression can rich up to 60% of total Vδ1^{pos} T cells (**Figure 4.13B and Figure 4.22A**). As previously observed by t-SNE analysis (**Figure 4.14C**), further statistical evaluation on the matched samples of the same patient, confirmed higher expression of CD69 on the specific T_{EMRA} subpopulation (**Figure 4.22B**). Notably, the expression of CD57 on the blood-circulating T_{EMRA} Vδ1^{pos} lymphocytes was inversely correlated to the expression of CD69, thus suggesting that an activating rather than a senescent phenotype is associated with the expression of CD69 on the T_{EMRA} Vδ1^{pos} cells (**Figure 4.22C**) Importantly, in line with the described ability of the liver-resident T_{EMRA} Vδ1^{pos} lymphocytes to recirculate between blood and normal liver tissue of autoimmune disease conditions[141]and also in CLM patients (**Figure 4.20**) we found that higher frequency CD69^{pos} T_{EMRA} Vδ1^{pos} cells in the tumor-free region highly correlates with the increased proportion of this subset in the PBMCs of CLM patients (**Figure 4.22D**). This evidence is indicative of the **increase of activated CD69^{pos} liver-derived T_{EMRA} Vδ1^{pos} cells in PBMCs of CLM patients.**

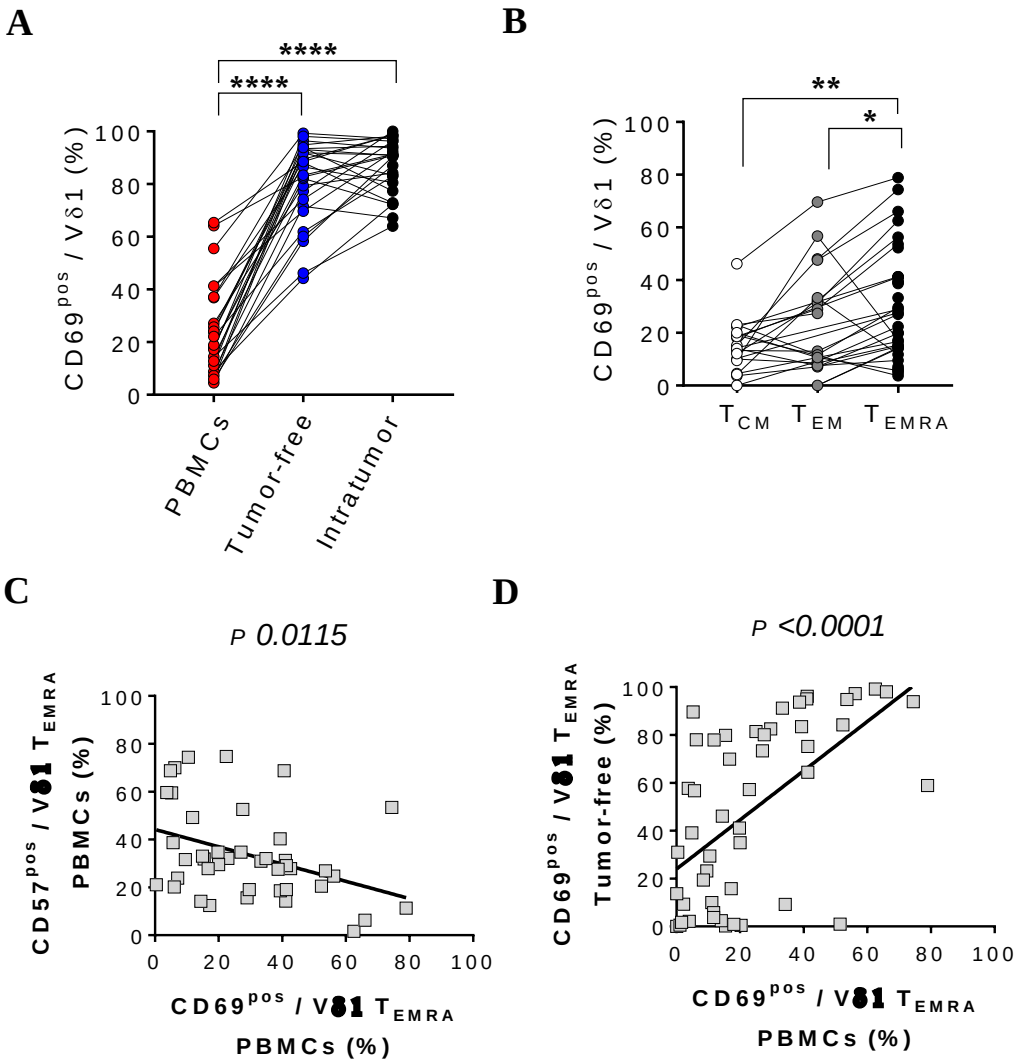

Figure 4.22. Increased frequency of PB CD69^{pos} Vδ1^{pos} T_{EMRA} cells in CLM patients depends on the occurrence of these cells in the liver. (A-B)*Statistical analysis showing the expressions (%) of CD69 receptor on matching Vδ1^{pos} T cell subset in PBMCs, tumor-free and intratumor tissues (A) (N=26) and among T_{CM}, T_{EM} and T_{EMRA} Vδ1^{pos} T cell subpopulations in PBMCs of CLM patients (B)(N=19). (**C-D**) Statistical analysis showing the correlations between the frequency of either CD57 on PBMCs (C) or CD69 on tumor-free (D) Vδ1^{pos} T_{EMRA} T cells and the frequency of CD69 on Vδ1^{pos} T_{EMRA} cells in PBMCs of CLM (n=40). Statistical significance was calculated with two-way, paired t-test. *P ≤ 0.05; **P ≤ 0.01; ***P ≤ 0.001; ****P ≤ 0.0001. For correlation analysis Pearson's coefficient was applied.*

The number of metastatic sites is a strong predictor of CLM patient's survival[15], and specifically in our cohort of CLM patients better survival was found when less than 4 metastatic tumors were present (**Figure 4.23A**). Importantly, higher frequency of CD69^{pos} Vδ1^{pos} T cells in the tumor-free tissue of CLM patients was associated with the development of a lower number of liver metastases (**Figure 4.23B**) suggesting the prognostic relevance of this subset.

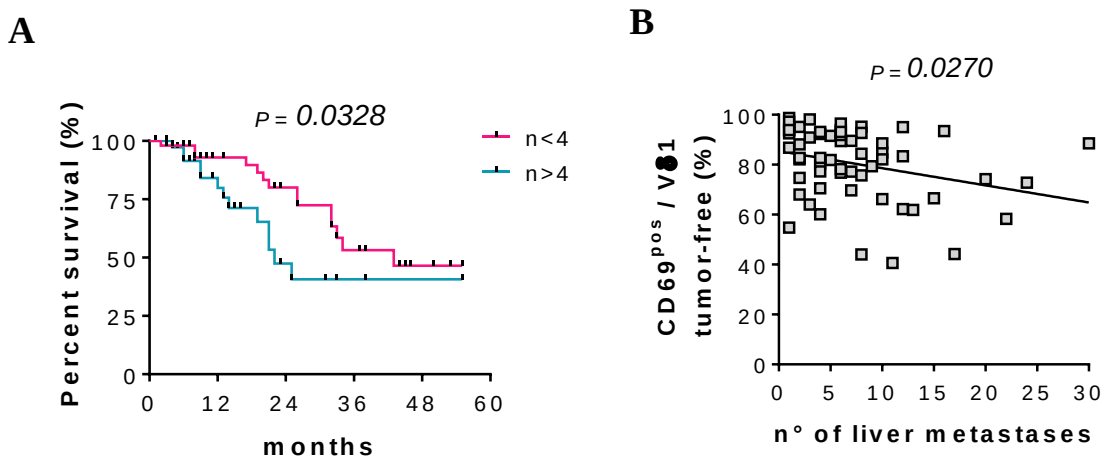

Figure 4.23. Prognostic relevance of CD69 marker in CLM patients. *(**A**) Statistical analysis showing the correlation between the frequency of CD69 on matching Vδ1^{pos} T subset in the tumor-free tissue of CLM (N=77) and the number (n°) of liver metastases. (**B**) Kaplan-Meier survival analysis of CLM patients according to the number of liver metastases: n<4 (pink, N=51) and n>4 (light blue; N=40). For correlation analysis Pearson's coefficient was applied. P ≤ 0.05 were considered statistically significant.*

The possible protective role of T_{EMRA} Vδ1^{pos} cells was further demonstrated by their higher cytotoxic potential. In fact, PB T_{EMRA} Vδ1^{pos} subpopulation from CLM patients, displayed higher levels of CD107a degranulation marker upon Phorbol-Myristate-Acetate (PMA)/Ionomycin stimulation similar to healthy controls. Additionally, CD69^{pos}Vδ1^{pos} T_{EMRA} cells from the tumor-free tissue of CLM patients showed increased expression of CD107a molecule thus, indicating an effector and not exhausted behavior of both tissue-associated and blood-circulating T_{EMRA} Vδ1^{pos} lymphocytes. On contrary, intratumor derived Vδ1^{pos} T_{EMRA} cells displayed highly variable response which resulted with significantly lower degranulation percentage (**Figure 4.24**).

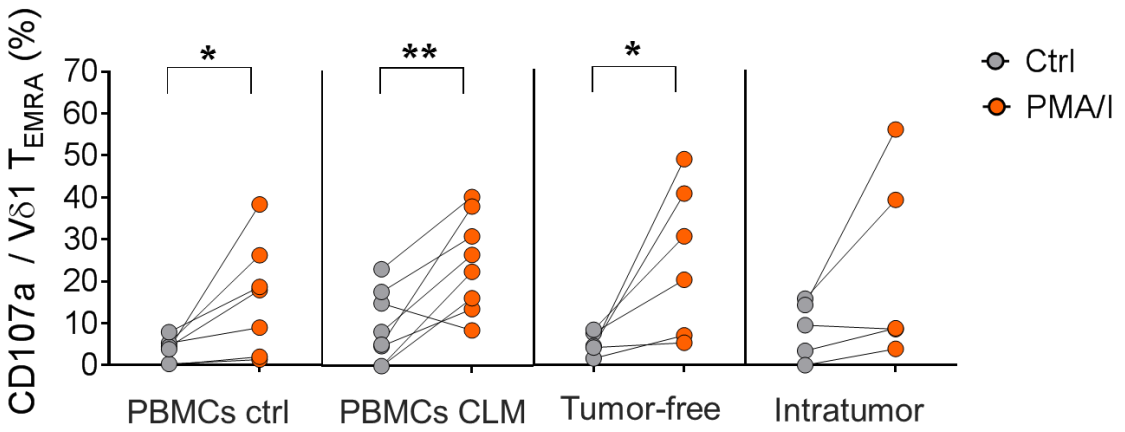

Figure 4.24. Cytotoxic potential of Vδ1^{pos} T_{EMRA} subpopulation in CLM patients. *Statistical analysis showing CD107a expression upon stimulation with PMA/Ionomycin (PMA/I) on Vδ1^{pos} T_{EMRA} subset from PBMCs of healthy donors (ctrl), PBMCs of CLM patients, tumor-free tissue and intratumor lesion (n>5). Statistical significance was calculated with two-way paired t-test. *P ≤ 0.05; **P ≤ 0.01; ***P ≤ 0.001; ****P ≤ 0.0001.*

Since Vδ1^{pos} T cells can be an important source of inflammatory cytokines in the tumor setting[46], we analyzed the intracellular production of interferon (IFN)-γ, tumor necrosis factor (TNF)-α and interleukin (IL)-17 after *in vitro* PMA/I stimulation. We found that TNF-α was the major cytokine produced by Vδ1^{pos} T_{EMRA} cell from both the PBMCs and the tumor-free tissue of CLM patients (**Figure 4.25A**). Importantly, the extent of TNF-α response was similar between T_{EMRA} Vδ1^{pos} cells of PBMCs of CLM patients and healthy donor, demonstrating that the effector function of tumor-related Vδ1^{pos} T_{EMRA} is conserved respect to physiological conditions (**Figure 4.25A**). Diversely, PB T_{EMRA} Vδ1^{pos} cells of CLM patients did not respond with high synthesis of IFN-γ as it was observed in healthy controls (**Figure 4.25B**). In a similar way we did not see IFN-γ release by T_{EMRA} Vδ1^{pos} lymphocytes of the tumor-free tissue (**Figure 4.25B**). Moreover, no IL-17 production was detectable by T_{EMRA} Vδ1^{pos} cells neither in PBMCs of healthy controls nor in PBMCs and tumor-free compartment of CLM patients (**Figure 4.25C**).

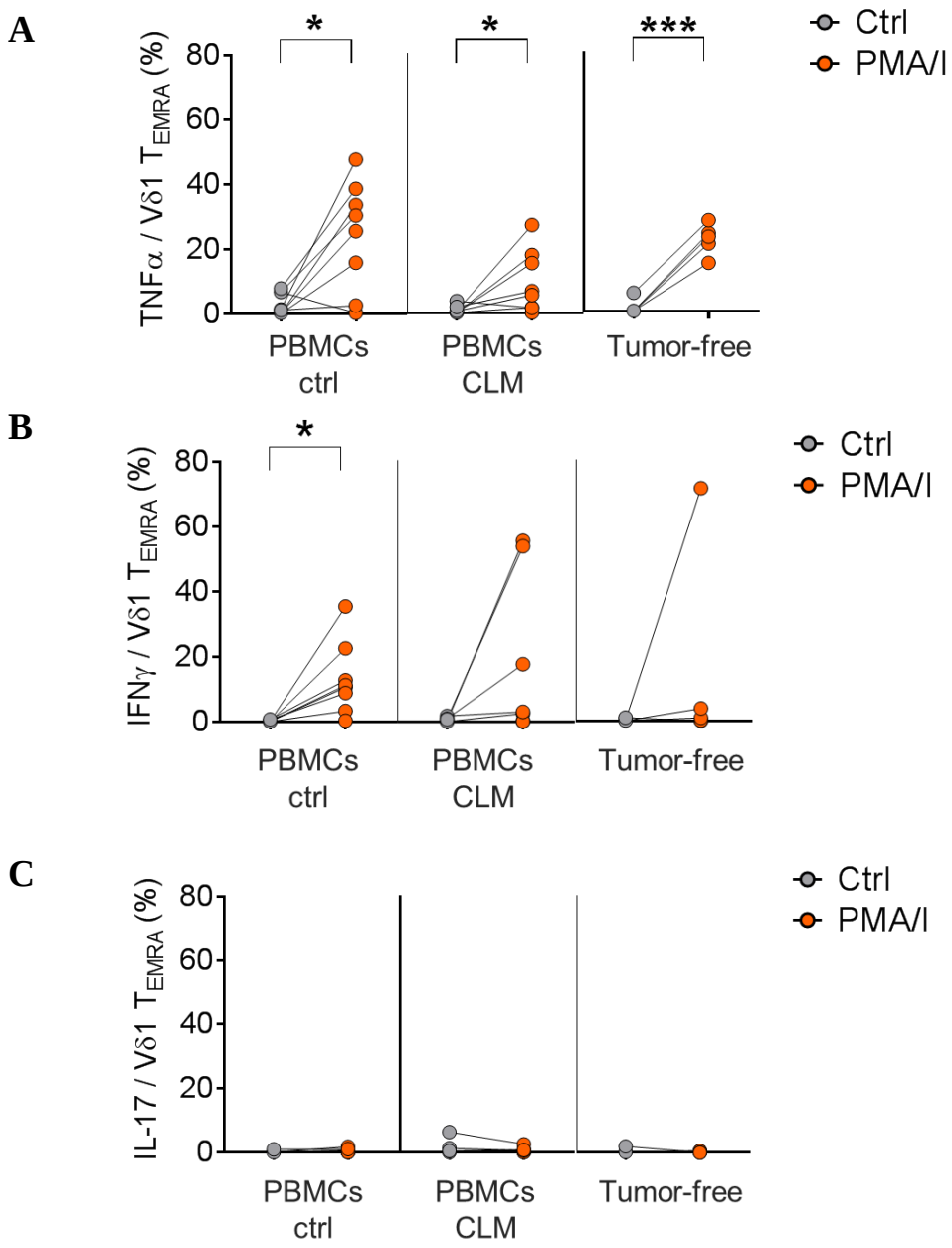

Figure 4.25. Cytokine production by Vδ1^{pos} T_{EMRA} subset in CLM patients. *(**A-C**) Statistical analysis showing TNF-α (A), IFNγ (B), IL-17 (C) intracellular production on Vδ1^{pos} T_{EMRA} subset from PBMCs of healthy donors (Ctrl) and from PBMCs and tumor-free tissue of CLM patients upon stimulation with PMA/I (n>5). Statistical significance was calculated with two-way paired t-test. *P ≤ 0.05; **P ≤ 0.01; ***P ≤ 0.001; ****P ≤ 0.0001*

Altogether, our functional analysis demonstrates that the degranulation capacity and TNF-α production in T_{EMRA} Vδ1^{pos} cells of CLM patients are conserved compared to physiological conditions, in both the PB and the tumor-free tissue compartments, suggesting a similar effector pattern between PB and tissue-derived subsets, which further supports the hypothesis of T_{EMRA} Vδ1^{pos} cells recirculation between liver tissue and blood.

4.3.1 CTLA4 expression on PB Vδ1^{pos} T cells is a favorable prognostic marker in CLM patients

An extensive screening of all phenotypical markers included in our high-dimensional flow cytometry analysis, revealed that the expression of CTLA4 on PB Vδ1^{pos} T cells was associated with a lower rate of metastatic-disease recurrence thus a prolonged recurrence-free survival (**Figure 4.26A**). CTLA4 is an important checkpoint inhibitor of T cells immune-response that increases upon activation.[153] Importantly, prognostic outcome of this marker was independent of other clinical variable including CHT, lymph nodal positivity of the primary tumor (N status) and presence of early liver metastases (developed in less than 1 year from CRC diagnosis) (**Figure 4.26B**).

A

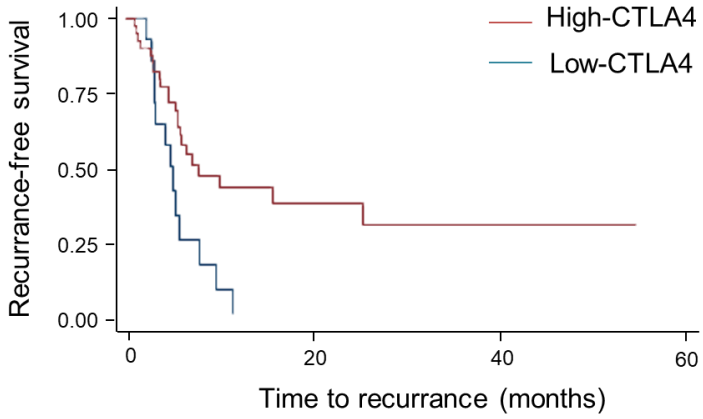

B

Parameter	*Hazard ratio*	*P value*
CTLA4/ Vδ1^{pos}	**0.39**	**0.038**
CHT	1.53	0.527
N status	1.65	0.356
Early CLM	0.54	0.250

Figure 4.26. Clinical relevance of CTLA4 expression on PB Vδ1^{pos} cells in CLM patients. (A) *Recurrence-free survival (RFS) analysis of CLM patients according to the level of expression of CTLA4 (> or < 27.15%) on Vδ1^{pos} cells from PBMCs of CLM patients. High-CTLA4 (red; N=35), Low-CTLA4 (light blue; N=19).* ***(B)*** *Statistical analysis of hazard ratio and corresponding P value of the RFS associated with different parameters including CTLA4 expression on Vδ1^{pos} cells from PBMCs of CLM patients, chemotherapy (CHT) administration, lymph nodal positivity (N status) of primary tumor and the presence of early CLM (developed in less than 1 year from CRC diagnosis). $P \leq 0.05$ were considered statistically significant.*

As we have shown, expression of CTLA4 was higher in CLM patients compared to healthy donors (**Figure 4.12 and Figure 4.15C**). In addition, similar expression of CTLA4 on Vδ1^{pos} T cells was observed between matched Vδ1^{pos} T cells from the PB and tumor-free tissue (**Figure 4.27A**). Interestingly, in the PB of CLM patients the occurrence of CTLA4^{pos} Vδ1^{pos} T cells strongly correlates with its expression on the specific CD69^{pos} Vδ1^{pos} T cell subset (**Figure 4.27B**).

Likewise, expression of CTLA4 on the PB CD69^{pos} Vδ1^{pos} T cell subset matched with higher percentage of CTLA4 levels in the liver tumor-free tissue of Vδ1^{pos} T_{EMRA} cells (**Figure 4.27C**).

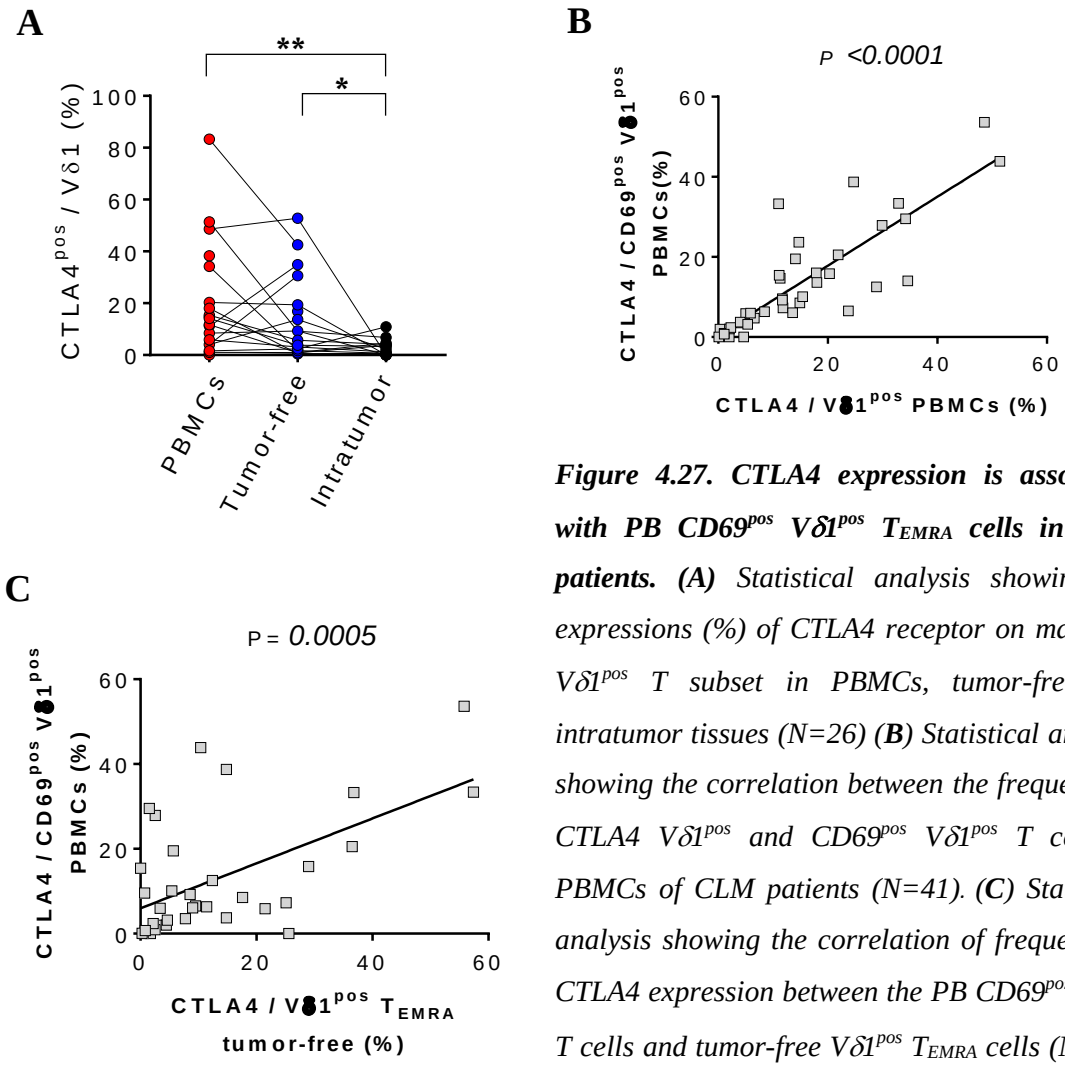

Figure 4.27. CTLA4 expression is associated with PB CD69^{pos} Vδ1^{pos} T_{EMRA} cells in CLM patients. ***(A)*** *Statistical analysis showing the expressions (%) of CTLA4 receptor on matching Vδ1^{pos} T subset in PBMCs, tumor-free and intratumor tissues (N=26)* ***(B)*** *Statistical analysis showing the correlation between the frequency of CTLA4 Vδ1^{pos} and CD69^{pos} Vδ1^{pos} T cells in PBMCs of CLM patients (N=41).* ***(C)*** *Statistical analysis showing the correlation of frequency of CTLA4 expression between the PB CD69^{pos}Vδ1^{pos} T cells and tumor-free Vδ1^{pos} T_{EMRA} cells (N=26). Statistical significance was calculated with two-way, paired t-test. *P ≤ 0.05; **P ≤ 0.01; ***P ≤ 0.001; ****P ≤ 0.0001. For correlation analysis Pearson's coefficient was applied.*

All these data firmly indicate that expression of CTLA4 on PB Vδ1^{pos} T cells depends on the frequency of tumor-related cluster of CD69^{pos} Vδ1^{pos} T_{EMRA} cells and constitutes a favorable prognostic marker for CLM patients.

4.3.2 Age-related changes of Vδ2^{pos} T cells in PBMCs of CLM patients

CD57 receptor is considered a universal marker of senescence, in both αβ and γδT cells. We found that the increased occurrence of T_{EMRA} Vδ2^{pos} in CHT patients highly correlated with the augmented percentage of CD57^{pos} Vδ2^{pos} cells (**Figure 4.28A**). In particular, the expression of CD57 followed the trend of CD27/CD45RA differentiation phenotype since Vδ2^{pos} T_{EMRA} cells showed higher CD57 expression compared to their T_{CM} and T_{EM} counterparts (**Figure 4.28B**). Interestingly, age-related changes were observed in the frequencies of both CD57^{pos} and T_{EMRA} Vδ2^{pos} cell subsets that were significantly higher in CLM subjects receiving CHT treatment after 60 years old (**Figure 4.28C**). The parallel senescent-related phenotypic changes observed with the increased expression of CD57 on Vδ2^{pos} T cells were also related to loss of the CD28 marker that inversely correlated with CD57 and, on the contrary, an increased expression of CD16 (**Figure 4.28D**), the FcγRIII receptor known to define highly differentiated human Vδ2^{pos} T_{EMRA} cells.[148]

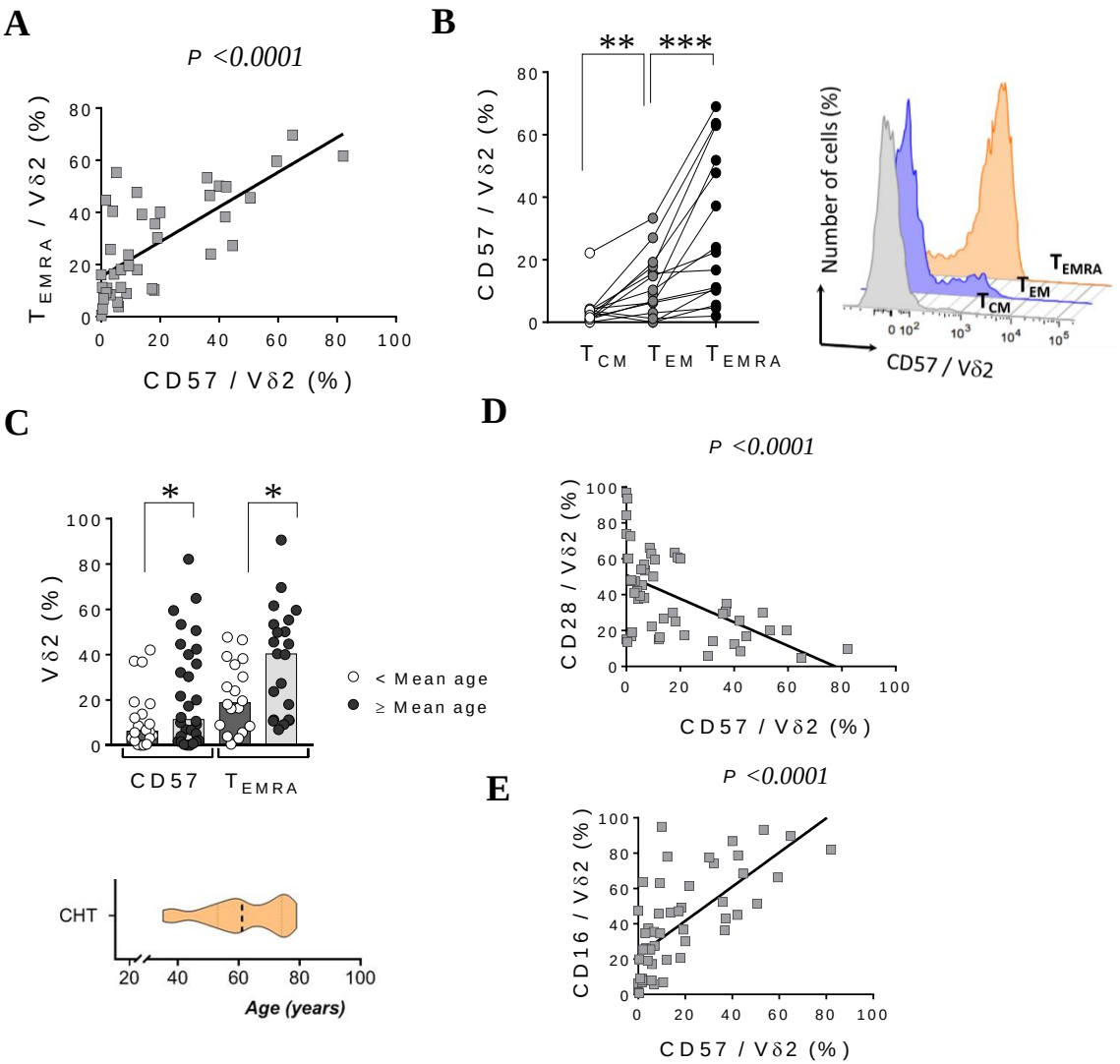

Figure 4.28. Age-related changes in the PB Vδ2^{pos} T cell subsets in CLM patients after CHT treatment. (A) *Scatter graph showing the correlation between the frequencies of CD57 on Vδ2^{pos} T and T_{EMRA} Vδ2^{pos} cells in CLM patients receiving CHT regimen (N=40)* ***(B)*** *Statistical analysis (left graph) and representative histogram plot showing the expressions of CD57 on matching T_{CM}, T_{EM} and T_{EMRA} Vδ2^{pos} T cell subsets in CLM patients receiving CHT regimen (n=15).* ***C)*** *Statistical analysis showing the expressions of CD57 and the frequencies of T_{EMRA} subset on Vδ2^{pos} T cells in CLM patients underwent CHT regimens. CLM patients was sub-divided in two groups: < mean age (empty circles; N ≥18) and ≥ mean age (black circles; N ≥21). The mean age (61 ±10.7 years old) estimated in CHT-treated CLM patient is shown in right upper graph.* ***(D-E)*** *Scatter graphs showing the correlations between the frequencies of CD57 on Vδ2^{pos} T cells and the expression of CD16 (n=51) (D) or CD28 (n=51) (E) on Vδ2^{pos} T cells in CLM patients receiving CHT regimens. Statistical significance was calculated with two-way, paired t-test or unpaired t-test. *P ≤ 0.05; **P ≤ 0.01; ***P ≤ 0.001; ****P ≤ 0.0001. For correlation analysis Pearson's coefficient was applied.*

Further functional characterization revealed that cytokines production, IFN-γ and TNF-α, by Vδ2^{pos}CD57^{pos} was impaired compared to the CD57^{neg} counterpart in CHT patients upon PMA/Ionomycin stimulation (**Figure 4.29**). Similar inhibitory relation of CD57 expression was observed on the degranulation activity observed in Vδ2^{pos} cells (**Figure 4.29**).

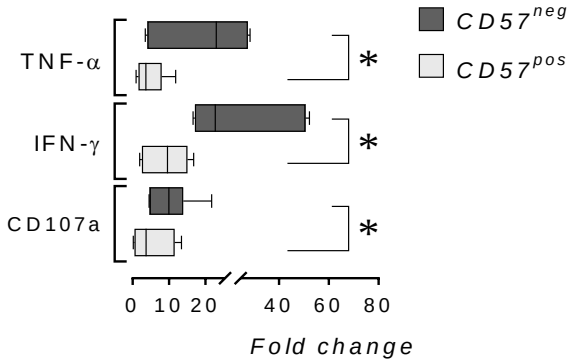

Figure 4.29. Functional analysis of PB Vδ2^{pos} T cell according to CD57 expression. *Statistical analysis showing the fold change increase of cellular membrane CD107a, and intracellular IFN-γ and TNF-α expression in PMA/Ionomycin stimulated cells, in relation to not stimulated controls, analyzed in both effector (T_{EMRA} and T_{EM}) CD27^{neg}CD57^{pos} and CD27^{neg}CD57^{neg} in CLM patients underwent CHT regimens (N=6). Statistical significance was calculated with two-way, paired t-test *P ≤ 0.05; **P ≤ 0.01; ***P ≤ 0.001; ****P ≤ 0.0001.*

5. Conclusions

During this PhD project we characterized the two main human subsets, Vδ1^{pos} and Vδ2^{pos}, of γδT cells in patients affected by colon-derived liver metastases (CLM). We performed an extensive phonotypical analysis of γδT cells derived from PBMCs, tumor-free and intratumor liver tissue compartments of CLM patients. We found several and considerable changes in the frequency, maturation and activation status of both Vδ1^{pos} and Vδ2^{pos} T cells that mainly implicated the peripheral blood (PB) γδT cell compartment of CLM patients.

In particular, we identified a tumor-related and activated cluster of CD69^{pos} Vδ1^{pos} T_{EMRA} cells endowed with high antitumor potential. Both the increase of PB Vδ1^{pos} T_{EMRA} cells as well as the induction of CD69 receptor in CLM patients were independent of chemotherapy and associated with the higher expression of antitumor receptor NKG2D and CD161 molecule and negative expression of CD28. The tumor-associated origin of the cluster was deduced by the strong correlation in the frequency of CD69 expression on Vδ1^{pos} T_{EMRA} cells between PB and tumor-free liver tissue. Moreover, we found a common TCR-repertoire between liver tissue and PB CD69^{pos} Vδ1 cells in CLM patients. Importantly, the increased occurrence of CD69 expression on tissue Vδ1^{pos} T cells was associated with the lower number of metastases in these patients, revealing the protective role of this subset in the control of metastatic spreading. In addition, higher expression of CTLA4, which expression depends on the frequency of the specific cluster of PB CD69^{pos} Vδ1^{pos} T cells, was linked to prolonged disease free survival in CLM patients.

Thus, we described the existence of the liver-derived and blood recirculating CD69^{pos}CD161^{pos}NKG2D^{pos}CD28^{neg} Vδ1^{pos} T_{EMRA} cells, which reflects the tumor-related Vδ1^{pos} T cells activation and metastases protection that has a potential to represent a novel immunotherapeutic target for CLM patients. Moreover, the occurrence of CTLA4 on PB CD69^{pos} Vδ1^{pos} T cells represents a candidate prognostic biomarker for CLM patients (**Figure 5.1)**.

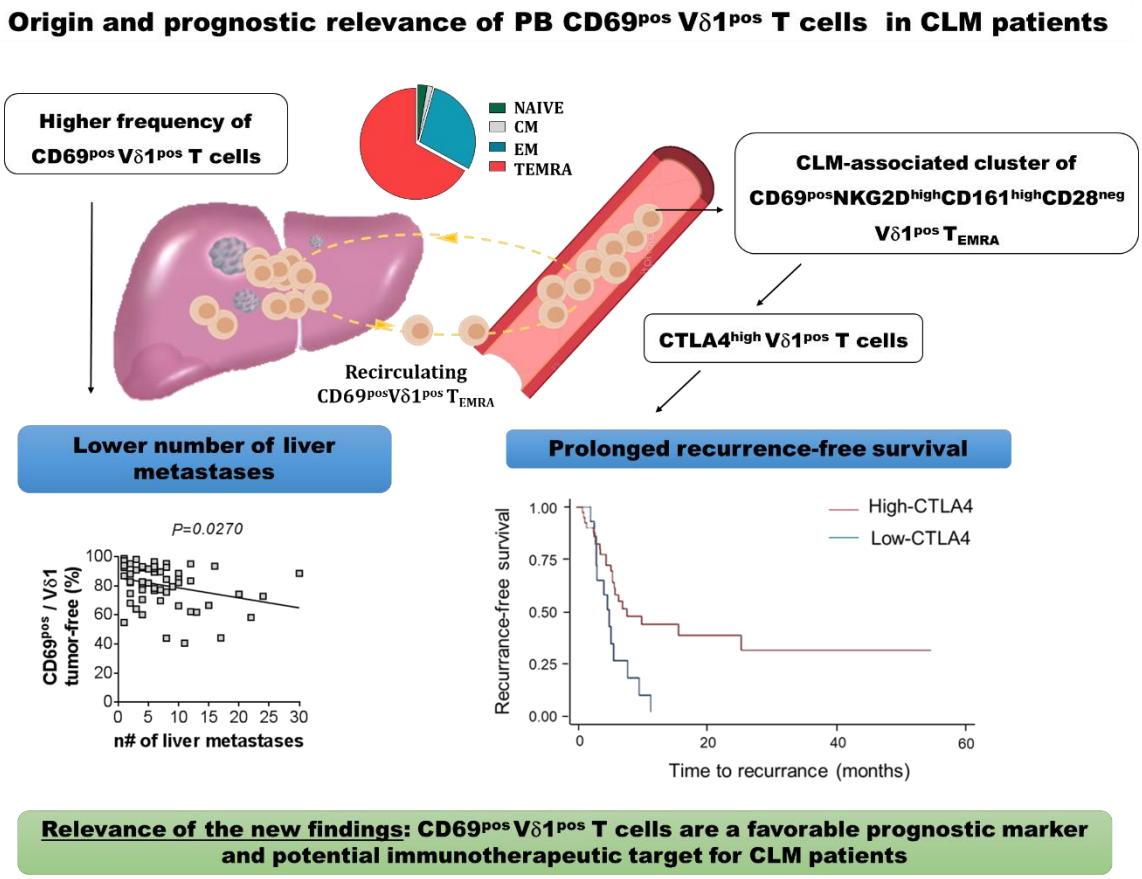

Figure 5.1 Model on the origin and prognostic relevance of the peripheral blood CD69^{pos} Vδ1^{pos} T cell subset in CLM patients. *From the upper left) According to the number of liver metastases, CLM patients present different frequency of CD69^{pos} Vδ1^{pos} T cells: patients with lower number of liver metastases, in the tumor-free area, present higher frequency of tissue CD69^{pos} Vδ1^{pos} cells that mainly are represented by two T_{EMRA} and T_{EM} subpopulations (upper pie chart). Liver CD69^{pos} T_{EMRA} Vδ1 T cells are able to enter the bloodstream (yellow dashed arrow) and define the new PB CLM-associated cluster of CD69^{pos} T_{EMRA} Vδ1^{pos} T cells characterized by high expression of NKG2D and CD161. Moreover, higher expression of CTLA4 on PB Vδ1^{pos} T cells which depends on the occurrence of CD69^{pos} T_{EMRA} Vδ1 T cells in the liver, is associated with prolonged recurrence free survival of CLM patients. Thus, determination of PB Vδ1^{pos} CD69^{pos} T cells in association with the expression of CTLA4 that relates on the activation status of Vδ1 T cells at the liver site might represent a favorable prognostic marker and potential immunotherapeutic target for CLM patients.*

The analysis of Vδ2^{pos} T cells revealed a major impact of chemotherapy (CHT) on the phenotype of this subset. We identified a large and persistent senescent CD57^{pos}CD28^{neg}CD16^{pos}T$_{EMRA}$ Vδ2^{pos} T cell cluster that was more pronounced in CHT treated patients compared to untreated patients and to healthy controls. An important component of this shift was the increased frequency of highly differentiated T$_{EMRA}$ Vδ2^{pos} T cells that, along with CD57^{pos} cells, showed better resistance to chemotherapeutic agents. Our study also revealed the induction of a premature CHT-related senescent phenotype that was particularly pronounce in elderly patients. Moreover, CD57 expression on Vδ2^{pos} T cells in CHT patients was associated with an impaired functional response. Indeed, both cytokines production, IFN-γ and TNF-α, and degranulation capacity (CD107a expression) were lower compared to the CD57^{neg} counterpart upon PMA/Ionomycin stimulation.

Thus, our data besides providing a further evidence of the existence of senescent Vδ2^{pos} T cells endowed with a specific phenotypic and functional profile also offer a hint on how anti-cancer treatment should be refine to improve the efficacy of Vδ2^{pos} T cell-based immunotherapy (**Figure 5.2**).

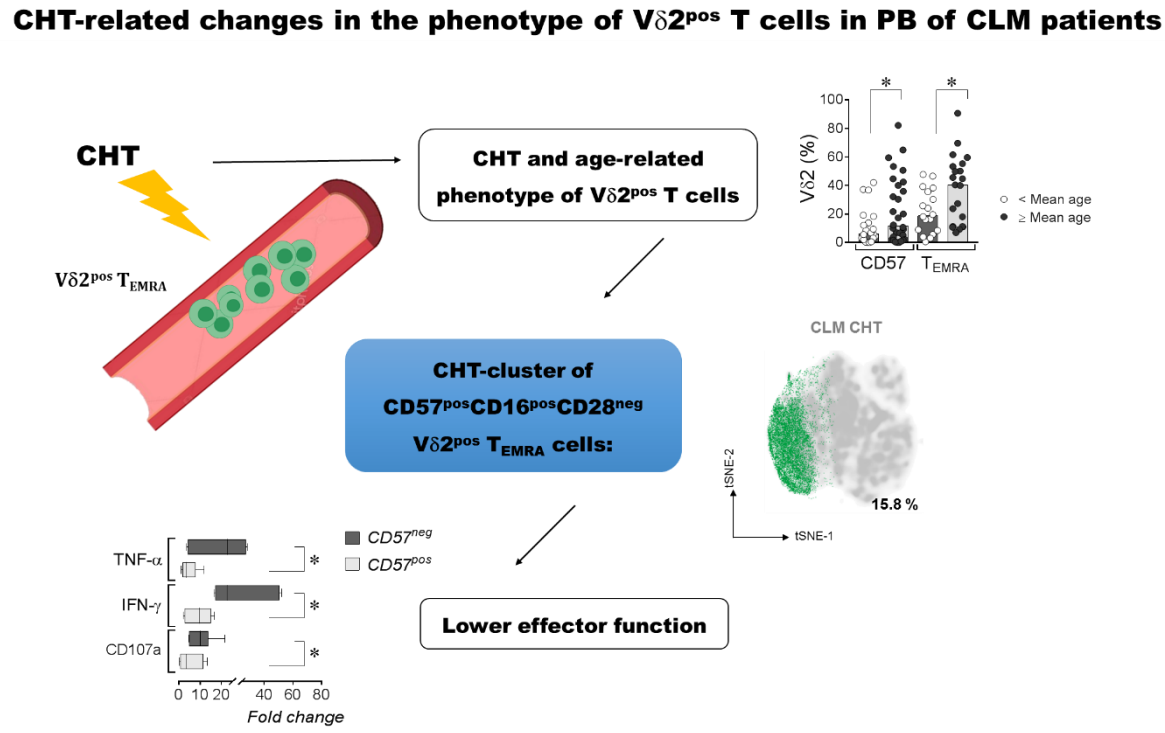

Relevance of the new finding: evidence of Vδ2^{pos} T cells senescent phenotype to consider for the improvement of anti-cancer treatment based on expanded Vδ2^{pos} T cells

Figure 5.2 CHT-related changes in the phenotype and function of Vδ2^{pos} T cells in PB of CLM patients. *From left to right) CHT has a major effect on the maturation status of PB Vδ2^{pos} T cells that result in the higher proportion of T_{EMRA} subpopulation and increased CD57 expression on Vδ2^{pos} T cells. This senescent phenotype is more pronounced in elderly patients and is associated with the higher expression of CD57 and CD16 that marks highly differentiated cells. Moreover, the identified CHT-cluster of CD57^{pos}CD16^{pos}CD28^{neg} Vδ2^{pos} T_{EMRA} is endowed with lower degranulation capacity (CD107a^{low}) and cytokine production (INF-γ^{low} and TNF-α^{low}). For these reasons, the occurrence of senescent Vδ2^{pos} T cells has considerable implications in the development of effective Vδ2^{pos} T cell-mediated therapeutic approaches.*

In conclusion, our study allowed the identification of the specific subpopulations of Vδ1^{pos} and Vδ2^{pos} T cells strictly associated with the pathological condition and CHT-treatment of CLM patients that will be extensively and separately discussed in the next paragraph.

6

Discussion

6.1 CD69 marker detects tumor-related and liver-recirculating Vδ1^{pos} T_{EMRA} cell in the peripheral blood of CLM patients

Vδ1^{pos} T cells constitute the main liver tissue-associated subset of total T lymphocytes and γδT cells, comprising up to 80-90% of total γδT cell population.[39,141] Nevertheless, the exact contribution of Vδ1^{pos} T cell subset in the progression of liver metastatic disease is still undefined.

Our work provides an extensive phenotypical characterization of human circulating and liver/tumor-associated Vδ1^{pos} T cells in CRC patients developing liver metastases. We observed substantial changes affecting both the frequency and maturation status of Vδ1^{pos} T cells of CLM patients compared to the one of healthy individuals. In particular, CLM patients are characterized by increased frequency of the specific T_{EMRA} subpopulation on PB Vδ1^{pos} T cells. T_{EMRA} cells correspond to the latest stage of αβ and γδ T cells differentiation, and thus are characterized by high effector function but low proliferative capacity. This feature, explains the higher resistance of PB Vδ1^{pos} T cells to CHT toxicity. Indeed, the absolute number of PB Vδ1^{pos} T cells does not change in CLM patients compared to healthy controls. Whereas CD3^{pos} and Vδ2^{pos} T lymphocytes appeared more sensitive to CHT toxic effect and lower absolute count of these cell subsets are found in the blood of CLM patients. For this reason, the increased frequency of Vδ1^{pos} T cells on total PB T lymphocytes, seen in CLM patients, is probably the indirect consequence of the CHT-dependent reduced number of αβT cells and Vδ2^{pos} T cells and not of Vδ1^{pos} T lymphocytes, which consist for about 70% of low proliferating, and thus CHT-resistant T_{EMRA} cells.

However, CHT is not the only cause of increased Vδ1^{pos} T_{EMRA} cells in PBMCs of CLM patients. In fact, several CHT-independent changes emerged from the phenotypical analysis of PB Vδ1^{pos} T cells.

First of all, we observed a significant upregulation of the CD69 molecule, a well-established marker of early T cell activation. Indeed, expression of CD69 on the surface of PB Vδ1^{pos} T cells from healthy individuals, have already been linked to higher cytotoxic responses compared to Vδ2^{pos} and CD69^{neg} T cells.[122] In particular, CD69^{pos} Vδ1^{pos} T cells displayed higher cytotoxicity against adherent and metastatic sphere-forming CRC-derived tumor cells.[122]

Our analysis revealed that expression of CD69 on PB Vδ1^{pos} T cells of CLM patients is strictly associated to T_{EMRA} subpopulation and to higher levels of NKG2D, a key regulator of γδT cells antitumor activity, suggesting the antitumor effector potential of this specific cancer-related Vδ1^{pos} T cell subpopulation. For this instance, it is known that NKG2D is constitutively expressed by γδT cells and its engagement, can potentiate TCR responsiveness thus resulting in degranulation and target cell lysis. NKG2D expression is involved in tumor cell recognition by both human PB[163,164] and tumor-infiltrating[165] γδT cells. In particular, MICA expression on epithelial tumors, including CRC, drives NKG2D-dependent Ag-recognition and tumor-killing activity of PB γδT cells.[163] In gastric cancer patients, high levels of NKG2D ligands' expression, MICA and MICB, on tumor cells represents a favorable prognostic marker associated with increased survival.[166] In fact MICA and MICB are prevalently expressed in epithelial tumors, where they contribute in the promotion of γδT cells antitumor functions.[167,168] For instance, Vδ1^{pos} T cell lines obtained from different tumors, including colon cancer, recognized MICA and MICB in both autologous and heterologous conditions.[165] Moreover, *in vitro* study, using human-derived CRC primary cell lines, demonstrated that the cell surface stabilization of NKG2D ligands had an inhibitory effect on the CRC cell lines metastatic ability,[169] confirming the important role of NKG2D-mediated antitumor response in CRC. It would be interesting to evaluate the degree of expression of NKG2D ligands on liver metastases and the related functional response of Vδ1^{pos} T cells.

Another receptor strictly correlated with the cluster of CD69^{po}NKG2D^{pos} Vδ1^{pos} T_{EMRA} cells is CD161. This receptor is found on both NK cells and T cells[170], however the exact functions associated with its expression remain controversial[171]. In NK cells, CD161 binding with its ligand LLT1 inhibits NK cell cytotoxicity and cytokine secretion.[170] Whereas a costimulatory role of CD161 has been proposed in case of T cells.[152] In fact, IL-12 and IL-18 stimulation can induce an innate-like and TCR-independent response, based on IFN-γ production, in both αβ and γδT cells[152]. Importantly, CD161 is also expressed on memory T cell subsets[172] with tissue-homing capacity[151]. For example, HCV-virus specific CD8^{pos} T cell subsets expressing CD161 are particularly enriched in the human liver, during chronic hepatitis.[173] Here, we found that CD161 is highly expressed on liver-derived Vδ1^{pos} T cells (44% of total Vδ1^{pos} T cells) and increased levels of this molecule are associated to the cluster of tumor-related (CHT-independent) activated (CD69^{pos}, NKG2D^{pos}) and highly differentiated ($T_{EMRA,}$ CD28^{neg}) Vδ1^{pos} T cells, which is increased in PBMCs of CLM

patients. Although the meaning of the higher expression of CD161 molecule in PB Vδ1^{pos} T cells of CLM patients is quite controversial, as multiple functions have been linked to this specific receptor, its antitumor relevance recently emerged from the transcriptomic analysis of several human malignancies.[174] In fact, in this study, Gentles and colleagues, identified CD161 as the most favorable cancer-wide prognostic gene,[174] stressing the importance of dissecting the specific features of CD161^{pos} γδT cells in CLM as well as other tumor settings.

To understand the origin of the cancer-related CD69^{pos} T_{EMRA} Vδ1^{pos} T subset two main facts must be considered. First of all, CD69 receptor is a largely accepted marker of tissue-residency for immune cell,[161] indeed, we found high levels of this molecule in both tumor-free and intratumor-derived γδT cell subsets. Second, TCR-sequencing analysis already revealed the existence of recirculating liver-associated Vδ1^{pos} T_{EMRA} cells in patients with end-stage liver disease, including mainly autoimmune conditions.[141] In CLM patients, we observed a direct correlation in the frequency of CD69 expression on T_{EMRA} Vδ1^{pos} T cells between blood and tumor-free compartments. Thus, we hypothesize that liver-derived recirculating CD69^{pos} T_{EMRA} Vδ1^{pos} T cells are enriched in the blood of CLM patients. Indeed, the analysis on one CLM patient, revealed that specific clones are shared between tumor-free Vδ1^{pos} T cells and PB CD69^{pos} Vδ1^{pos} T cells and that same clones are absent on the CD69^{neg} Vδ1^{pos} T cell counterpart. A more detailed TCR-repertoire analysis on more CLM patients will clarify our hypothesis on the existence of recirculating tumor-specific and liver-derived clones associated with CD69 expression on PB Vδ1^{pos} T cells. Moreover, TCR-sequencing analysis will reveal possible clonal expansion of tumor-induced Vδ1^{pos} T cells in CLM patients.

So far adaptive-like responses that imply the expansion of specific Vδ1^{pos} T clones have been described only in the presence of human cytomegalovirus (CMV) infections.[69] For this reason, it would be relevant to evaluate if the CMV serological status of CLM patients is associated anyhow to the higher abundance of Vδ1^{pos} T_{EMRA} or to the upregulation of CD69 expression on PB Vδ1^{pos} T cells.

A possible function of CD69^{pos} Vδ1^{pos} T_{EMRA} cells recirculation could be to keep the liver immunological memory and thus act as immune-sentinels. Similar role has, in fact, been proposed in case of skin-derived CD4^{pos} T cells, which are found in the blood of healthy individuals.[175] In this study, *Klicznik* and colleagues, found that CD4^{pos}CD69^{pos}CD103^{pos} T cells exit from skin tissue and constitute a unique population in the blood with specific

cytokine profile and gene signature consistent with host-defense and tissue-repair responses.[175] This general role of functionally specialized T memory subsets could be apply also for CD69^{pos} Vδ1^{pos} T_{EMRA} cells in CLM patients. It is possible that tumor-reactive Vδ1^{pos} T_{EMRA} clones are induced at the early stage of CRC development and persist in the circulation of CLM patients. This persistence of recirculating Vδ1^{pos} T_{EMRA} cells could be a mechanism of control of tumor progression. Indeed, CLM patients with higher frequency of CD69^{pos} Vδ1^{pos} T cells within the tumor-free compartment experience a lower number of liver metastasis further suggesting the antitumor-protective role of this subset.

The antitumor role of Vδ1^{pos} T cells has been explored in different human hematological malignancies including, lymphoma and leukemias.[98,124] For example a significant amelioration of disease-free survival has been observed in patients with acute leukemia upon allogenic bone marrow transplantation after αβT cells depletion.[176] Whereas analysis of intratumoral Vδ1^{pos} T cells of colon tumors revealed their cytotoxic activity in response to both autologous and heterologous tumor targets.[177] Moreover expanded Vδ1^{pos} T cells from melanoma patients, produced high amount of both TNF-α and IFN-γ and killed melanoma cell lines.[106] However, protumor role associated with the Vδ1^{pos} T cell subset have also been described.[110] In particular, in breast cancer, the higher occurrence of infiltrating γδT cells correlated with worse clinical outcome and the protumor role of Vδ1^{pos} T cells was associated with the production of IL-17.[178] Similar, infiltration of IL-17^{high} γδT cells in CRC patients was associated with their lower survival.[177]

By immunohistochemistry analysis we observed that the majority of γδT cells are located at the invasive margin of liver metastases. This preferential localization could be the result of ongoing interaction with tumor cells. For instance, Vδ1^{pos} T cells of the liver tumor-free compartment exhibit a more cytotoxic phenotype compared to the intratumoral counterpart, which results in higher prevalence of Vδ1^{pos} T_{EMRA} and increased expression of activating NKG2D receptor. Of notice this same cells, differently from intratumor ones, present increased levels of CTLA4. This molecule is involved in the immune regulation of T cells and it is induced upon antigen-specific activation.[153] The signaling pathway regulated by CTLA4 binding to B7 ligands on the surface of antigen presenting cells[155] is generally targeted by therapeutic approaches aiming at favoring cytotoxic T cell responses[179]. Indeed, CTLA4 activation generates inhibitory signals, which eventually limit T cell activation.[155] Interestingly, we found that the expression of CTLA4 on tumor-free T_{EMRA} cells directly correlates with its higher expression on the subset of PB CD69^{pos} Vδ1^{pos} T cells thus

suggesting their recirculation. Remarkably, CLM patients with higher levels of CTLA4 on PB Vδ1^{pos} T cells showed prolonged recurrence free survival, underlining the prognostic significance of CTLA4 marker expression on Vδ1^{pos} T cells and its possible association with tumor-reactive clones. A tumor-reactive phenotype associated with the expression of CTLA4 have been also described for CD8^{pos} T cells.[180] From the analysis of six different human malignancies it was revealed that CTLA4 gene transcripts were specifically enriched on tumor Ag-specific T cells from both primary and metastatic lesions. Furthermore, this subset of tumor-reactive CD8^{pos} T cells showed cytotoxic-activity against autologous tumor cells.[180]

Expression of CTLA4 is associated with an exhausted phenotype[181] and corresponded to the 9% of PB CD69^{pos} Vδ1^{pos} T_{EMRA} cells. Nevertheless, Vδ1^{pos} T_{EMRA} subpopulation, displayed high degranulation capacity in response to PMA/Ionomycin stimulation with similar degree of response between PB and tissue-derived subsets. Moreover, patient-derived Vδ1^{pos} T_{EMRA} were capable of producing high amount of the inflammatory cytokine TNF-α. The release of this cytokine, in the tumor context, is associated with controversial an opposing functions related to the binding of two different receptors.[182] TNF receptor type I (TNFR1), which is broadly expressed on many cell types, and TNF receptor type II (TNFR2) that is more restricted to immune cells and some type of tumor cells. In particular, it was reported that TNFR2 expression on CD8^{pos} effector T cells drives the activation and cytotoxic activity of this subset.[182] Regarding γδT cells, the role TNF-α production remains largely undefined. *Li et al.* demonstrated that TNF-α/TNFR2 signals is necessary for the antitumor cytotoxic response of Vδ2^{pos} T cells,[183] while no reports exist on the effect of TNF-α pathway on Vδ1^{pos} T cells. Thus, a more detailed analysis should be performed to evaluate the TNF-α-mediated antitumor role in CLM patients.

Although we did not report any direct antitumor-activity of Vδ1^{pos} T cells from CLM patients, our data strongly support the existence of tumor-related subset/clones within the cluster of CD69^{pos}CD161^{pos}NKG2D^{pos}CD28^{neg} Vδ1^{pos} T_{EMRA} cells. We showed that this cluster is induced in the presence of metastatic liver disease and has important prognostic relevance for both the survival and disease free recurrence of these patients. The further identification of specific and tumor-reactive clones within the CD69^{pos} Vδ1^{pos} T cell subsets will represent an important achievement for the future immunotherapeutic treatment of CLM patients. However, we cannot excluded that the cluster of CD69^{pos} Vδ1^{pos} T cells include

different subsets endowed with diverse functions including regulatory activity. For instance, a minor subpopulation of $CD86^{pos}V\delta1^{pos}$ T cells also emerged from the t-SNE analysis.

Considering the adaptive nature of $V\delta1^{pos}$ T cells, the identification of antitumor-$V\delta1^{pos}$ T cells/clones has crucial relevance for γδT cells-based immunotherapeutic approaches. The use of diverse γδT cell subsets, a part from the Vγ9Vδ2 T cell subpopulation, or the identification of tumor specific clones would definitely improve the efficacy of γδT cells-based cancer therapy. Up to date, all the clinical trials reported, relied on the adoptive transfer of *in vitro* expanded $V\delta2^{pos}$ T cells. Whereas, in the last years, new protocols have been published for the *in vitro* activation and expansion of $V\delta1^{pos}$ T cells.[125] In this setting, expanded delta one T (DOT) cells from healthy donors displayed potent cytotoxicity against chronic lymphocytic leukemia (CLL) cells in both *in vitro* and *in vivo* models. This tumor-killing activity was mainly driven by the acquisition of an innate-like and natural cytotoxicity receptors-dependent phenotype.[120,125] The adaption of the same protocol for the expansion of CLM-derived $V\delta1^{pos}$ T cells could be of potential interest to obtain more patient/tumor-specific reactive clones and could be applied also for the expansion of liver-resident subsets. Indeed, some proliferative capacitive has been observed on *in vitro* cultured T_{EMRA} cells.

In conclusion in this work we describe a cancer-related subpopulation of $CD69^{pos}CD161^{pos}NKG2D^{pos}CD28^{neg}$ $V\delta1^{pos}$ T_{EMRA} cells with possible liver-recirculating capacity and important prognostic relevance in CLM patients. In general, our experimental approach represents a valid strategy for the identification of tumor-related cell subset that could be easily extendable to other immune-cell population and cancer conditions to finally improve current therapeutic strategies.

6.2 Impact of CHT-induced age-related changes of Vδ2^{pos} T cells on immunotherapeutic approaches for CLM patients.

The analysis of the Vδ2^{pos} γδT cell subset in CLM patients, revealed the existence of previously described senescent T cells.[184] We focused our study on the effect of CHT treatment by comparing control groups, including non CHT treated CLM patients and healthy donors, with CHT cohort. We found that patients receiving CHT showed a significantly higher Vδ2^{pos} T cell population with an immune-senescent profile, consisting of CD57^{pos}CD28^{neg}CD16^{pos}T$_{EMRA}$, as also revealed by *t-SNE* analysis. Increased occurrence of CHT-mediated senescent Vδ2^{pos} T cells can be triggered by two major mechanisms. Primarily, CD57^{pos}T$_{EMRA}$ Vδ2^{pos} T cells display better resistance to DNA-damaging chemotherapeutic agents compared to other subpopulations, a further evidence of their senescent properties and of the existence of Vδ2^{pos} T senescent cells *in vivo*. Additionally, the age of the patient constituted an important factor for the increased amount of Vδ2^{pos} T senescent cells. For instance, increased proportions of both CD57^{pos} and T$_{EMRA}$ Vδ2^{pos} T cells were found among patients over 60 years old, thus indicating the presence of an enhanced number of senescent Vδ2^{pos} T cells in the elderly population.

Of note, the senescent profile of Vδ2^{pos} T cells persisted post-cancer treatment, on the average of six weeks after completion of CHT, suggesting a lower recovery rate compared to Vδ1^{pos} T cell subset that did not show increased expression of CD57 marker. A longer observation period, at different time points, will be necessary to determine if immune-reconstitution of Vδ2^{pos} T cells can counterbalance their senescence signature. Moreover, further studies will be needed to determine if the frequency of senescent CD57^{pos}T$_{EMRA}$ Vδ2^{pos} cells has any implication on the overall survival of CLM patients and on their response to therapy. In fact, prolonged expression of CD57 on αβT cells in gastric cancer was associated with lower patients' survival.[185] Senescence process is potentially reversible upon inhibition of p38 mitogen-activated protein kinase (MAPK) signaling.[186] If senescence is indeed reversible, then the specific re-appearance of T cells after CHT-induced could represent and effective approach to improve cancer immunotherapies.

Lately *Weili Xu et al*. proposed that CD57 is the only marker that defines senescent status on Vδ2^{pos} T cells and correlates with the shortening of telomere lengths.[145] In addition, the authors did not see any correlation between expression and kinetics of both CD27 and CD45RA markers on Vδ2^{pos} T cells along progressive shortening of telomere ends.[145]

Therefore, there is still controversy on how to exactly define replicative senescence of Vδ2^{pos} T cells (i.e. to use the CD57 marker, either alone or in combination with CD27 and CD45RA or other markers) in both physiological and pathological conditions. We found that, at least in a human cancer setting, expression of both CD27 and CD45RA markers correlates with CD57^{pos} and CD28^{neg} senescent Vδ2^{pos} T cell phenotype. This phenotypic profile defines different effector functions of Vδ2^{pos} T cells. Indeed, Vδ2^{pos} T_{EMRA} cells result to be resistant to phosphoantigen stimulation, but rather respond to activation via FcγRIII (CD16).[148] On the other hand, preserved proliferating capacity *in vitro* of T_{EMRA} Vδ2^{pos} cell subset has been recently reported.[187,188]

In conclusion, the present work shows that Vδ2^{pos} T cell immune-senescence is more pronounced in aged CHT treated patients than in controls. The majority of cancer patients are over the age of 65 years at diagnosis,[189] therefore, large prospective trials in the elderly population are needed to better understand mechanisms underlying T cell senescence in cancer and cancer therapy. Therefore, the potential of Vδ2^{pos} T cells in cancer immunotherapy has to be investigated more extensively.

Bibliography

1. Bray, F. *et al.* Global cancer statistics 2018: GLOBOCAN estimates of incidence and mortality worldwide for 36 cancers in 185 countries. *CA: a cancer journal for clinicians* **68**, 394–424 (2018).
2. AIRTUM. *I Numeri del cancro in Italia 2018*. (2018).
3. Xu, J. *et al.* Trends in Liver Cancer Mortality Among Adults Aged 25 and Over in the United States, 2000-2016. *NCHS Data Brief* 1–8 (2018).
4. Siegel, R. L. *et al.* Colorectal Cancer Statistics , 2017. *CA: a cancer journal for clinicians* **67**, 177–193 (2017).
5. Jasperson, K. W., Tuohy, T. M., Neklason, D. W. & Burt, R. W. Hereditary and Familial Colon Cancer. *Gastroenterology* **138**, 2044–2058 (2011).
6. Chan, A. T. & Giovannucci, E. L. Primary Prevention of Colorectal Cancer. *Gastroenterology* **138**, 2029–2043 (2011).
7. Burt, R. Inheritance of Colorectal Cancer. *drug discovery today disease mechanisms* **4**, 293–300 (2008).
8. Ekbom, A., Helmich, C. & Zack, M. Increased risk of large bowel cancer in Chron's disease with colonic involvement. *Lancet* 357–359 (1990).
9. Grady, W. M., Markowitz, S. D. & Hutchison, F. The molecular pathogenesis of colorectal cancer and its potential application to colorectal cancer screening. *Digestive Diseases and Sciences* **60**, 762–772 (2016).
10. Rady, W. & Carethers, J. Genomic and epigenetic instability in colorectal cancer. *Gastroenterology* **135**, 1079–1099 (2008).
11. Nakayama, G., Tanaka, C. & Kodera, Y. Current Options for the Diagnosis , Staging and Therapeutic Management of Colorectal Cancer. 25–32 (2014).
12. Seyfriend, T. & Huysentruit, L. On the Origin of Cancer Metastasis. *Critical reviews in oncogenesis* **18**, 43–73 (2014).
13. Turdean, S., Simona, G., Turcu, M., Voidăzan, S. & Anca, S. Liver Metastases: Incidence and Clinicopathological Data. *Acta Medica Marisiensis* **58**, 254–258 (2012).
14. Zarour, L. R. *et al.* Colorectal Cancer Liver Metastasis: Evolving Paradigms and Future Directions. *Cmgh* **3**, 163–173 (2017).
15. Donadon, M. *et al.* The Shifting Paradigm of Prognostic Factors of Colorectal Liver Metastases : From Tumor-Centered to Host immune-Centered Factors. *Frontiers in Immunology* **8**, (2018).
16. Riihimäki, M., Hemminki, A., Sundquist, J. & Hemminki, K. Patterns of metastasis in colon and rectal cancer. *Scientific Reports - Nature* **6**, 1–9 (2016).
17. Simmonds, P. *et al.* Surgical resection of hepatic metastases from colorectal cancer: A systematic review of published studies. *British Journal of Cancer* **7**, 982–999 (2006).
18. Chow, F. C. & Chok, K. S. Colorectal liver metastases: An update on multidisciplinary approach. *World Journal of Hepathology* **11**, 150–172 (2019).
19. Zouhairi, M. El, Charabaty, A. & Pishvaian, M. J. Molecularly Targeted Therapy for Metastatic Colon Cancer: Proven Treatments and Promising New Agents. *Gastrointestinal Cancer Research* **4**, 15–21 (2011).
20. Lu, Z. *et al.* Bevacizumab with preoperative chemotherapy versus preoperative chemotherapy alone for colorectal cancer liver metastases. *Medicine* 1–6 (2016).
21. Ferrara, N., Hillan, K. J., Gerber, H., Novotny, W. & Francisco, S. S. Discovery and development of bevacizumab, an anti-vegf antibody for treating cancer. *Nature Reviews Drug Discovery* **3**, 1–10 (2004).
22. Chen, K., Gong, Y., Zhang, Q., Shen, Y. & Zhou, T. Efficacy and safety of addition of bevacizumab

to FOLFIRI or irinotecan/bolus 5-FU/LV (IFL) in patients with metastatic colorectal cancer. *Medicine* 1–7 (2016).

23. Roock, W. De *et al.* KRAS wild-type state predicts survival and is associated to early radiological response in metastatic colorectal cancer treated with cetuximab. *Annals of Oncology* **19**, 508–515 (2008).

24. Seshaxharuylu, P., Ponnusamy, M., Haridas, D. & Jain, M. Targeting the EGFR signaling pathway in cancer therapy. *Expert Opinion on Therapeutich Targets* **16**, 15–31 (2013).

25. Pollock, R., Broglio, K. R., Hess, K. & Curley, S. A. Recurrence and Outcomes Following Hepatic Resection , Radiofrequency Ablation , and Combined Resection / Ablation for Colorectal Liver Metastases. *Annals of Surgery* **239**, 818–827 (2004).

26. Krenkel, O. & Tacke, F. Liver macrophages in tissue homeostasis and disease. *Nature Reviews Immunology* **17**, 307–319 (2017).

27. Lau, A. H. & Thomson, A. W. Dendritic cells and immune regulation in the liver. *gut* **52**, 307–313 (2003).

28. Williamson, T., Sultanpuram, N. & Sendi, H. The role of liver microenvironment in hepatic metastasis. *Clinical and Translational Medicine* **8**, (2019).

29. Donadon, M. *et al.* Increased Infiltration of Natural Killer and T Cells in Colorectal Liver Metastases Improves Patient Overall Survival. *Journal of Gastrointestinal Surgery* **21**, 1226–1236 (2017).

30. Tosolini, M., Camus, M., Berger, A., Wind, P. & Lagorce-page, C. Type, Density, and Location of Immune Cells Within Human Colorectal Tumors Predict Clinical Outcome ´. *Science* **313**, (2006).

31. Ascierto, P. A. *et al.* The additional facet of immunoscore: immunoprofiling as a possible predictive tool for cancer treatment. *Journal of Translational Medicine* **11**, 8–11 (2013).

32. Macdonald, F. & Zaiss, D. M. W. The Immune System's Contribution to the Clinical Efficacy of EGFR Antagonist Treatment. *Frontiers in Immunology* **8**, 1–7 (2017).

33. Aldeghaither, D., Connell, A. O. & Weiner, L. M. Enhancing antibody-dependent cell-mediated cytotoxicity: a strategy for improving antibody-based immunotherapy. *AntibodyTherapeutics* **1**, 7–12 (2018).

34. Bank, I. *et al.* A functional T3 molecule associated with a novel heterodimer on the surface of immature human thymocytes. *Nature* **322**, 179–181 (1986).

35. Brenner, M. *et al.* Identification of a putative second T-cell receptor. *Nature* **322**, 145–149 (1986).

36. Chien, Y., Iwashima, M., Kaplan, K., Elliot, J. & Davis, M. A new T-cell receptor gene located within the alpha locus and expressed early in T-cell differentiation. *Nature* **327**, 677–682 (1987).

37. Bluestone, J. A., Schwartz, R. H. & Coligan, J. E. Thymus-dependent and thymus-independent developmental pathways for peripheral T cell receptor-gamma delta-bearing lymphocytes. *JThe Journal of Immunology* **140**, 4091–4096 (1988).

38. Bos, J. *et al.* T-cell receptor gamma delta bearing cells in normal human skin. *Journal of Investigative Dermatology* **94**, 37–42 (1990).

39. Kenna, T. *et al.* Distinct subpopulations of γδ T cells are present in normal and tumor-bearing human liver. *Clinical Immunology* **113**, 56–63 (2004).

40. Goodman, T. & Lefrançois, L. Expression of the gamma-delta T-cell receptor on intestinal CD8+ intraepithelial lymphocytes. *Nature* **333**, 855–858 (1988).

41. Chien, Y., Meyer, C. & Bonneville, M. γδ T Cells: First Line of Defense and Beyond. *Annual Review of Immunology* **32**, 121–155 (2014).

42. Ogata, M. & Itoh, T. Gamma/delta intraepithelial lymphocytes in the mouse small intestine. *Anatomical science international* (2016).

43. Bergstresser, P., Tigelaar, P., Dees, J. & Streilein, J. Thy- 1 antigen- bearing dendritic cells populate murine epidermis. *Journal of Investigative Dermatology* **81**, 286–288 (1983).

44. Wu, D., Wu, P., Qiu, F., Wei, Q. & Huang, J. Human γδT-cell subsets and their involvement in tumor immunity. *Cellular and Molecular Immunology* **14**, 245–253 (2017).

45. Adams, E. J., Gu, S. & Luoma, A. M. Human gamma delta T cells: evolution and ligand recognition. *Cellular Immunology* **296**, 31–40 (2016).

46. Vantourout, P. & Hayday, A. Six-of-the-best: unique contributions of γδ T cells to immunology. *Nature Reviews Immunology* **13**, 88–100 (2013).

47. Schild, H. The nature of major histocompatibility complex recognition by γδ T cells. *Cell* **76**, 29–37 (1994).

48. Kroca, M., Johansson, A., Sjo, A. & Ta, A. Vγ9Vδ2 T Cells in Human Legionellosis. *Clinical and Diagnostic Laboratory Immunology* **8**, 949–954 (2001).

49. Munk, M. E., Gatrill, A. J. & Kaufmann, S. H. E. Target cell lysis and IL-2 secretion by gamma/delta T lymphocytes after activation with bacteria. *Journal of Immunology* **145**, 2434–2439 (1990).

50. Paoli, P. D. E. *et al.* A subset of gamma delta lymphocytes is increased during HIV-1 infection. *Clinical Experimental Immunology* **83**, 187–191 (1991).

51. De, J. *et al.* Major Expansion of γδ T Lymphocytes following Cytomegalovirus Infection in. *The Journal of Infectious Diseases* **179**, 1–8 (1999).

52. Sutton, C. E., Mielke, L. A. & Mills, K. H. G. IL-17-producing γδ T cells and innate lymphoid cells. *European Journal of Immunology* **42**, 2221–2231 (2012).

53. Pardoll, D. M. *et al.* Differential expression of two distinct T-cell receptors during thymocyte development. *Nature* **326**, 79–81 (1987).

54. Havran, W. L. & Allison, J. P. Developmentally ordered appearance of thymocytes expressing different T-cell antigen receptors. *Nature* **335**, 443–445 (1988).

55. Lefranc, M. The human T-cell rearranging gamma (TRG) genes and the gamma T-cell receptor. *Biochimie* **70**, 901–908 (1988).

56. Kranz, D. *et al.* Chromosomal locations of the murine T-cell receptor alpha-chain gene and the T-cell gamma gene. *Science* **227**, 941–945 (1985).

57. Greisser, H. *et al.* The human T cell receptor alpha-delta locus: a physical map of the variable, joining and constant region genes. *European Journal of Immunology* **18**, 641–644 (1988).

58. Bassing, C., Swat, W. & Alt, F. The mechanism and regulation of chromosomal V(D)J recombination. *Cell* **109**, S45–S55 (2002).

59. Lefranc, M., Giudicelli, V., Duroux, P., Jabado-Michaloud, J. & Folch, G. IMGT®, the international ImMunoGeneTics information system® 25 years on. *Nucleic Acids Research* **43**, 413–422 (2014).

60. Chien, Y. & Konigshofer, Y. Antigen recognition by γδ T cells. *Immunological Reviews* **215**, 46–58 (2007).

61. Elliott, J., Rock, E., Patten, P., Davis, M. & Chien, Y. The adult T-cell receptor 5-chain is diverse and distinct from that of fetal thymocytes. *Nature* **331**, 627–631 (1988).

62. Rock, B. E. P., Sibbald, P., Davis, M. M. & Chien, Y. CDR3 Length in Antigen-specific Immune Receptors. *Journal of Experimental Medicine* **179**, 323–328 (1994).

63. Havran, W. L. & Allison, J. P. Origin of Thy-1+ dendritic epidermal cells of adult mice from fetal thymic precursors. *Nature* **344**, 68–70 (1990).

64. Yoichi, S., Rania, H. M. & Masanori, K. Origin and evolution of Dendritic epidermal T Cells. *Frontiers in Immunology* **9**, 1–5 (2018).

65. Casorati, B. Y. G., Lanzavecchia, A. & Migonet, N. Molecular analysis of human gamma/delta+ clones from thymus and peripheral blood. *Journal of Experimental Medicine* **170**, 1521–1535 (1989).

66. Dimova, T. *et al.* Effector Vγ9Vδ2 T cells dominate the human fetal γδ T-cell repertoire. *PNAS* **112**, E556–E565 (2015).

67. Davey, M. S. *et al.* Clonal selection in the human Vδ1 T cell repertoire indicates γδ TCR-dependent adaptive immune surveillance. *Nature Communications* **8**, 1–15 (2017).

68. Davey, M. S., Willcox, C. R., Baker, A. T., Hunter, S. & Willcox, B. E. Recasting Human Vδ1 Lymphocytes in an Adaptive Role. *Trends in Immunology* **39**, 446–459 (2018).

69. Ravens, S. *et al.* Human γδ T cells are quickly reconstituted after stem-cell transplantation and show adaptive clonal expansion in response to viral infection. *Nature immunology* **18**, (2017).

70. Fahl, S. P., Coffey, F. & Wiest, D. L. Origins of γδ T Cell Effector Subsets: A Riddle Wrapped in an Enigma. *The Journal of Immunology* **193**, 4289–4294 (2014).

71. Willcox, B. E. & Willcox, C. R. γδ TCR ligands: the quest to solve a 500-million- year-old mystery. *Nature Immunology* **20**, 121–128 (2019).

72. Witherden, D. A. & Havran, W. L. EPCR: a stress trigger for γδ T cells. *Nature immunology* **13**, 812–814 (2012).

73. O'Brien, R. L. *et al.* γδ T-cell receptors: Functional correlations. *Immunological Reviews* **215**, 77–88 (2007).

74. Sabourin, C. *et al.* Self/non-self discrimination by human γδ T cells: simple solutions for a complex issue? *Immunological Reviews* **215**, 123–135 (2007).

75. Paul, S. & Lal, G. Regulatory and effector functions of gamma-delta (γδ) T cells and their therapeutic potential in adoptive cellular therapy for cancer. *International Journal of Cancer* **139**, 976–985 (2016).

76. Harly, C., Peigné, C. & Scotet, E. Molecules and mechanisms implicated in the peculiar antigenic activation process of human Vγ9Vδ2 T cells. *Frontiers in Immunology* **5**, 1–13 (2015).

77. Gober, H. *et al.* Human T Cell Receptor γδ Cells Recognize Endogenous Mevalonate Metabolites in Tumor Cells. *The Journal of experimental medicine* **197**, 163–168 (2003).

78. Poupot, M. & Fournié, J. J. Non-peptide antigens activating human Vγ9/Vδ2 T lymphocytes. *Immunology Letters* **95**, 129–138 (2004).

79. Harly, C. *et al.* Key implication of CD277/butyrophilin-3 (BTN3A) in cellular stress sensing by a major human γδ T-cell subset. *Blood* **120**, 2269–2279 (2012).

80. Silva-santos, B. & Strid, J. Working in 'NK Mode': Natural Killer Group 2 Member D and Natural Cytotoxicity Receptors in Stress-Surveillance by γδ T Cells. *Frontiers in Immunology* **9**, 1–8 (2018).

81. Kong, Y. *et al.* The NKG2D ligand ULBP4 binds to TCR g9/d2 and induces cytotoxicity to tumor cells through both TCRγδ and NKG2D. *Blood* **114**, 310–317 (2009).

82. Spada, F. M. *et al.* Self-recognition of CD1 by gamma/delta T cells: implications for innate immunity. *The Journal of experimental medicine* **191**, 937–48 (2000).

83. Uldrich, A. P. *et al.* CD1d-lipid antigen recognition by the γδ TCR. *Nature immunology* **14**, 1137–45 (2013).

84. Willcox, C. R. *et al.* Cytomegalovirus and tumor stress surveillance by binding of a human γδ T cell antigen receptor to endothelial protein C receptor. *Nature Immunology* **13**, 872–879 (2012).

85. Fonslow, B. R. *et al.* γδ T cells recognize a microbial encoded B cell antigen to initiate a rapid antigen specific Interleukin 17 response. **10**, 54–56 (2013).

86. Scotet, E. *et al.* Tumor recognition following Vγ9Vδ2 T cell receptor interactions with a surface F1-ATPase-related structure and apolipoprotein A-I. *Immunity* **22**, 71–80 (2005).

87. Bruder, J. *et al.* Target specificity of an autoreactive pathogenic human γδ-T cell receptor in myositis. *Journal of Biological Chemistry* **287**, 20986–20995 (2012).

88. Vermijlen, D., Gatti, D., Kouzeli, A., Rus, T. & Eberl, M. γδ T cell responses: How many ligands will it take till we know? *Seminars in Cell and Developmental Biology* **84**, 75–86 (2018).

89. Jensen, K. D. C. *et al.* Thymic Selection Determines γδ T Cell Effector Fate: Antigen-Naive Cells Make Interleukin-17 and Antigen-Experienced Cells Make Interferon-g. *Immunity* **29**, 90–100 (2008).

90. Schulz, S. M., Köhler, G., Holscher, C., Iwakura, Y. & Alber, G. IL-17A is produced by Th17, γδ T cells and other CD4- lymphocytes during infection with Salmonella enterica serovar Enteritidis and has a mild effect in bacterial clearance. *International Immunology* **20**, 1129–1138 (2008).

91. Lockhart, E., Green, A. M. & Flynn, J. L. IL-17 production is dominated by gammadelta T cells rather than CD4 T cells during Mycobacterium tuberculosis infection. *Journal of Immunology* **177**, 4662–4669 (2006).

92. Welte, T. *et al.* Vγ4+T Cells Regulate Host Immune Response to West Nile Virus Infection. **10**, 54–56 (2013).

93. Dodd, J., Riffault, S., Kodituwakku, J. S., Hayday, A. C. & Openshaw, P. J. M. Pulmonary V{gamma}4+ {gamma}{delta} T Cells Have Proinflammatory and Antiviral Effects in Viral Lung Disease. *J Immunol* **182**, 1174–1181 (2009).

94. Strid, J., Sobolev, O., Zafirova, B., Polic, B. & Hayday, A. The intraepithelial T cell response to NKG2D-ligands links lymphoid stress surveillance to atopy. *Science* **334**, 1293–7 (2011).

95. Sharp, L. L., Jameson, J. M., Cauvi, G. & Havran, W. L. Dendritic epidermal T cells regulate skin homeostasis through local production of insulin-like growth factor 1. *Nature immunology* **6**, 73–79 (2005).

96. Gerber, D. J. *et al.* IL-4-producing gamma delta T cells that express a very restricted TCR repertoire are preferentially localized in liver and spleen. *Journal of immunology* **163**, 3076–3082 (1999).

97. Bukowski, J. F., Morita, C. T. & Brenner, M. B. Recognition and destruction of virus-infected cells by human gamma delta CTL. *Journal of Immunology* **153**, 5133–5140 (1994).

98. Siegers, G. M. & Lamb, L. S. Cytotoxic and regulatory properties of circulating Vδ1+ γδ t cells: A new player on the cell therapy field? *Molecular Therapy* **22**, 1416–1422 (2014).

99. Jameson, J. *et al.* A Role for Skin γδ T Cells in Wound Repair. *Science* **296**, 747–750 (2002).

100. Nanno, M., Shiohara, T., Yamamoto, H., Kawakami, K. & Ishikawa, H. γδ T cells: Firefighters or fire boosters in the front lines of inflammatory responses. *Immunological Reviews* **215**, 103–113 (2007).

101. Girardi, M. *et al.* Regulation of Cutaneous Malignancy by γδ T Cells. *Science* **294**, 605–610 (2001).

102. Street, S. E. A. *et al.* Innate Immune Surveillance of Spontaneous B Cell Lymphomas by Natural Killer Cells and γδ T Cells. *Journal of Experimental Medicine* **199**, 879–884 (2004).

103. Corvaisier, M., Moreau-Aubry, A., Diez, E. & Bennouna, J. Vγ9Vδ2 T cell response to colon carcinoma cells. *Journal of Immunology* **175**, 5481–5488 (2005).

104. Zocchi, M. R., Ferrarini, M. & Rugarli, C. Selective lysis of the autologous tumor by δTCS1+ γ/δ+ tumor- infiltrating lymphocytes from human lung carcinomas. *European Journal of Immunology* **20**, 2685–2689 (1990).

105. Liu, Z., Guo, B. E. N. L., Gehrs, B. C., Nan, L. I. & Lopez, R. D. Ex vivo expanded human Vgamma9Vdelta2+ gammadelta-T cells mediate innate antitumor activity against human prostate cancer cells in vitro. *Journal of Hurology* **173**, 1552–1556 (2005).

106. Cordova, A. *et al.* Characterization of Human γδ T Lymphocytes Infiltrating Primary Malignant Melanomas. *PLoS ONE* **7**, 1–9 (2012).

107. Correia, D. V & Silva-santos, B. Tumor cell recognition by γδ T lymphocytes. *OncoImmunology* **2**, 1–5 (2013).

108. Silva-Santos, B., Serre, K. & Norell, H. γδ T cells in cancer. *Nature Reviews Immunology* **15**, 683–91 (2015).

109. Chen, H., Zou, M., Teng, D., Zhang, J. & He, W. Characterization of the diversity of T cell receptor γδ complementary determinant region 3 in human peripheral blood by Immune Repertoire Sequencing. *Journal of Immunological Methods* **443**, 9–17 (2017).

110. Zhao, Y., Niu, C. & Cui, J. Gamma-delta (γδ) T Cells: Friend or Foe in Cancer Development. *Journal of Translational Medicine* **16**, 1–13 (2018).

111. Wakita, D. *et al.* Tumor-infiltrating IL-17-producing γδ T cells support the progression of tumor by

promoting angiogenesis. *European Journal of Immunology* **40**, 1927–1937 (2010).

112. Lo Presti, E., Dieli, F. & Meraviglia, S. Tumor-infiltrating γδ T lymphocytes: Pathogenic role, clinical significance, and differential programing in the tumor microenvironment. *Frontiers in Immunology* **5**, 1–8 (2014).

113. Wu, P. *et al.* γδT17 cells promote the accumulation and expansion of myeloid-derived suppressor cells in human colorectal cancer. *Immunity* **40**, 785–800 (2014).

114. Daley, D., Zambirinis, C., Seifert, L. & Akkad, N. γδ T Cells Support Pancreatic Oncogenesis by Restraining αβ T Cell Activation. *Cell* **166**, 1485–1499 (2016).

115. Kalyan, S. & Kabelitz, D. Defining the nature of human γδ T cells: A biographical sketch of the highly empathetic. *Cellular and Molecular Immunology* **10**, 21–29 (2013).

116. Sebestyen, Z., Prinz, I., Silva-, B. & Kuball, J. Translating gammadelta (γδ) T cells and their receptors into cancer cell therapies. *Nature Reviews Drug Discovery* (2019).

117. Wrobel, P. *et al.* Lysis of a Broad Range of Epithelial Tumour Cells by Human cd T Cells: Involvement of NKG2D ligands and T-cell Receptor- versus NKG2D-dependent Recognition. *Scandivian Journal of Immunology* **66**, 320–328 (2007).

118. Tokuyama, H. *et al.* Vγ9Vδ2 T cell cytotoxicity against tumor cells is enhanced by monoclonal antibody drugs — Rituximab and trastuzumab. *International Journal of Cancer* **122**, 2526–34 (2008).

119. Correia, D. V *et al.* Differentiation of human peripheral blood Vδ1+ T cells expressing the natural cytotoxicity receptor NKp30 for recognition of lymphoid leukemia cells. *Blood* **118**, 992–1001 (2011).

120. Correia, D. V *et al.* Differentiation of human peripheral blood Vδ1+ T cells expressing the natural cytotoxicity receptor NKp30 for recognition of lymphoid leukemia cells. *Blood* **118**, 992–1001 (2011).

121. Poggi, A. *et al.* Vδ1 T Lymphocytes from B-CLL Patients Recognize ULBP3 Expressed on Leukemic B Cells and Up-Regulated by Trans -Retinoic Acid. *Cancer Research* **64**, 9172–9179 (2004).

122. Wu, D. *et al.* Ex vivo expanded human circulating Vδ1 γδT cells exhibit favorable therapeutic potential for colon cancer. *OncoImmunology* **4**, e992749 (2015).

123. Devaud, C., Rousseau, B., Netzer, S. & Pitard, V. Anti-metastatic potential of human Vδ1+ γδ T cells in an orthotopic mouse xenograft model of colon carcinoma. *Cancer Immunology Immunotherapy* **62**, 1199–1210 (2013).

124. Silva-santos, B., Mensurado, S. & Coffelt, S. B. γδ T cells: pleiotropic immune effectors with therapeutic potential in cancer. *Nature Reviews Cancer* **19**, 392–404 (2019).

125. Almeida, A. R. *et al.* Delta One T Cells for Immunotherapy of Chronic Lymphocytic Leukemia: Clinical-Grade Expansion/Differentiation and Preclinical Proof of Concept. *Clinical cancer research: an official journal of the American Association for Cancer Research* **22**, 5795–5804 (2016).

126. Wang, H. *et al.* Indirect Stimulation of Human Vγ2Vδ2 T Cells through Alterations in Isoprenoid Metabolism. *The Journal of Immunology* **187**, 5099–5113 (2011).

127. Marcu-malina, V. *et al.* Redirecting γδT cells against cancer cells by transfer of a broadly tumor-reactive γδT-cell receptor. *Blood* **118**, 50–60 (2011).

128. Bennouna, J. *et al.* Phase-I study of Innacell ™ , an autologous cell-therapy product highly enriched in γ9δ2 T lymphocytes , in combination with IL-2, in patients with metastatic renal cell carcinoma. *Cancer Immunology Immunotherapy* **2**, 1599–1609 (2008).

129. Sakamoto, M., Nakajima, J., Murakawa, T., Fukami, T. & Yoshida, Y. Adoptive Immunotherapy for Advanced Non-small Cell Lung Cancer Using Zoledronate-expanded γδ T Cells: A Phase I Clinical Study. *Journal of Immunotherapy* **34**, 202–211 (2011).

130. Kunzmann, V. *et al.* Tumor-promoting Versus Tumor-antagonizing Roles of γδ T Cells in Cancer Immunotherapy : Results From a Prospective Phase I / II Trial. *Journal of Immunotherapy* **35**, 205–213 (2012).

131. Wistuba, Hamprecht K Martens, A. *et al.* Proportions of blood-borne Vδ1+ and Vδ2+ T-cells are associated with overall survival of melanoma patients treated with ipilimumab. *European Journal of*

Cancer **64**, 116–126 (2017).

132. de Weerdt, I., Hofland, T., Lameris, R Endstra, S., Jongejan, A Moerland, P. & de Bruin, R. Improving CLL Vγ9Vδ2-T-cell fitness for cellular therapy by ex vivo activation and ibrutinib. *Blood* **132**, 2260–2272 (2018).

133. Bruin, C. G. De *et al.* A bispecific nanobody approach to leverage the potent and widely applicable tumor cytolytic capacity of Vγ9Vδ2-T cells. *OncoImmunology* **7**, 1–14 (2017).

134. Salter, A. I., Pont, M. J. & Riddell, S. R. Chimeric antigen receptor– modified T cells: CD19 and the road beyond. *Blood* **131**, 2621–2630 (2018).

135. Tacke, F., Luedde, T. & Trautwein, C. Inflammatory Pathways in Liver Homeostasis and Liver Injury. *Clinical Review Allergy Immunology* **36**, 4–12 (2009).

136. Hammerich, L. & Tacke, F. Role of gamma-delta T cells in liver inflammation and fibrosis. *World Journal of Gastrointestinal Pathophysiology* **5**, 107–113 (2014).

137. Nuti, S. *et al.* Dynamics of intra-hepatic lymphocytes in chronic hepatitis C: enrichment for V alpha24+ T cells and rapid elimination of effector cells by apoptosis. *European Journal of Immunology* **28**, 3448–3455 (1998).

138. Agrati, C. *et al.* γδ T Cell Activation by Chronic HIV Infection May Contribute to Intrahepatic V d 1 Compartmentalization and Hepatitis C Virus Disease Progression Independent of Highly Active Antiretroviral Therapy. *AIDS RESEARCH AND HUMAN RETROVIRUSES* **17**, 1357–1363 (2001).

139. Hou, L. *et al.* Early IL-17 production by intrahepatic T cells is important for adaptive immune responses in viral hepatitis. *Journal of Immunology* **190**, 621–629 (2014).

140. Yi, Y. *et al.* The functional impairment of HCC-infiltrating γδ T cells , partially mediated by regulatory T cells in a TGFb- and IL-10-dependent manner. *Journal of Hepatology* **58**, 977–983 (2013).

141. Hunter, S. *et al.* Human liver infiltrating γδ T cells are composed of clonally expanded circulating and tissue-resident populations. *journal of Hepatology* **69**, 654–665 (2018).

142. Dieli, F. *et al.* Differentiation of Effector/ Memory Vδ2 T Cells and Migratory Routes in Lymph Nodes or Inflammatory Sites. *Journal of Experimental Medicine* **198**, 391–397 (2003).

143. Rosa, S. C. De *et al.* Ontogeny of γδ T Cells in Humans. *Journal of Immunology* **172**, 1637–1645 (2004).

144. Kepp, O. & Zitvogel, L. Immunological Effects of Conventional Chemotherapy and Targeted Anticancer Agents. *Cancer cell* **28**, 690–714 (2015).

145. Xu, W. *et al.* Mapping of γ/δ T cells reveals Vδ2+ T cells resistance to senescence. *EBioMedicine* **39**, 44–58 (2019).

146. Boćko, D., Kosmaczewska, A., Ciszak, L., Teodorowska, R. & Frydecka, I. CD28 costimulatory molecule-expression, structure and function. *Archivum Immunologiae et Therapiae Experimentalis* **50**, 169–177 (2002).

147. Ribot, J. C., Mancio-silva, L. & Silva-santos, B. B7 − CD28 Costimulatory Signals Control the Survival and Proliferation of Murine and Human γδ T Cells via IL-2 Production. *Journal of Immunology* **189**, 1202–1208 (2012).

148. Angelini, D. F. *et al.* FcγRIII discriminates between 2 subsets of Vγ9Vδ2 effector cells with different responses and activation pathways. *Blood* **104**, 1801–1808 (2004).

149. Misslitz, A. *et al.* Thymic T Cell Development and Progenitor Localization Depend on CCR7. *Journal of Experimental Medicine* **200**, 481–491 (2004).

150. Ziegler, Steven F.Ramsdell, F. & Alderson, M. R. The activation antigen CD69. *Stem Cells* **12**, 456–465 (1994).

151. Iiai, T., Watanabe, H., Suda, T., Okamoto, H. & Abo, T. CD161+ T (NT) cells exist predominantly in human intestinal epithelium. *Clinical Experimental Immunology* **129**, 92–98 (2002).

152. Fergusson, J. R. *et al.* CD161 Defines a Transcriptional and Functional Phenotype across Distinct Human T Cell Lineages. *Cell Reports* **9**, 1075–1088 (2014).

153. Walunas, T. *et al.* CTLA-4 can function as a negative regulator of T cell activation. *Immunity* **1**, 405–413 (1994).

154. Agata, Y. *et al.* Expression of the PD-1 antigen on the surface of stimulated mouse T and B lymphocytes. *International Immunology* **8**, 765–772 (1996).

155. Sansom, D. CD28, CTLA-4 and their ligands: who does what and to whom? *Immunology* **101**, 169–177 (2000).

156. Mair, F., Hartmann, F. J., Mrdjen, D. & Tosevski, V. The end of gating? An introduction to automated analysis of high dimensional cytometry data. *European Journal of Immunology* **46**, 34–43 (2016).

157. Brandes, M., Willimann, K. & Moser, B. Professional Antigen-Presentation Function by Human γδ T Cells. *Science* **309**, 264–268 (2005).

158. Cui, Y., Li, H., Zhou, H., Zhang, T. & Li, Q. Correlations of Tumor-associated Macrophage Subtypes with Liver Metastases of Colorectal Cancer. *Asian Pacific Journal of Cancer Prevention* **14**, 1003–1007 (2013).

159. Keskinov, A. A. & Shurin, M. R. Myeloid regulatory cells in tumor spreading and metastasis. *Immunobiology* **220**, 236–242 (2015).

160. Halama, N. *et al.* Tumoral Immune Cell Exploitation in Colorectal Cancer Metastases Can Be Targeted Effectively by Anti-CCR5 Therapy in Cancer Patients Article Tumoral Immune Cell Exploitation in Colorectal Cancer Metastases Can Be Targeted Effectively by Anti-CCR5 Therapy in Cancer Patients. *Cancer Cell* **29**, 587–601 (2016).

161. Cibrián, D. & Sánchez-madrid, F. CD69: from activation marker to metabolic gatekeeper. *European Journal of Immunology* **47**, 946–953 (2017).

162. Sites, M. *et al.* Human Tissue-Resident Memory T Cells Are Defined by Core Transcriptional and Functional Signatures in Lymphoid and Mucosal Sites. *Cell Reports* **20**, 2921–2934 (2017).

163. Bauer, S. *et al.* Activation of NK Cells and T Cells by NKG2D , a Receptor for Stress-Inducible MICA. *Science* **285**, 727–730 (1999).

164. Correia, D. V *et al.* The MHC class Ib protein ULBP1 is a nonredundant determinant of leukemia/ lymphoma susceptibility to γδ T-cell cytotoxicity. *Blood* **115**, 2407–2412 (2010).

165. Groh, V., Rhinehart, R., Secrist, H. & Spies, T. Broad tumor-associated expression and recognition by tumor-derived γδ T cells of MICA and MICB. *Proceedings of the National Academy of Sciences of the United States of America* **96**, 6879–6884 (1999).

166. Kamei, R., Yoshimura, K., Yoshino, S., Inoue, M. & Asao, T. Expression levels of UL16 binding protein 1 and natural killer group 2 member D affect overall survival in patients with gastric cancer following gastrectomy. *Oncology letters* **1991**, 747–754 (2018).

167. Zhao, Y. *et al.* Prognostic value of MICA/B in cancers: a systematic review and meta-analysis. *Oncotarget* **8**, 96384–96395 (2017).

168. Groh, V. *et al.* Cell stress-regulated human major histocompatibility complex class I gene expressed in gastrointestinal epithelium. *Proceedings of the National Academy of Sciences of the United States of America* **93**, 12445–12450 (1996).

169. Andrade, L. F. De *et al.* Antibody-mediated inhibition of MICA and MICB shedding promotes NK cell – driven tumor immunity. *Science* **359**, 1537–1542 (2018).

170. Lanier, L. L., Chang, C. & Phillips, J. H. Human NKR-P1A. A disulfide-linked homodimer of the C-type lectin superfamily expressed by a subset of NK and T lymphocytes. *Journal of Immunology* **153**, 2417–2428 (1994).

171. Fergusson, J. R., Fleming, V. M. & Klenerman, P. CD161-expressing human T cells. *Frontiers in Immunology* **2**, 1–7 (2011).

172. Maggi, L. *et al.* CD161 is a marker of all human IL-17-producing T-cell subsets and is induced by RORC. *European Journal of Immunology* **40**, 2174–2181 (2010).

173. Northfield, J. W. *et al.* CD161 Expression on Hepatitis C Virus–Specific CD8+ T Cells Suggests a

Distinct Pathway of T Cell Differentiation. *Hepatology* **47**, 396–406 (2008).

174. Gentles, A. J. *et al.* The prognostic landscape of genes and infiltrating immune cells across human cancers. *Nature medicine* **21**, 938–945 (2015).

175. Klicznik, M. M., Morawski, P. A., Höllbacher, B., Varkhande, S. R. & Motley, S. Exit of human cutaneous resident memory CD4 T cells that enter the circulation and seed distant skin sites. *Science Immunology* **4**, 1–15 (2019).

176. Godder, K. T. *et al.* Long term disease-free survival in acute leukemia patients recovering with increased cd T cells after partially mismatched related donor bone marrow transplantation. *Bone Marrow Transplantation* **39**, 751–757 (2007).

177. Meraviglia, S. *et al.* Distinctive features of tumor-infiltrating γδ T lymphocytes in human colorectal cancer. *OncoImmunology* **6**, 1–12 (2017).

178. Coffelt, S. B. *et al.* IL-17-producing γδ T cells and neutrophils conspire to promote breast cancer metastasis. *Nature* **522**, 345–348 (2015).

179. Peggs, K. S., Quezada, S. A., Korman, A. J. & Allison, J. P. Principles and use of anti-CTLA4 antibody in human cancer immunotherapy. *Current Opinion in Immunology* **18**, 206–213 (2006).

180. Duhen, T. *et al.* Co-expression of CD39 and CD103 identifies tumor-reactive CD8 T cells in human solid tumors. *Nature Communications* **9**, 1–13 (2018).

181. Yi, J. S., Cox, M. A. & Zajac, A. J. T-cell exhaustion: characteristics, causes and conversion. *Immunology* **2**, 474–481 (2010).

182. Ye, L., Wei, X., Zhang, M., Niu, Y. & Zhou, Q. The Significance of Tumor necrosis Factor Receptor Type ii in CD8+ Regulatory T Cells and CD8+ effector T Cells. *Frontiers in Immunology* **9**, 1–8 (2018).

183. Li, H., Luo, K. & Pauza, C. D. TNF-a is a positive regulatory factor for human Vγ9Vδ2 T cells. *Journal of Immunology* **181**, 7131–7137 (2008).

184. Xu, W. & Larbi, A. Markers of T Cell Senescence in Humans. *International Journal of Molecular Science* **18**, 1–13 (2017).

185. Akagi, J. & Baba, H. Prognostic value of CD57+ T lymphocytes in the peripheral blood of patients with advanced gastric cancer. *International Journal of Clinical Oncology* **13**, 528–535 (2008).

186. Lanna, A., Henson, S. M., Escors, D. & Akbar, A. N. The kinase p38 activated by the metabolic regulator AMPK and scaffold TAB1 drives the senescence of human T cells. *Nature Immunology* **15**, 965-972 (2014).

187. Pizzolato, G., Kaminski, H., Tosolini, M. & Franchini, D. Single-cell RNA sequencing unveils the shared and the distinct cytotoxic hallmarks of human TCRVδ1 and TCRVδ2 γδ T lymphocytes. *PNAS* **116**, 2–11 (2019).

188. Odaira, K., Kimura, S., Fujieda, N. & Kakimi, K. CD27- CD45+ γδ T cells can be divided into two populations, CD27-CD45int and CD27-CD45hi with little proliferation potential. *Biochemical and Biophysical Research Communications* **478**, 1298–1303 (2016).

189. Hurria, A. Jones, L. & Muss H.B. Cancer Treatment as an Accelerated Aging Process: Assessment, Biomarkers, and Interventions. *American Society of Clinical Oncology Educational Book* **35,** e516-e522 (2016).